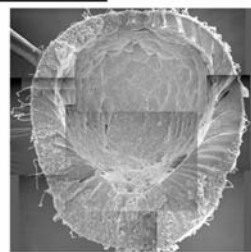
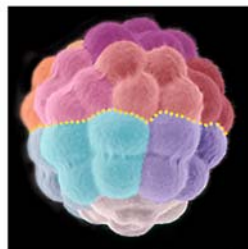
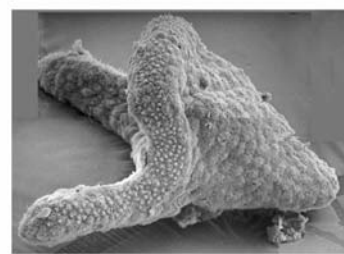


An Atlas of the Development of the Sea Urchin *Lytechinus variegatus*



John B. Morrill
and
Lauren Marcus
Division of Natural Sciences
New College of Florida
Sarasota, Florida
2005



PREFACE

From the 1970s to the present, the sea urchin *Lytechinus variegatus* has provided material for numerous descriptive and experimental studies on cells and embryos that range from oogenesis through metamorphosis of the free-swimming pluteus larva. The *Lytechinus* egg is an ideal cell because of its size, relative transparency and rapid development at room temperature. Many original research articles and reviews on the developmental biology of sea urchins contain elegant photo-micrographs and detailed methodologies for this species. Accordingly, we have assembled sets of cytoembryological micrographs to serve as a visual guide to the morphological aspects of the developmental biology of this species.

The atlas begins with a timetable of development at 20, 23, and 25 °C and a cell lineage chart through tenth cleavage. The rest of the atlas is divided into twelve sections listed in the table of contents. Each plate of figures has abbreviated legends. Lengthy descriptive legends and texts are not included. The plates of micrographs were acquired from the research of John Morrill and numerous students, in his cell and developmental biology program, at New College of Florida over 20 years.

ACKNOWLEDGMENTS

We are indebted to many students in the New College cell and developmental biology program who contributed specimens and micrographs during the course of their senior thesis research projects. We thank the following for the use of their negatives of light and scanning electron micrographs: John Collins, Sherry Doty, Deni Gallileo, Charles Hall, Mark Hastings, Kristin Kalmbacher, Randall Lanier, Lucia Massard, Shawn Murphy, Lisa Muscanara, Corey Nislow, Elizabeth Pare, Adam Rasky, Nicole Reudiger, Laurinda Santos, Alex Slawson, James Tietsworth, John Valdes, and Joshua Waxman. Confocal micrographs of Feulgen stained nuclei are from studies by Nicole Reudiger and Alan Stonebraker as well as Robert Summers. Transmission electron micrographs are from studies by Vivian Lombillo and Corey Nislow in collaboration with Robert Summers.

Special appreciation and gratitude is due to Dr. Robert Summers who over a period of 15 years provided everyone in our laboratory with instructional advice on various specimen preparations and instrumental techniques, especially confocal and transmission electron microscopy during and following his annual visitations to our laboratory.

Finally, we thank the New College Foundation and the Division of Natural Sciences, New College for financial support.

CONTENTS

Section	Page
Preface	i
Acknowledgements	ii
Table of Contents	iii - v
SECTION 1. Timetable of Development and Cell Lineage Chart	1-5
Time Table of Development	3
Cell Lineage Chart Through Tenth Cleavage	4,5
SECTION 2. Overviews of Development: Unfertilized Egg to Four Arm Pluteus	7-15
PLATE 1. Light Micrographs of Unfertilized Egg to Hatching Blastula	8,9
PLATE 2. SEM Micrographs of Unfertilized Egg to Pre-Hatched Blastula	10,11
PLATE 3. Hatched Blastula to Prism Larva; Light and SEM Micrographs	12,13
PLATE 4. Prism to Four Arm Pluteus and Larval Skeleton	14,15
SECTION 3. One Cell Egg	17-21
PLATE 5. Unfertilized Egg	18,19
PLATE 6. Fertilization and Post Fertilization Events	20,21
SECTION 4. First Cleavage to Pre-Hatched Blastula (5.5 hr. P.F.)	23-45
PLATE 7. First Cleavage – 2 Cell Stage	24,25
PLATE 8. Second Cleavage – 4 Cell Stage	26,27
PLATE 9. Third Cleavage – 8 Cell Stage	28,29
PLATE 10. Fourth Cleavage – 16 Cell Stage	30,31
PLATE 11. Fifth Cleavage – 28 and 32 Cell Stages	32,33
PLATE 12. Sixth Cleavage – 60 Cell Stage	34,35
PLATE 13. Seventh Cleavage – Early Blastula	36,37
PLATE 14. Confocal Images of Nuclei of Seventh Cleavage Embryos	38,39
PLATE 15. Confocal Images of Nuclei of Eighth Cleavage Embryos	40,41
PLATE 16. Confocal Images of Nuclei of Ninth Cleavage, Pre-Hatched Blastulae	42,43
PLATE 17. SEM Micrographs of Pre-Hatched Blastulae (5.5 hr P.F.)	44,45

Section	Page
SECTION 5. Hatched Blastula	47-51
PLATE 18. Hatching Time Table, Light Micrographs of a Hatching Embryo and SEMS of Fractured Hatched Blastulae	48,49
PLATE 19. SEM Micrographs of the Vegetal Pole of Hatched Blastulae	50,51
SECTION 6. Mesenchyme Blastula	53-61
PLATE 20. Primary Mesenchyme Cell Ingression	54,55
PLATE 21. Confocal Optical Sections of a Mid-Mesenchyme Blastula	56,57
PLATE 22. SEM Views of Morphological Features of Early Mesenchyme Blastula	58,59
PLATE 23. SEM Views of Late Mesenchyme Blastula	60,61
SECTION 7. Primary Mesenchyme Cells from Late Mesenchyme Mesenchyme Blastula to Late Gastrula	63-77
PLATE 24. Primary Mesenchyme Cell Migration – Late Mesenchyme Blastula to Primary Invagination of Archenteron	64,65
PLATE 25. SEM Views of Migrating Cells	66,67
PLATE 26. TEM Views of Primary Mesenchyme Cells and Primary Mesenchyme Cell Cytoplasmic Syncytium	68,69
PLATE 27. SEM Views of Formation of the Cytoplasmic Syncytium	70,71
PLATE 28. SEM Views of Ventro-Lateral Branch of Cytoplasmic Syncytium	72,73
PLATE 29. Formation of Syncytial Ring	74,75
PLATE 30. Syncytial Ring of the Late Gastrula	76,77
SECTION 8. Archenteron Formation	79-93
PLATE 31. Initiation of Primary Invagination by Ingression of Secondary Mesenchyme Cells	80,81
PLATE 32. Primary Invagination	82,83
PLATE 33. Secondary Elongation	84,85
PLATE 34. Confocal images of Feulgen Stained Nuclei During Secondary Elongation	86,87
PLATE 35. Archenteron Lengths and Numbers of Endodermal Cells	88,89
PLATE 36. TEM Views of the Archenteron of Gastrulae	90,91
PLATE 37. SEM Views of the Extra Cellular Matrix of the Archenteron Lumen	92,93

Section	Page
SECTION 9. Post Gastrula Prism and Pluteus Larvae	95-102
PLATE 38. Prism Stage Larvae	96,97
PLATE 39. Two Arm Pluteus	98,99
PLATE 40. Four Arm Pluteus Larvae	100,101
PLATE 41. Growth of Larval Skeleton	102
SECTION 10. Development of Animal Pole Ectoderm	103-107
PLATE 42. Early Development	104,105
PLATE 43. Apical Plate Ectoderm	106,107
SECTION 11. Ectodermal Cilia	109-119
PLATE 44. SEM Views of Cilia	110,111
PLATE 45. SEM Views of Acron Cilia of Mesenchyme Blastula	112,113
PLATE 46. SEM Views of Acron Cilia of Late Gastrula and Prism Stage Larva	114,115
PLATE 47. TEM Views of Cilia and Cilia Collar Microvilli	116,117
PLATE 48. SEM Views of Cilia With and Without the Hyaline Layer and Abnormal Lollipop Cilia	118,119
SECTION 12. Hyaline Layer of Gastrulae and Larvae	121-127
PLATE 49. Diagram of Hyaline Layer	122,123
PLATE 50. TEMs of the Hyaline Layer	124,125
PLATE 51. SEM Views of the Hyaline Layer and Apical Lamina	126,127
SECTION 13. Extracellular Matrices	129-135
PLATE 52. LM and SEM Views of Extracellular Matrices of the Cleavage Cavity and Blastocoel	130,131
PLATE 53. ECM Vesicle Exudate and Coated ECM Fibers	132,133
PLATE 54. Origins of ECM Vesicles.	134,135

Section 1:

Time Table of Development

&

Cell Lineage Chart

Time Table of Development of *Lytechinus variegatus*
From Sarasota Bay, Florida¹

Cleavage Cycle	Stage	Times Post Fertilization (hr:min)		
		20°C	23°C	25°C
1st	2 cells	1:05-1:15	1:05	0:40-0:60
2nd	4 cells	1:55	1:30	1:10-1:30
3rd	8 cells	2:30	2:00	1:30-1:55
	12 cells		2:22	
4th	16 cells	2:50-3:15	2:25	1:58-2:15
	28 cells	3:40-3:50		
5th	32 cells	3:40-4:00	2:48	2:07-2:30
	56 cells			
6th	60 cells	4:50	3:20	2:25-3:15
7th	116 cells		3:50	3:30-3:40
8th	216 cells			3:50-4:30
9th	408 cells			5:00-5:30
10th	828 cells			6:00-7:30
	First Cilia Visible	8:55	6:05	5:30-6:00
	Hatching Blastula	9:00-10:45	6:45-8:30	6:00-7:00
	PMC Ingression Begins	10:30	9:30	7:10-7:20
	PMC Ingression Ends	14:00	10:30	8:30
	PMC Migration			9:00-10:30
	1° Invagination Begins	15:00		10:00
	PMC Aggregations			11:00-11:30
	1° Invagination Ends	18:00	12:15	11:30
	2° Elongation Begins		12:30	11:50
	2° Elongation Ends	20:00-21:00	15:40	12:30-13:00
	Early Prisms	21:00-24:00	17:00	13:00-16:00
	Late Prisms	27:00-28:00		14:00-15:30
	Early 2-Arm Pluteus	33:00-34:00	25:00	16:00
	(Mouth Opens)			
	Late 2-Arm Pluteus	40:00-46:00		17:00-19:00
	(Oral Arm Buds)			
	Definitive 4-Arm Pluteus	65:00		26:00

1. The times are for embryos cultured in 2, 4, and 8 inch Carolina culture dishes with occasional stirring. Following the hatched blastula stage, swimming blastulae were collected and transferred to fresh seawater.

Duration of the cell cycle at 25°C is approximately 25 to 30 minutes from the 2nd to 6th cleavage, 40 to 40 minutes at 7th cleavage, 40 to 50 minutes at 8th cleavage, 1 hour to 1 hour 20 minutes at 9th cleavage, and 2 hours at 10th cleavage.

CELL LINEAGE CHART EXPLANATIONS

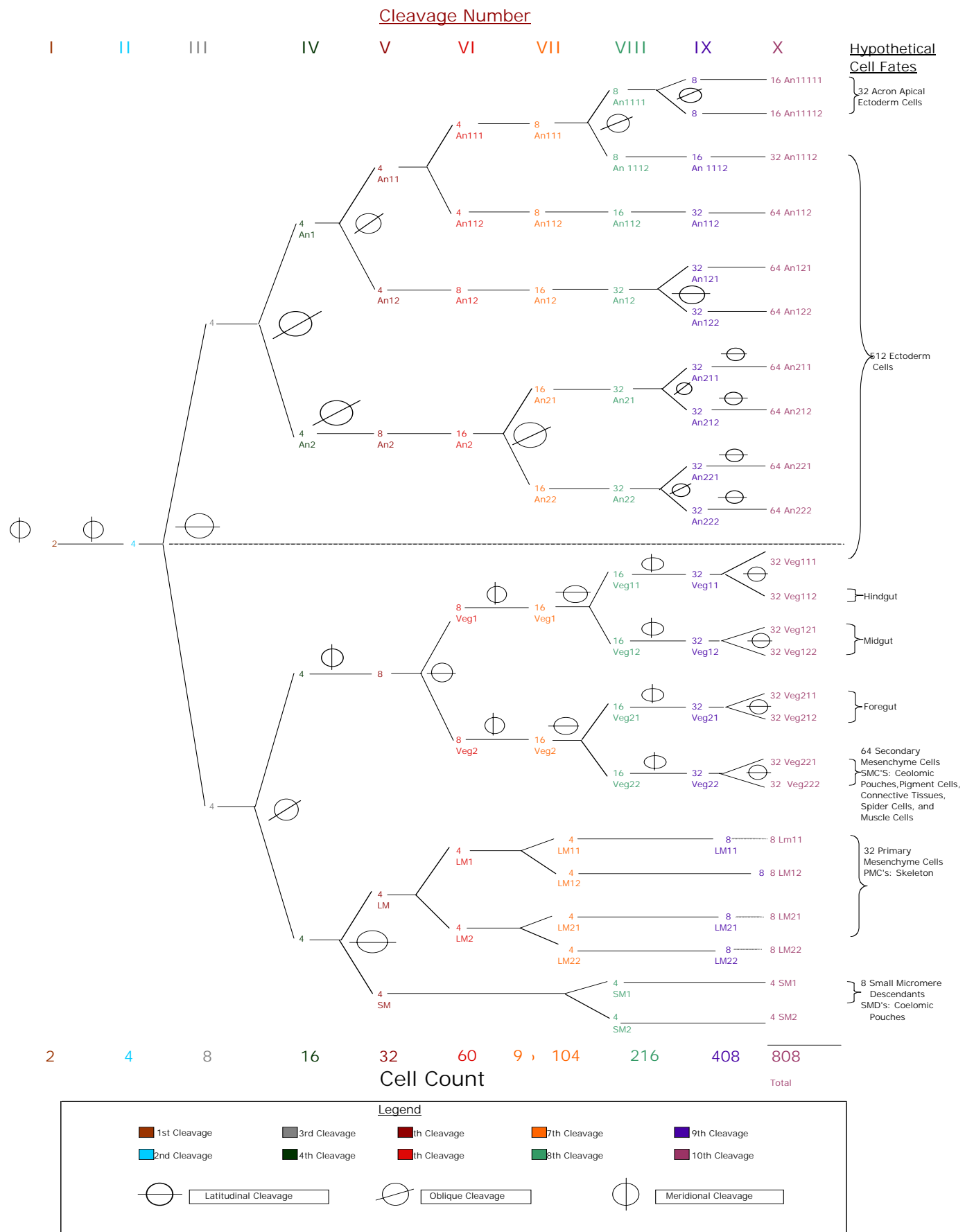
This chart is based on direct observations of live and fixed embryos from the first to the 8th cleavage.

During and following the 8th cleavage, cells begin to form cilia and drop out of the cell cycle. SEM analyses show cilia formations have no apparent pattern. Following the 8th cleavage, synchronous and parasynchronous cell division no longer occurs. In effect there is not a 9th or 10th synchronous cell division. However, we have formatted the 9th and 10th cleavages and their cell numbers in keeping with published data.

The first two meridional cleavages divide the egg into four equal quadrants. The third cleavage is equatorial and divides the egg into animal and vegetal hemispheres. Beginning with the 4th cleavage the planes of cell divisions are markedly different in the two hemispheres. In the vegetal hemisphere the macromeres and their descendants undergo alternating latitudinal and meridional divisions. In the animal hemisphere the planes of cell division are tangential to the A-V polar axis. Cells are arranged in the animal hemisphere to conform to an overall hemispherical shape.

Cell Lineage Chart Through Tenth Cleavage in the Sea Urchin

Lytechinus variegatus



Section 2:

Overviews of Development:

Unfertilized Egg to Four Arm Pluteus

PLATE 1

Unfertilized Egg to Hatching Blastula Stage; Light Micrographs

- A. Unfertilized egg with jelly coat stained with toluidine blue. (Jc, jelly coat)
- B. Unfertilized egg (Fp, Female pronucleus)
- C. SEM of sperm attached to surface of vitelline envelope.
- D. Fertilized egg showing male (M) and female (F) pronuclei, Fertilization envelope (Fe), Perivitelline space (Pv).
- E. Fertilized egg, 1-cell mitotic spindle “streak” stage.
- F. Two-cell stage (animal pole view)
- G. Four-cell stage.
- H. Eight-cell stage (lateral view) with cleavage cavity (Cc).
- I. Sixteen cell stage lateral view. Me, mesomeres, Ma, macromeres, Mi, micromeres.
- J. Twenty-eight cell stage (vegetal pole view).
- K. Thirty-two cell stage (vegetal pole view) showing four small micromeres (blue dots), four large micromeres (red dots), and eight macromeres (yellow dots).
- L. Sixty-cell stage, lateral view. (A) animal pole (V) vegetal pole (Cc) cleavage cavity
- M. Sixty-cell stage. Vegetal pole view showing four small micromeres (Sm=blue dots), eight large micromeres (Lm=red dots), and eight vegetal two macromeres (Veg₂=yellow dots).
- N. Seventh cleavage stage (96 cells; early blastula).
- O. Seventh cleavage, (96 cells; early blastula) vegetal pole view showing fifteen vegetal two (Veg₂) macromeres (yellow) eight large micromeres (red dots), and four small micromeres (blue dots).
- P. Prehatched blastula (eighth/ninth cleavage cycle).
- Q-T. Time lapse photos of hatching blastula. Blastocoelic cavity (Bc) Arrow points to rupture in fertilization envelope (Fe).

PLATE 1

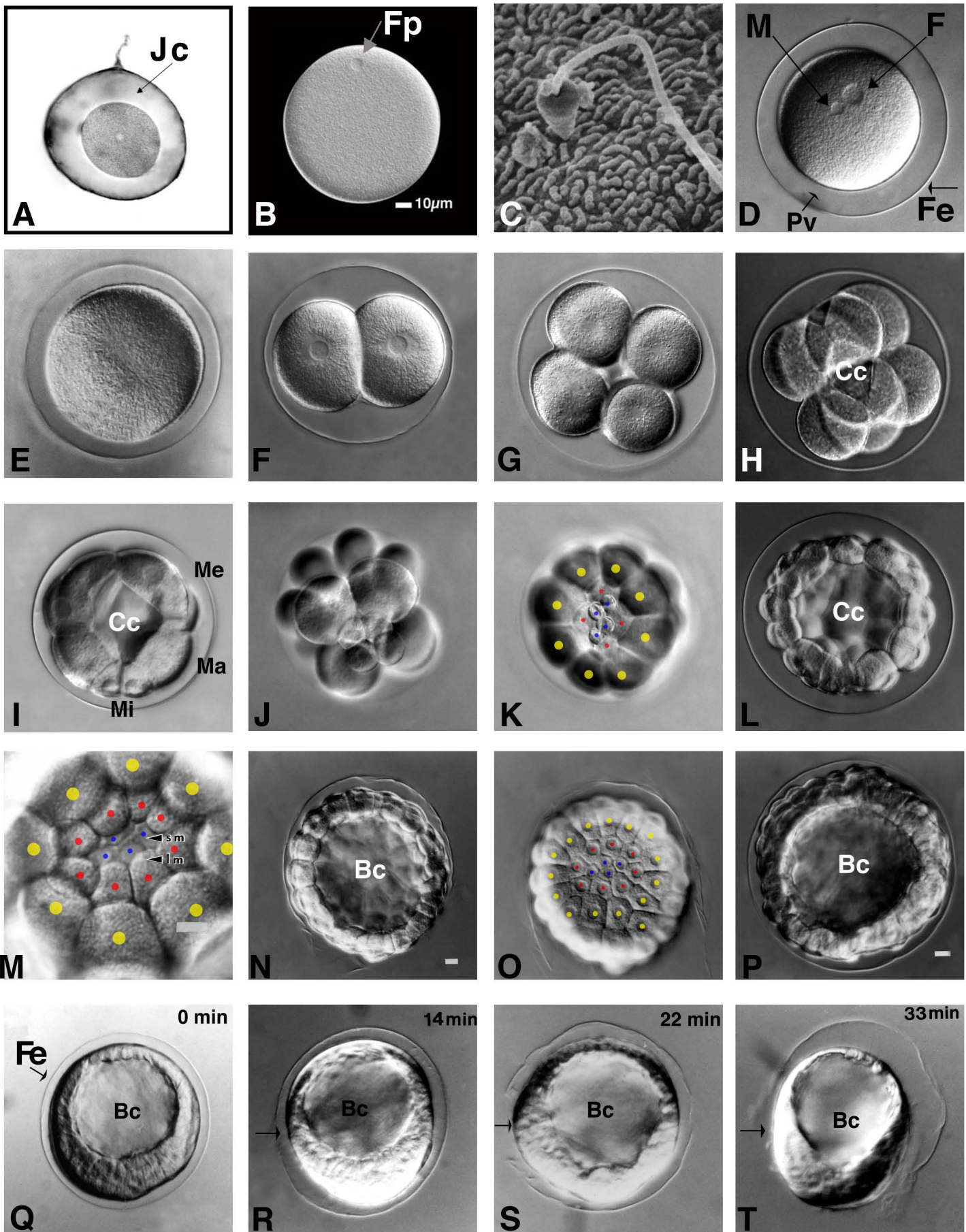


PLATE 2
Unfertilized Egg to PreHatched Blastula; SEM Micrographs

- A. Unfertilized egg without jelly coat
- B. Two-cell stage. Arrow points to hyaline layer across cleavage furrow.
- C. Four-cell stage (lateral view). Cell surface (Cs), area without hyaline layer, (Hl).
- D. Eight-cell stage (lateral view) A, animal pole; V, vegetal pole; arrow, subequatorial cleavage plane results in four large animal hemisphere and four smaller vegetal hemisphere blastomeres.
- E-F. Twelve-cell stage shows the formation of four micromeres (red dots) and four macromeres (yellow dots) before the division of the four animal hemisphere blastomeres (green dots). (E) lateral view. (F) vegetal pole view.
- G-H. Sixteen-cell stage. (G) Lateral view (H) Animal pole view shows arrangement of the eight mesomeres.
- I-J. Twenty-eight cell stage. (I) Oblique lateral view. (J) Vegetal pole view.
- K-L. Thirty-two cell stage. (K) Vegetal pole view. (L) Oblique animal pole view showing arrangement of five of the animal one (An_1) tier of blastomeres.
- M-O. Sixty- Cell stage (7^{th} Cleavage). (M) Lateral view with cells colored to show cell arrangements. Yellow dashed line lies between animal and vegetal hemispheres. (N) Lateral view with vegetal pole up. (O) Vegetal pole view shows arrangements of four small micromeres, four large micromeres, and eight vegetal two macromeres (Veg_2).
- P-Q. 7^{th} Cleavage. (P) Lateral view. (Q) Vegetal pole view with four small micromeres=blue dots, eight large micromeres= red dots, sixteen Veg_1 and sixteen Veg_2 macromeres =yellow dots.
- R-S. 8^{th} Cleavage. (R) Oblique vegetal view. Dashed Line encircles the eight small micromeres, blue dots. (S) Animal pole view of the same embryo showing the arrangement of blastomeres.
- T. 9^{th} Cleavage (5 hours post fertilization) Oblique vegetal view of embryo with torn fertilization envelope. Circles indicate where cilia are forming.

PLATE 2

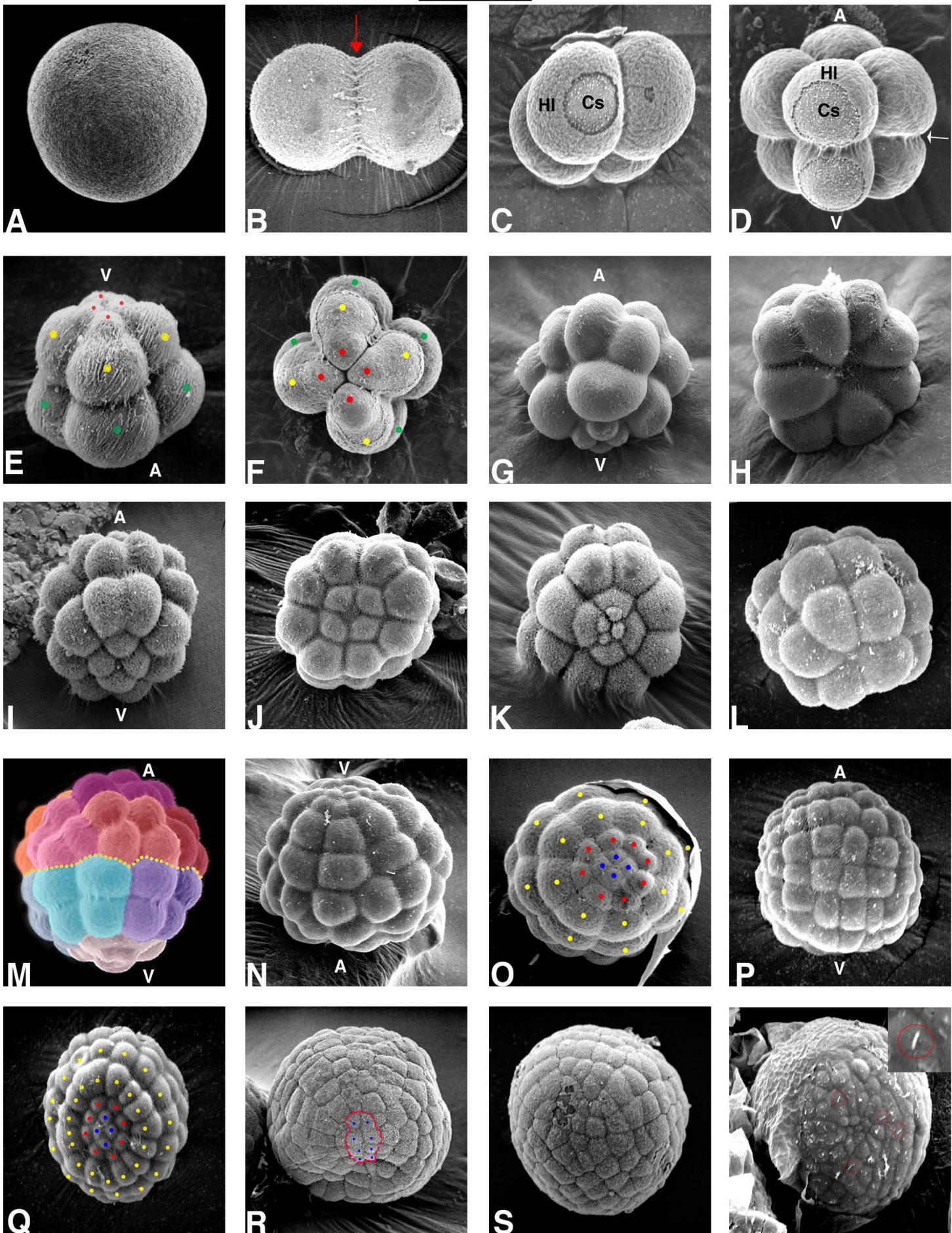


PLATE 3
Hatched Blastula to Prism Larva; Light and SEM Micrographs

- A- Ovoid Hatched Blastula. (A) LM. (B) SEM of dry fractured embryo showing overlapping ectodermal cells along the lateral walls (Okazaki pattern, Op).
- C. Early Mesenchyme Blastula LM of ingressing primary mesenchyme cells (PMCs).
- D. Early Mesenchyme Blastula SEM micrographs of fractured embryo shows ingressing PMCs and patterns of ectodermal cells along the animal-vegetal axis.
- E. LM of late Mesenchyme Blastula with PMCs migrating in blastocoel.
- F. LM of late Mesenchyme Blastula with PMCs migrating along ectodermal wall of vegetal hemisphere.
- G. SEM of fractured late mesenchyme embryo showing migrating PMCs in vegetal hemisphere.
- H-J. SEMs of migrating PMCs. (H) Late Mesenchyme Blastula. (I and J) Early primary invagination of archenteron.
- K. SEM micrograph of early gastrula showing primary invagination of archenteron (A) and Lateral arm (La) of PMC syncytium.
- L. LM of gastrula at end of primary invagination
- M. SEM of gastrula at end of primary invagination of archenteron.
- N. SEM of gastrula beginning of secondary elongation of archenteron.
- O. SEM of mid gastrula- secondary elongation of archenteron.
- P. LM of Late gastrula (oral/ventral view) showing elongated archenteron. Triradiate spicules (arrows) and PMC syncytium.
- Q. LM cross section view of late gastrula. Ab. Aboral side. Or. Oral side. Arrows, spicule centers.
- R. SEM near vegetal pole of late gastrula showing PMC ring of cells and bilateral PMC lateral arms. Or. Oral side. Ab. Aboral side.
- S. SEM of a late gastrula with elongated archenteron and apical cilia acron
- T. SEM of deciliated prism larva showing oral (Or) ectoderm, post oral arm buds (Po) and a bilaterally symmetrical blastopore (B) or (proctodeum).

PLATE 3

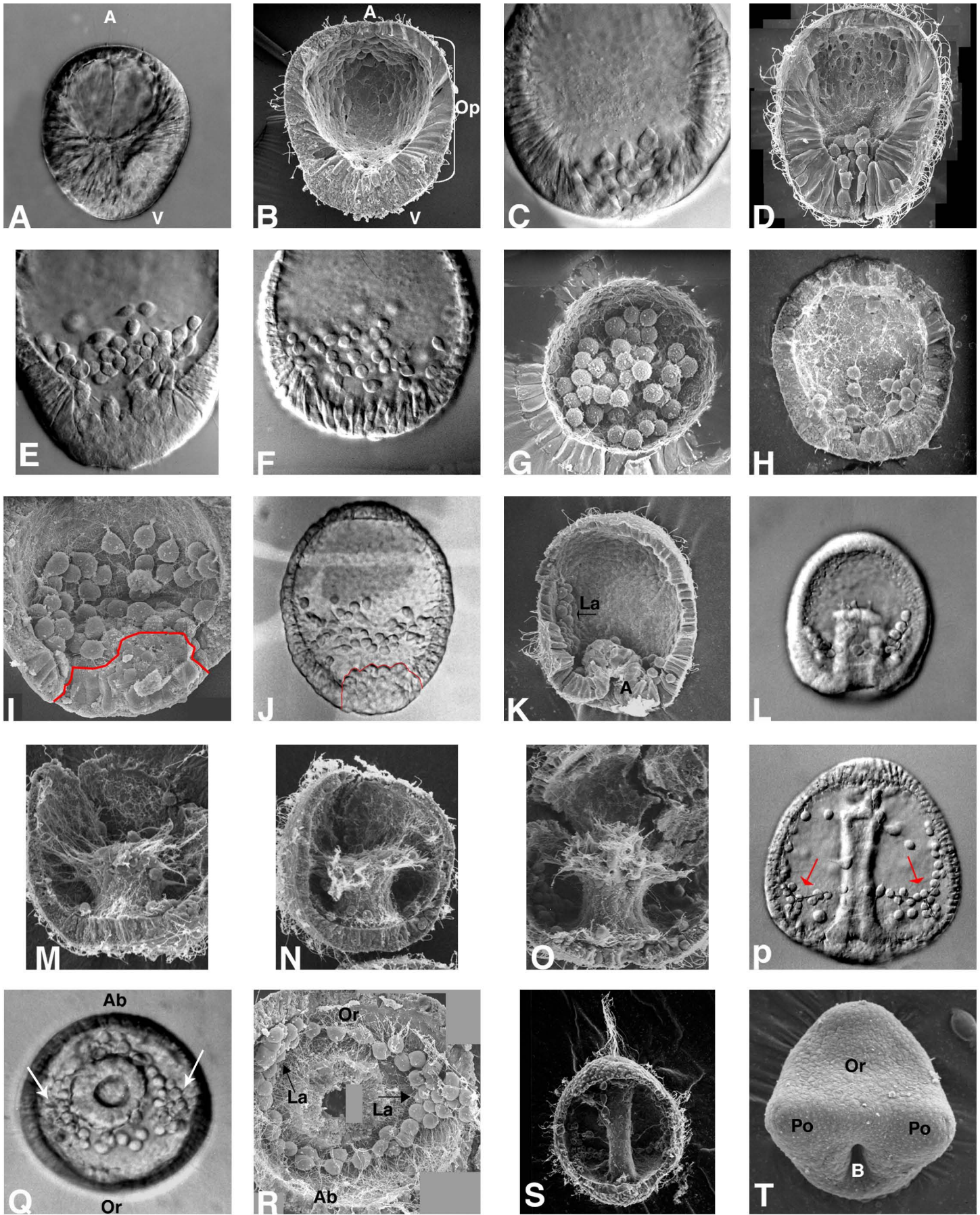
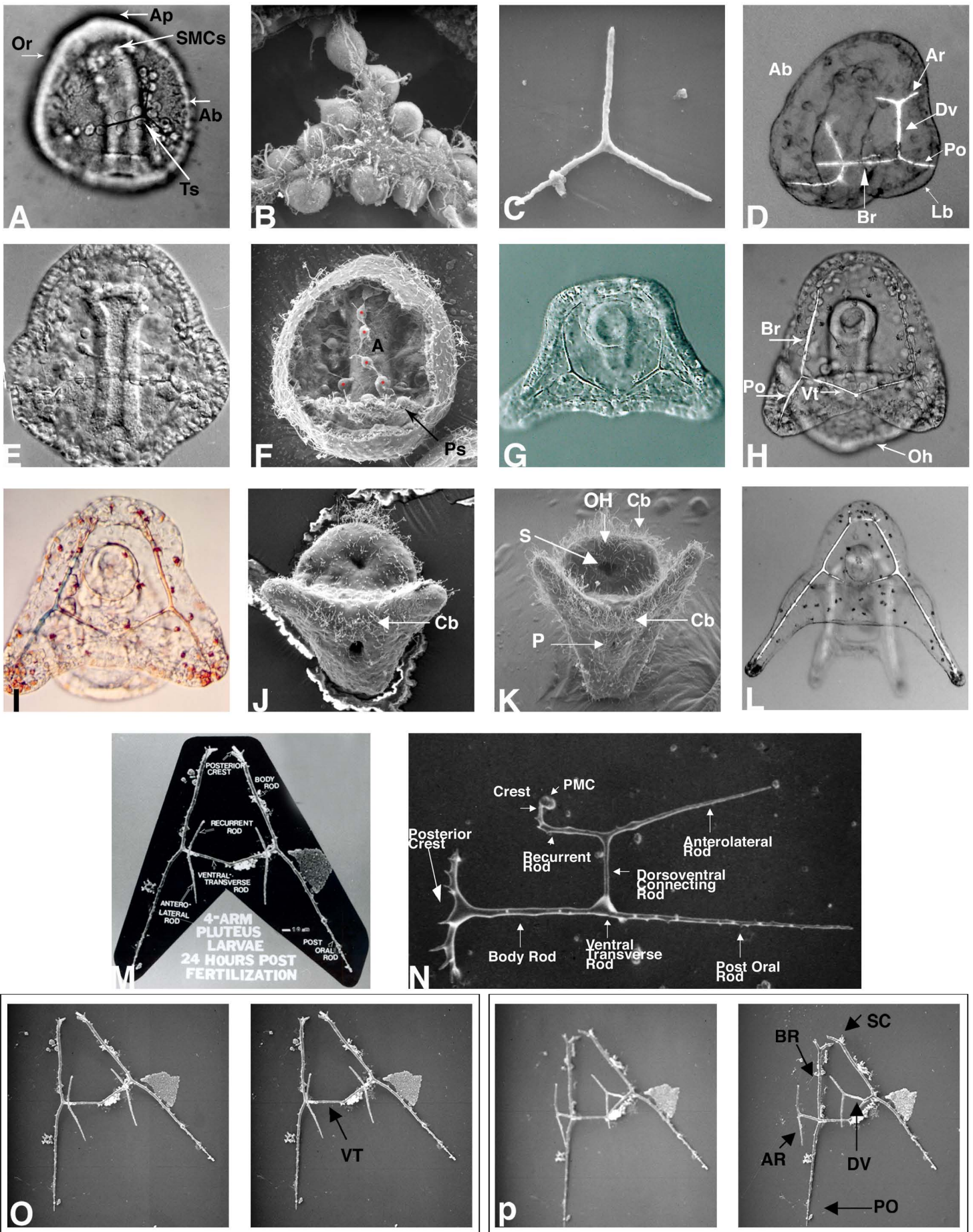


PLATE 4
Prism to Four Arm Pluteus Larva

- A. LM lateral view, early prism larva shows curving archenteron with secondary mesenchyme cells (SMCs) attached to tilted apical plate (Ap). Triradiate spicule (Ts) and PMCs are in focal plane. Or, oral side. Ab, aboral side.
- B. SEM of basal lamina side of PMC syncytium with many anchoring filopodia.
- C. SEM of isolated triradiate spicule of late gastrula, early prism.
- D. LM lateral view of Prism larva with the right half of the branching larval skeleton in focus. Lb, post oral limb bud. Po, postoral rod. Dv, dorsoventral connecting rod. Ar, anterior lateral rod. Br, Body rod. Ab, aboral side.
- E. LM oral side view of compressed prism larva
- F. SEM of fractured prism larva (aboral view). Ps, PMC syncytium. Red dot cells, SMC connective tissue cells migrating along basal lamina surface of archenteron (A).
- G-I. LM of short 2-arm pluteus larvae. (G) Anal plate view of early stage with truncated posterior body. (H) Later stage with rounded posterior body showing ventral transverse rod (Vt), post oral rod (Po), body rod (Br) of larval skeleton, oral hood (Oh). (I) Anal Plate view showing distribution of red echinochrome pigment cells.
- J-K. Two arm pluteus larvae with ciliary band (Cb). S, stomodeum. P, proctodeum. Oh, oral hood.
- L. Four arm pluteus larva (anal side view) showing right and left halves of larval skeleton in polarized light and pigment cells accumulated at the tips of the aboral arms.
- M. SEM of isolated 4-arm pluteus larval skeleton.
- N. SEM of lateral view of one half of 4-arm larval skeleton.
- O. Stereo pair of isolated skeleton in (M). Stage tilt 0°
- P. Stereo pair of isolated skeleton in (M). Stage tilt 40°. Ar, anterior lateral rod. BR, body rod. DV, dorsoventral rod. Po, postoral rod. Rc, recurrent rod. SC, schietel or posterior crest. Vt, ventral transverse rod.

PLATE 4



Section 3:

One Cell Egg

PLATE 5
Unfertilized Egg

- A. Spawning of female gametes induced by KCl injection into body cavity
- B. Immature oocyte with germinal vesicle (Gv) breaking down. Nc, nucleolus.
- C. Mature egg with small female pronucleus (Pn).
- D. Mature egg with jelly coat (Jc) stained with toluidine blue.
- E. Newly shed eggs are separated by invisible jelly coats.
- F. After 30 to 60 minutes in sea water the jelly coats dissolve allowing eggs to come in close contact.
- G. Light micrographs of unfertilized eggs centrifuged 15 min. at 2,000g. Female pronucleus is located at the centripetal (+) pole and the yolk granules near the centrifugal pole (↓).
- H. SEM micrograph of outer surface of the vitelline envelope (4,000 X).
- I. SEM micrograph of outer surface of the vitelline envelope (10,000X). Bar, 10 μ m.
- J. SEM micrograph of outer surface of the vitelline envelope (30,000X). Bar, 1.0 μ m
- K. TEM micrograph of cortical region of unfertilized egg without the vitelline envelope (24,000 X). Mv, microvilli. Cg, cortical granule. Y, yolk. Bar, 1.0 μ m

PLATE 5

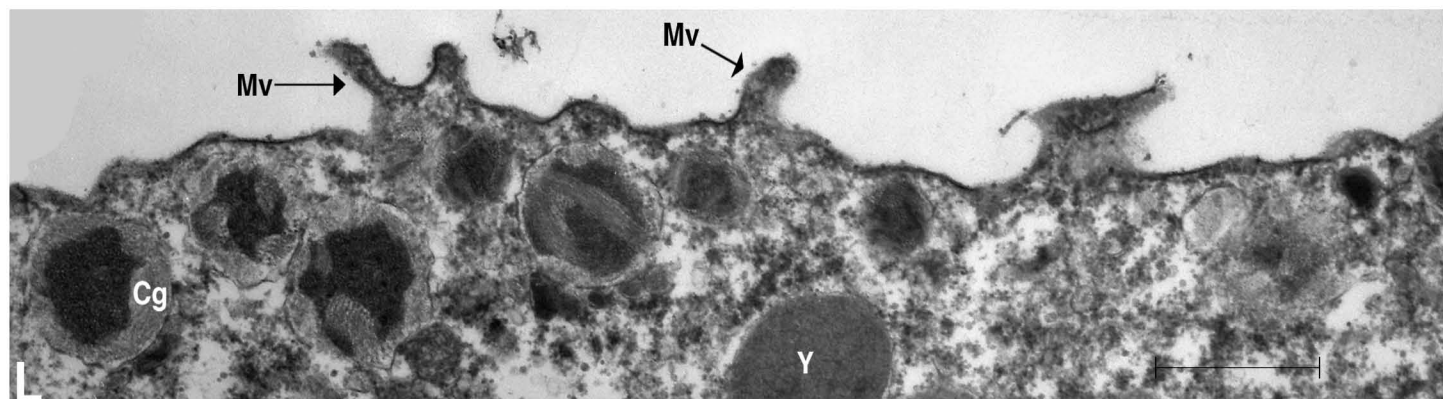
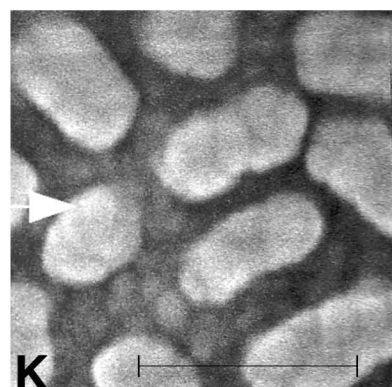
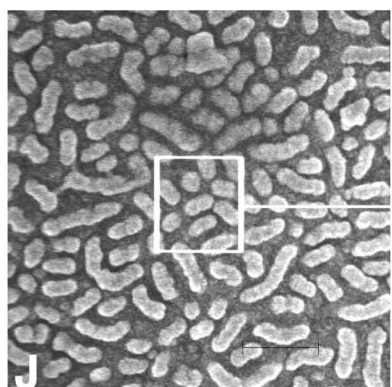
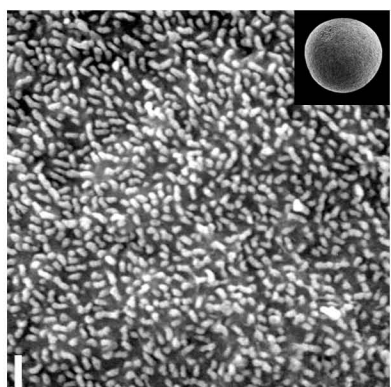
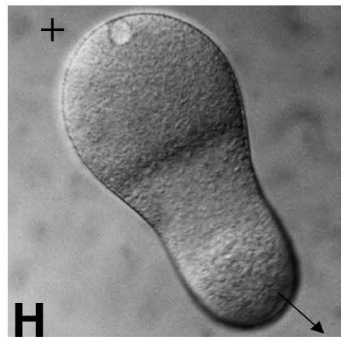
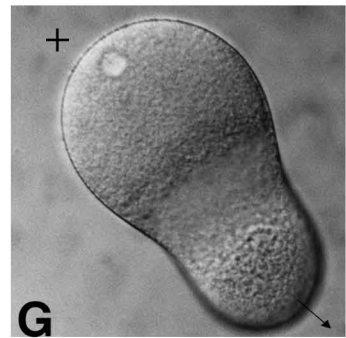
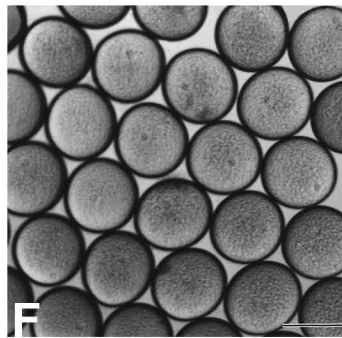
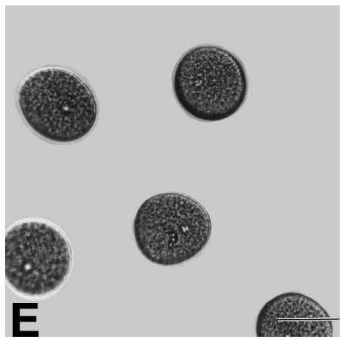
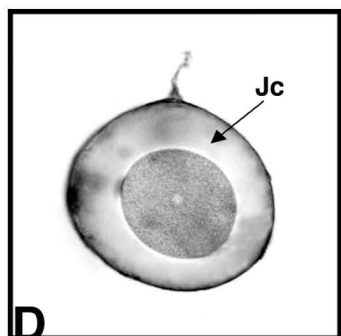
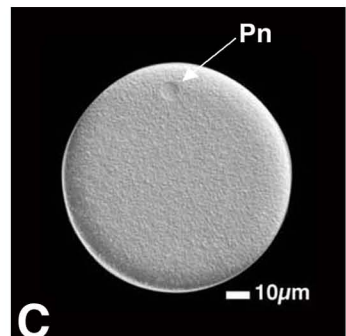
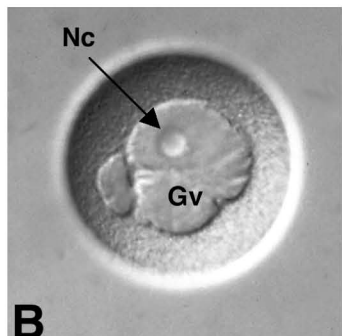
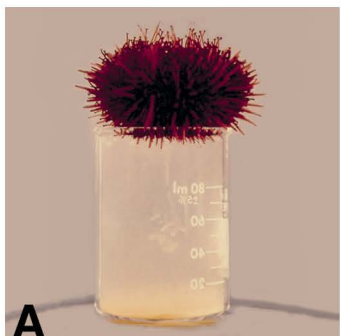
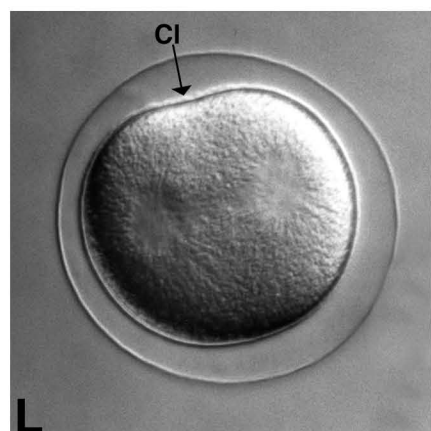
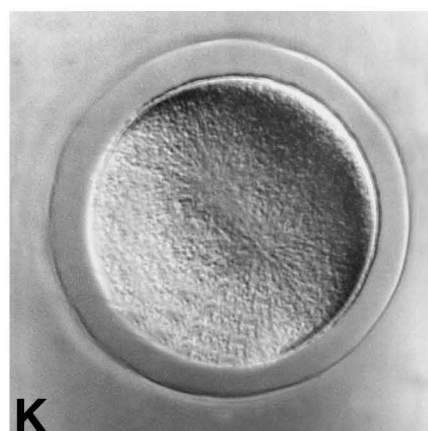
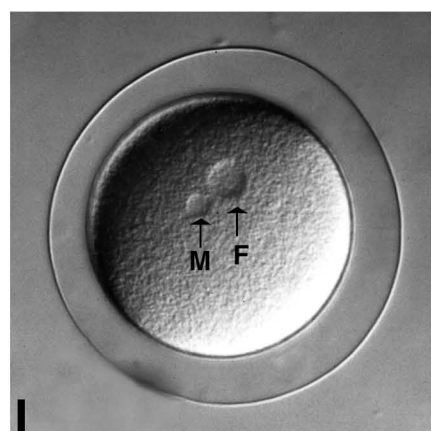
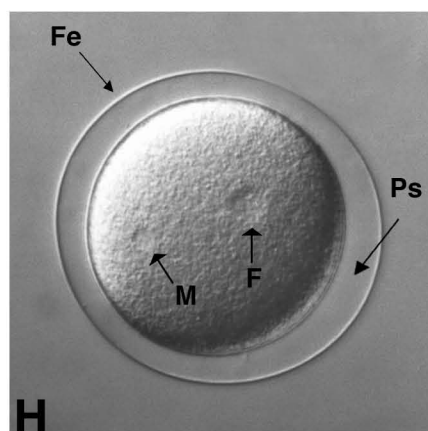
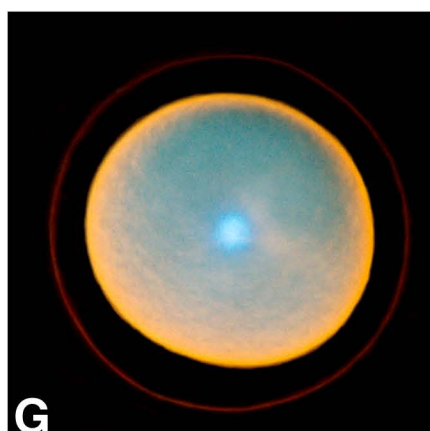
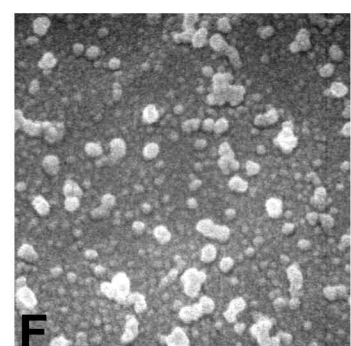
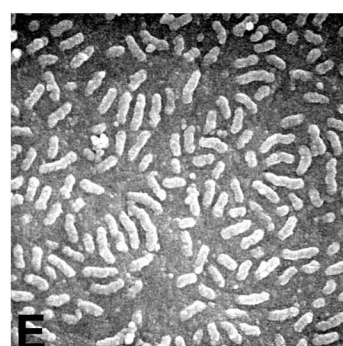
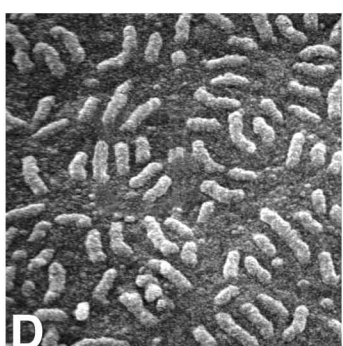
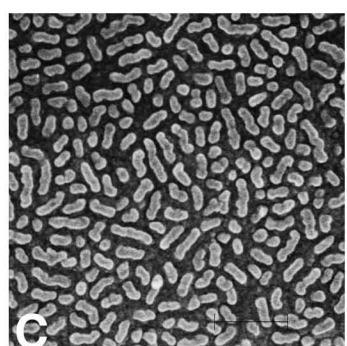
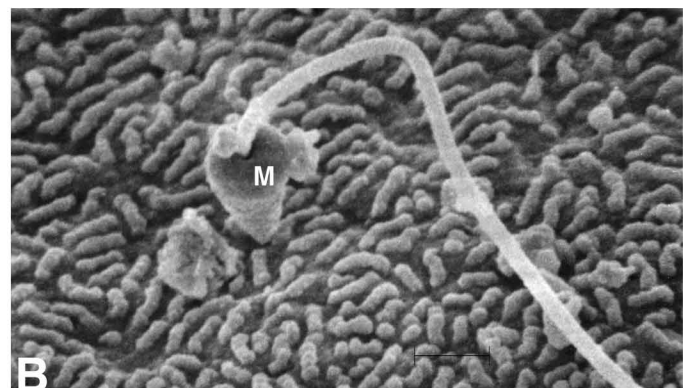
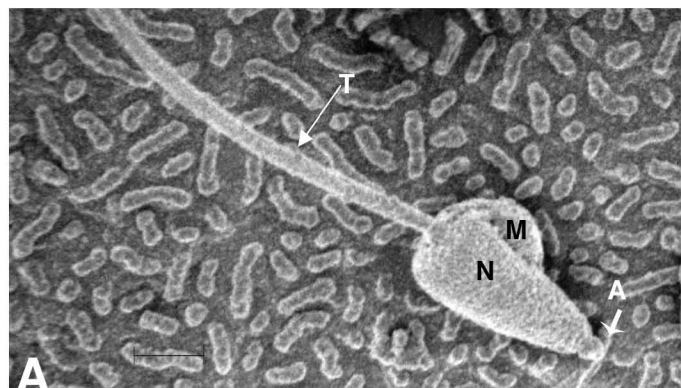


PLATE 6
Fertilization and Post Fertilization Events

- A,B SEM micrographs of sperm attached to outer surface of vitelline envelope of dejellied eggs (10,000 X). A, acrosome. N, nucleus. M, midpiece. T, tail. Bar, 1.0 μ m
- C-F SEM micrographs of densities of vitelline envelope surface protrusions of fertilized egg. (C) 1 second post fertilization. (D, E) 2 minutes post fertilization. (F) 2.5 hours (32-64 cell stage) post fertilization (10,000 X). Bar, 1.0 μ m
- G-M Light micrographs of 1-cell fertilized eggs with fertilization envelopes, and perivitelline space. Following the cortical granule reaction and formation of the fertilization envelope and perivitelline space, the male and female pronuclei migrate toward each other (H, I, J) in the center of the egg. On dissolution of the nuclear envelopes the mitotic apparatus of the first cell division forms and visualized the "streak" stage (K), followed by the nuclear division and interaction of the first cleavage furrow (L). Fe, fertilization envelope. Ps, perinuclear space. M, male pronucleus. F, female pronucleus. Cl, cleavage furrow initiated.

PLATE 6



Section 4:

First Cleavage to Pre-Hatched Blastula (5.5 hr. post fertilization)

PLATE 7

First Cleavage

2-Cell Stage

- A-F. Light micrographs of sequential phases of cell shapes and nuclei from initiation of the first cleavage furrow (A) to the metaphase spindles (F) in the late 2-cell stage embryo. Ms, metaphase chromosomes.
- G-L. SEM micrographs of microvilli and surfaces of blastomeres of embryos in which the fertilization envelope and hyaline layer were removed by treating eggs with 1.0M urea for 10 minutes post fertilization and subsequently cultured in calcium free sea water.

PLATE 7

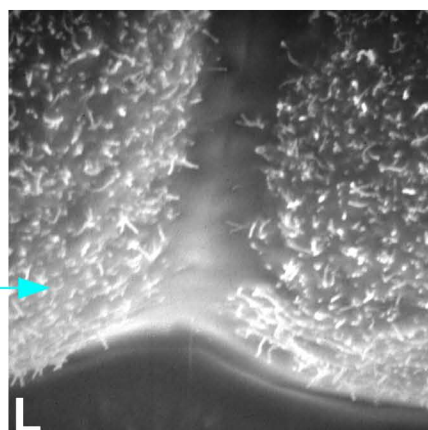
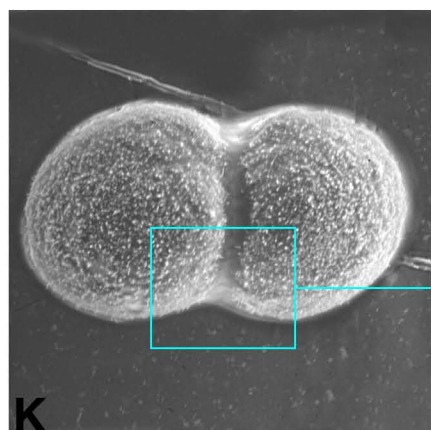
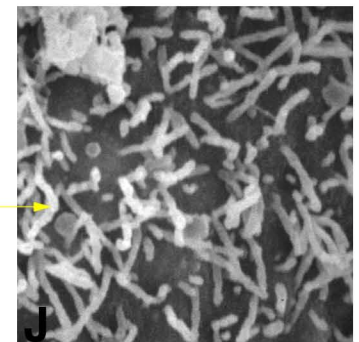
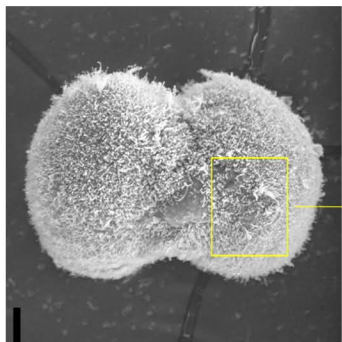
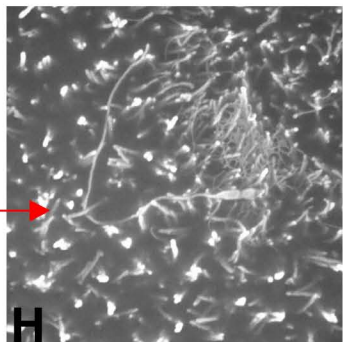
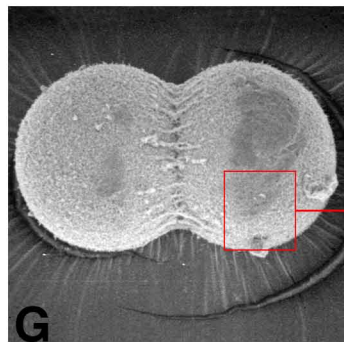
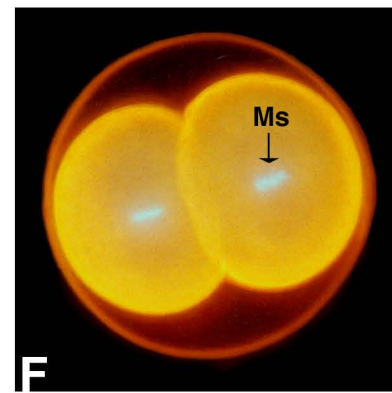
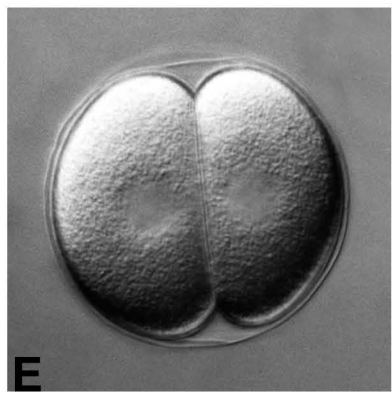
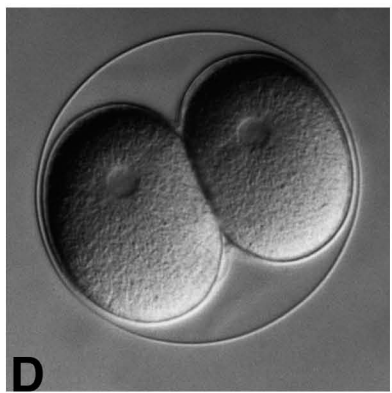
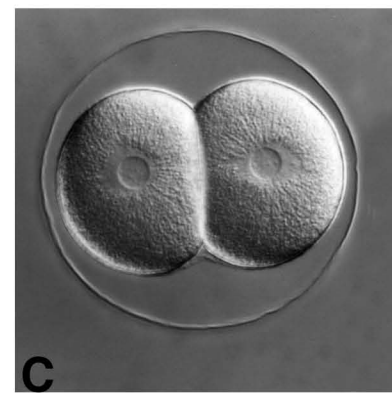
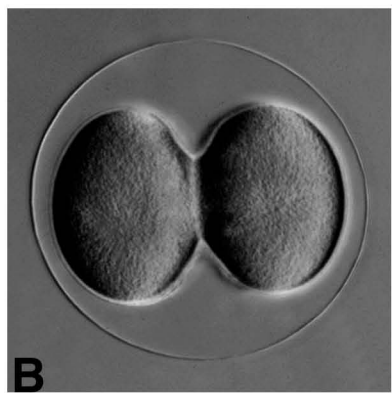
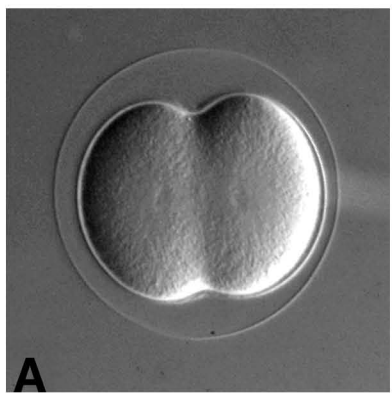


PLATE 8

Second Cleavage

4-Cell Stage

- A Light micrograph of initiation of second cleavage furrow (arrow).
- B Light micrograph of initiation of second cleavage showing asters (A) of three blastomeres.
- C Light micrograph of polar view of 4-cell embryo without a fertilization envelope. Cc, cleavage cavity.
- D Light micrograph of late 4-cell embryo with nuclei entering prophase of third cell division.
- E Light micrograph of 4-cell embryo with nuclei stained with Hoechst 2385.
- F SEM micrograph (lateral view) of 4-cell embryo with a hyaline layer.
- G SEM micrograph of 4-cell embryo with hyaline layer removed.
- H SEM micrograph of microvilli in G (10,000 X). Bar, 1.0 μ m.
- I SEM micrograph of dry fractured 4-cell embryo showing cleavage cavity cell surface of one blastomere, the cleavage furrow and the constriction of the hyaline layer in the furrow region (1,000 X). Bar, 1.0 μ m.
- J Cleavage furrow area enlarged shows numerous microvilli (5,000X). Bar, 1.0 μ m.
- K Boxed area in J at 10,000 X shows the microvilli are 1.0 to 1.5 μ m long. Bar, 1.0 μ m.

PLATE 8

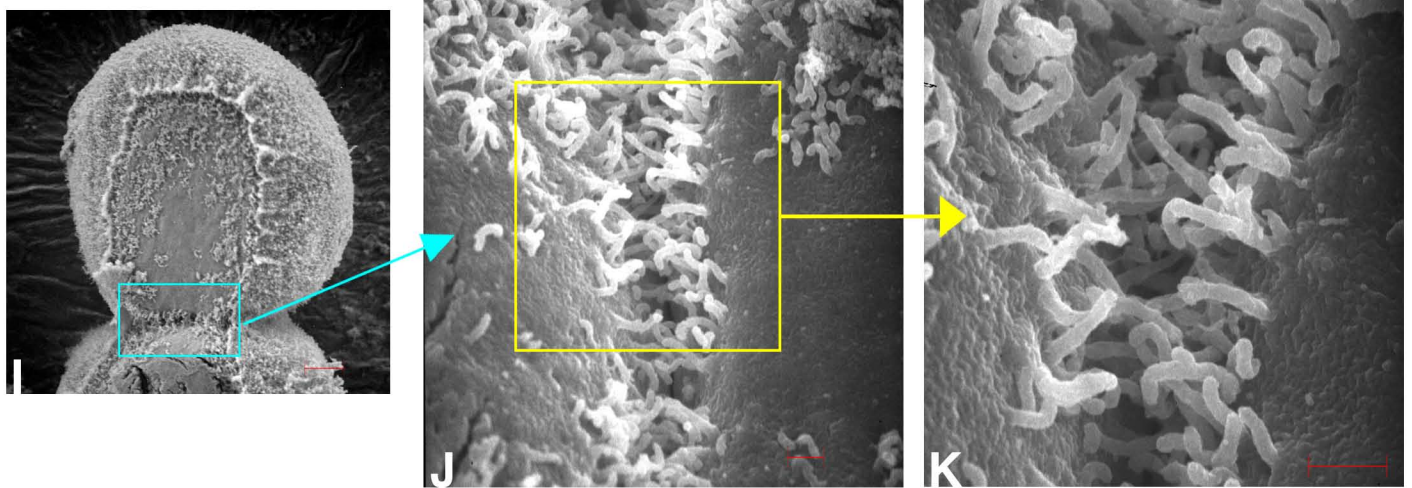
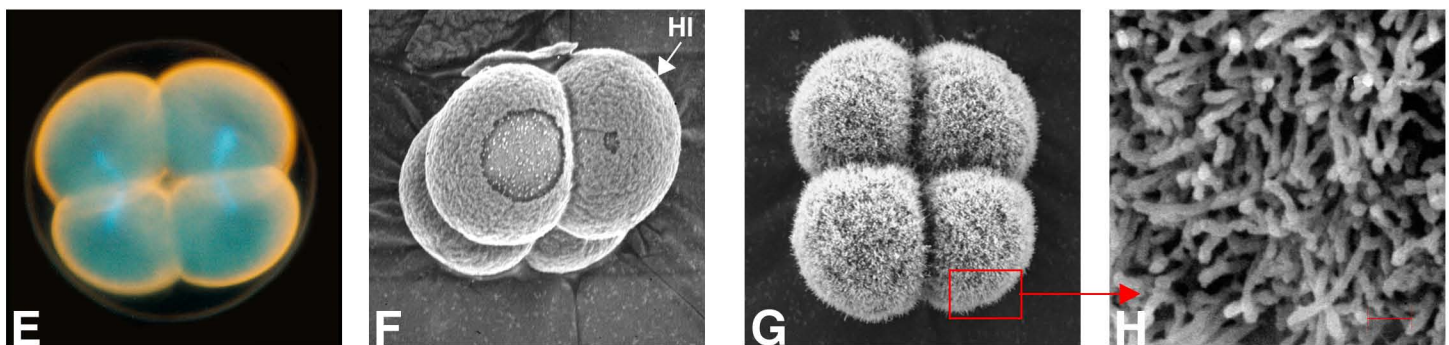
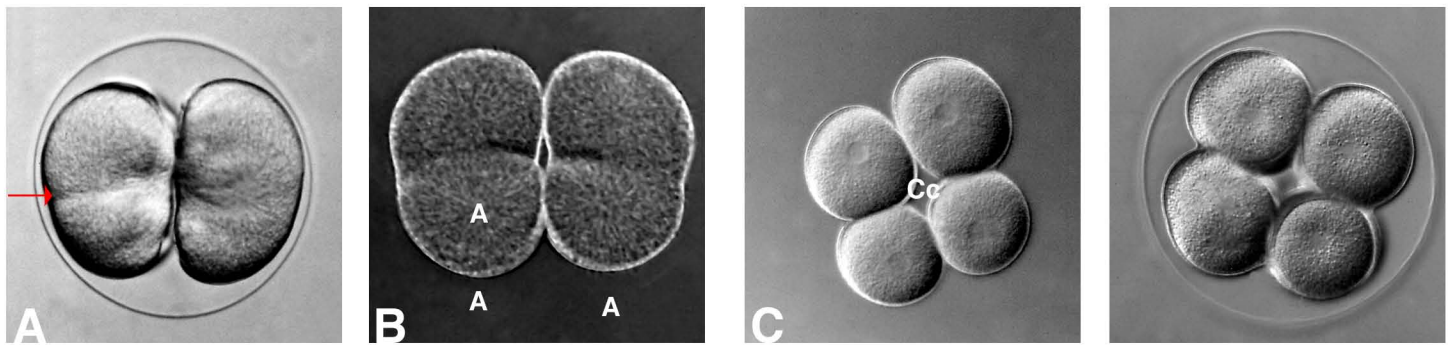


PLATE 9

Third Cleavage

8 and 12 Cell Stages

- A. Lateral view of eight cell stage showing cleavage cavity (Cc).
- B. Vegetal polar view of embryo where the third cleavage plane was subequatorial resulting in four smaller vegetal hemisphere blastomeres.
- C. SEM (lateral view) of embryo with subequatorial third cleavage plane. Blastomeres are covered with hyaline layer except where it was plucked off two blastomeres.
- D. SEM of 8-cell embryo fractured along the animal-vegetal axis. Cc, cleavage cavity.
- E. SEM of 8-cell embryo (freeze substituted fixation, or FSF) showing subequatorial third cleavage.
- F. Image (2,000 X) of boxed area in E shows fixation artifact of hyaline layer resulting from FSF. Bar, 1.0 μ m.
- G. SEM of fractured 8-cell embryo
- H. Image (4,000X) of boxed area in G shows numerous microvilli in cleavage furrow area. Bar, 0.1 μ m.
- I. SEM of 12-cell stage with vegetal blastomeres dividing unequally to form four micromeres and four macromeres. The four animal hemisphere cells have not begun to divide. Mi, micromeres. Ma, macromeres. Me, mesomeres. A, animal pole. V, vegetal pole.
- J. Stereo pair SEM of 12-cell stage (vegetal pole view) shows vegetal hemisphere blastomeres divide before animal hemisphere blastomeres. The hyaline layer is plucked off the presumptive micromeres and macromeres.

PLATE 9

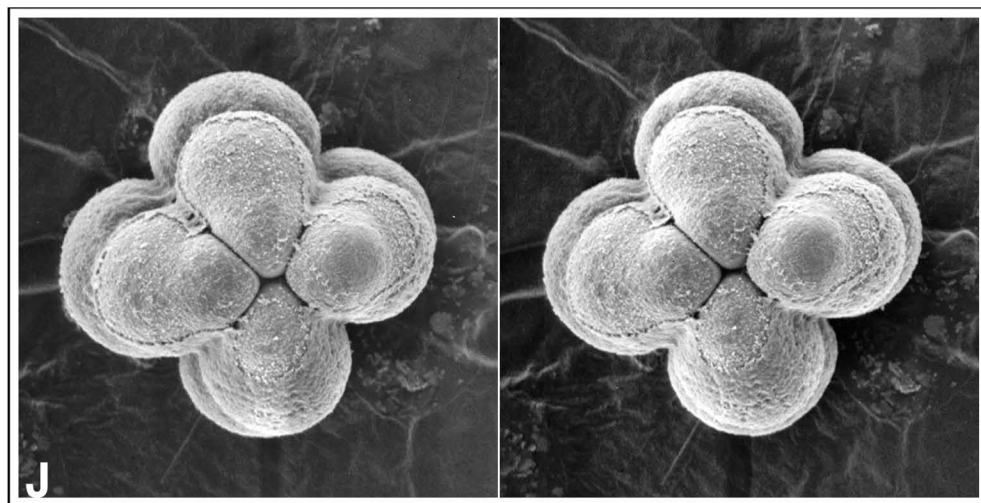
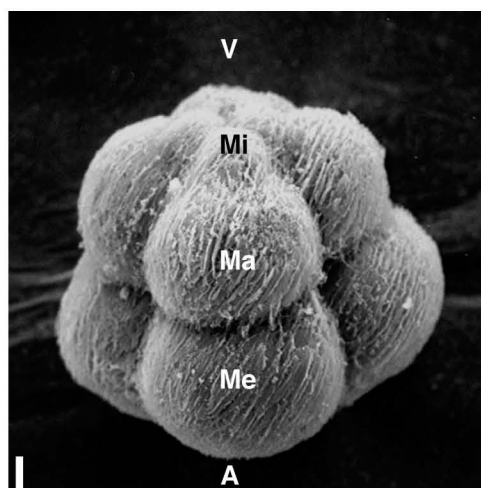
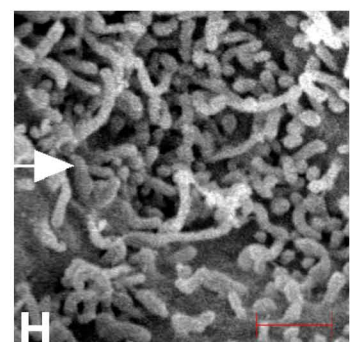
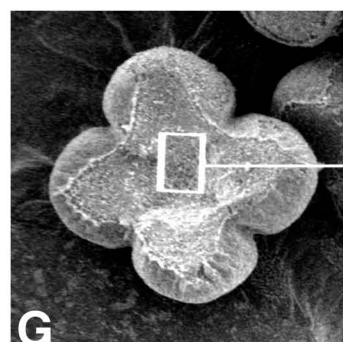
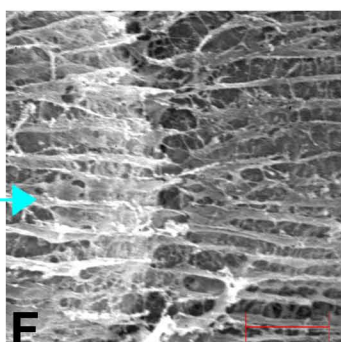
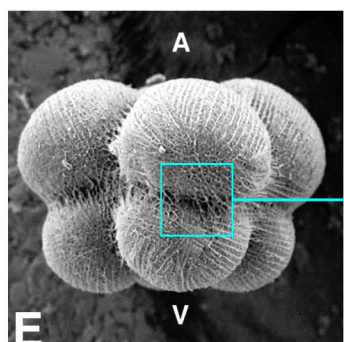
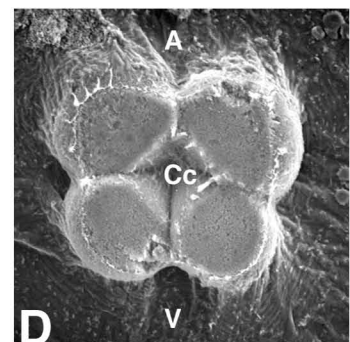
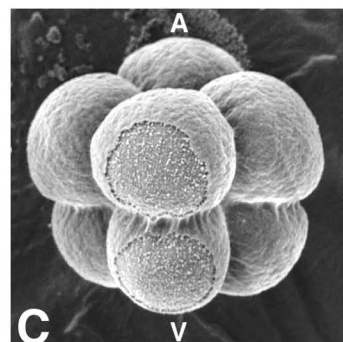
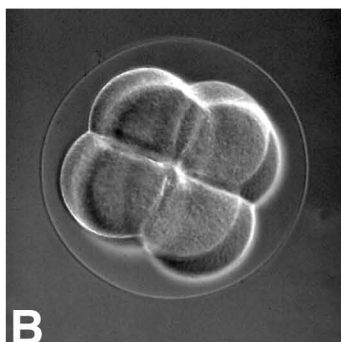
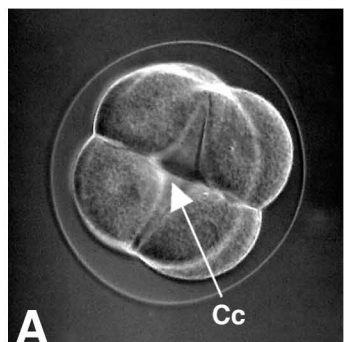


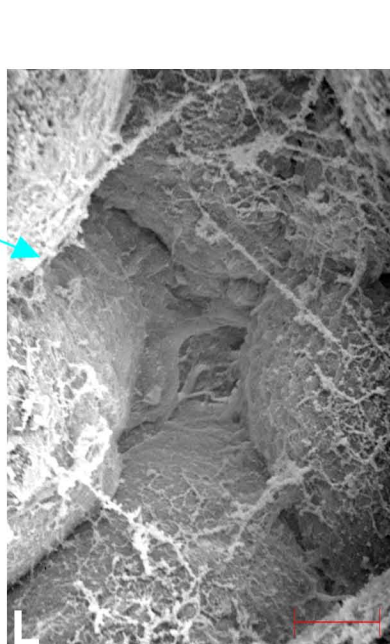
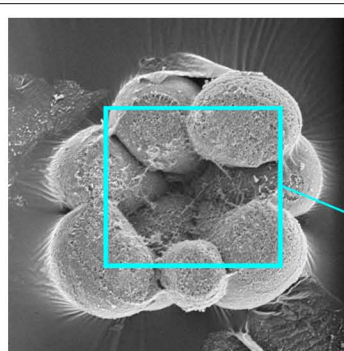
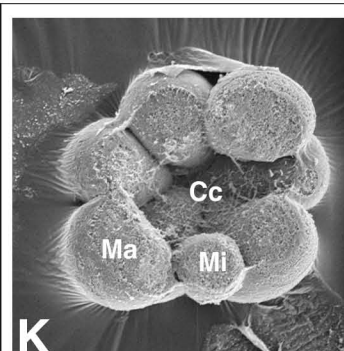
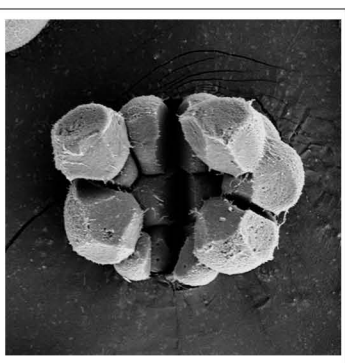
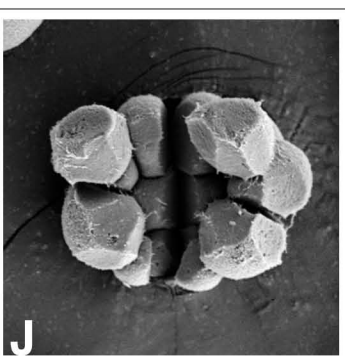
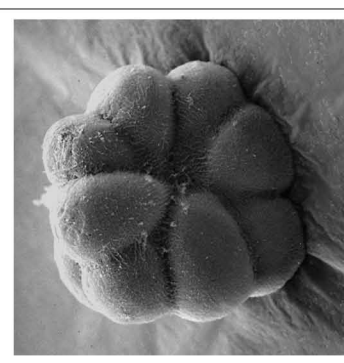
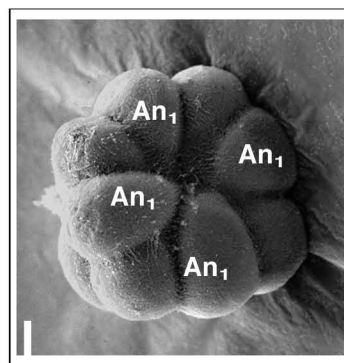
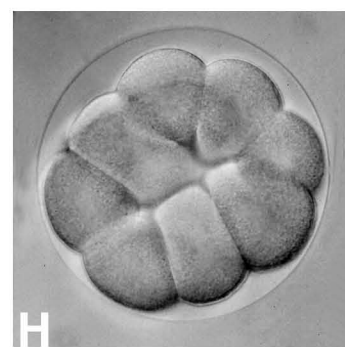
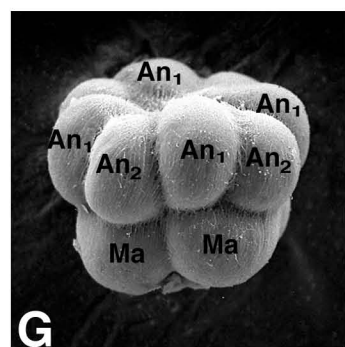
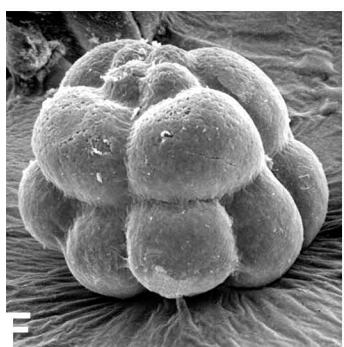
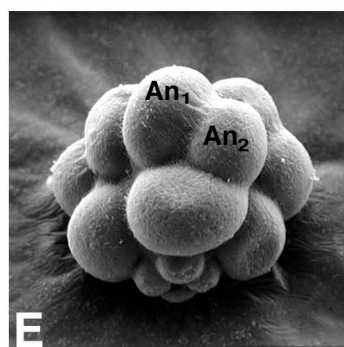
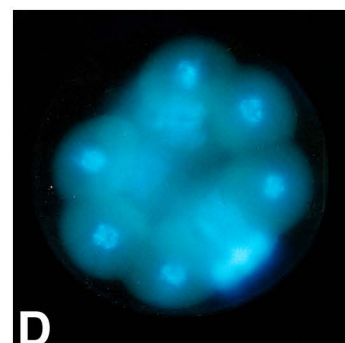
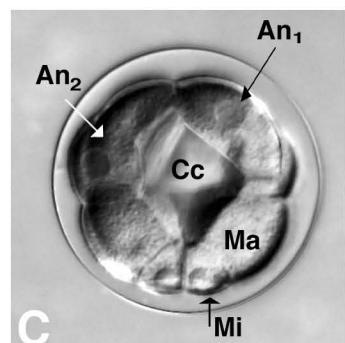
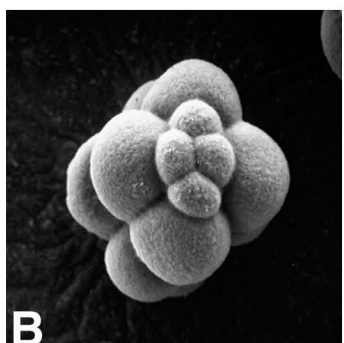
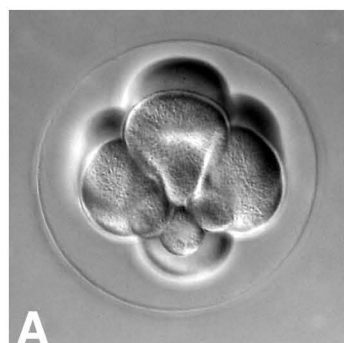
PLATE 10

Fourth Cleavage

16-Cell Stage

- A. Fourth cleavage. Vegetal blastomeres dividing unequally to form four micromeres and four macromeres.
- B. SEM of 16-cell stage embryo (vegetal pole view).
- C. Lateral view of 16-cell stage embryo with large cleavage cavity. Cc, cleavage cavity. An₁, animal 1 tier of mesomeres. An₂, animal 2 tier of mesomeres. Ma, macromeres. Mi, micromeres.
- D. Fluorescent image of Hoechst 2385 stained nuclei.
- E. SEM (lateral view) of 16-cell embryo tilted to show an An₁ and An₂ pair of mesomeres.
- F. SEM (lateral view) of 16-cell embryo with vegetal pole up.
- G. SEM (lateral view) of 16-cell embryo shows arrangements of An₁ and An₂ tiers of mesomeres.
- H. Light micrograph, animal pole view of 16-cell embryo.
- I. SEM stereo pair of arrangement of An₁ and An₂ tiers of mesomeres (animal pole view).
- J. SEM stereo pair of fractured 16-cell embryo shows the polygonal shapes of the blastomeres after blastomere compaction.
- K. SEM stereo pair of 16-cell embryo before blastomere compaction. Cc, cleavage cavity. Ma, macromere. Mi, micromere.
- L. SEM of enlarged view of fiberous, extracellular matrix (ECM) preserved after gluteraldehyde-osmium fixation. Bar, 10µm.
- M. SEM stereo pair micrographs of 16 cell embryo showing preservation of cleavage cavity ECM with Osmium FSF.

PLATE 10



10 μm

PLATE 11

Fifth Cleavage

28 and 32-Cell Stages

- A. Fluorescent image of nuclei of 28-cell stage embryo showing arrangement of the eight macromeres and metaphase plates of the four micromeres.
- B. SEM micrograph of the vegetal pole showing macromeres (Ma) and micromeres (Mi).
- C. Stereo pair SEM micrographs of 28-cell stage embryo
- D, E. Images of 29 - cell embryos. One micromere has divided unequally to form small (blue dot) and large (red dot) micromeres. Macromeres, yellow dots.
- F, G. Thirty-two cell stage embryos. Blue dots, small micromeres. Red dots, large micromeres. Yellow dots, macromeres.
- H. SEM of 32-cell stage embryo with hyaline layer removed.
- I. Stereopair SEM of boxed area in H show dense arrays of microvilli in blastomeres and in cleavage furrows.
- J. SEM of 32-cell embryo shows relative sizes of small and large micromeres and tier of eight macromeres.
- K. Light micrograph of a thick section of a thirty-two cell stage embryo shows arrangements and sizes of the two tiers of mesomeres, the macromeres, and large and small micromeres. An₁, animal 1 tier mesomere. An₂, animal 2 tier mesomere. Ma, macromere. Lm, large macromere. Sm, small micromere. Cc, cleavage cavity.
- L. DIC light micrograph of a thick section of a 32-cell stage embryo freeze substitute fixation (FSF) shows the preservation of the cleavage cavity (Cc) extracellular matrix (ECM).
- M. Stereo pair SEM of vegetal pole view of a 32-cell stage embryo.
- N. Stereo pair SEM of a fractured post 32-cell stage embryo shows the blastomeres are connected by many “processes.” A, animal pole.
- O. Boxed area in N at higher magnification. Bar, 1µm.

PLATE 11

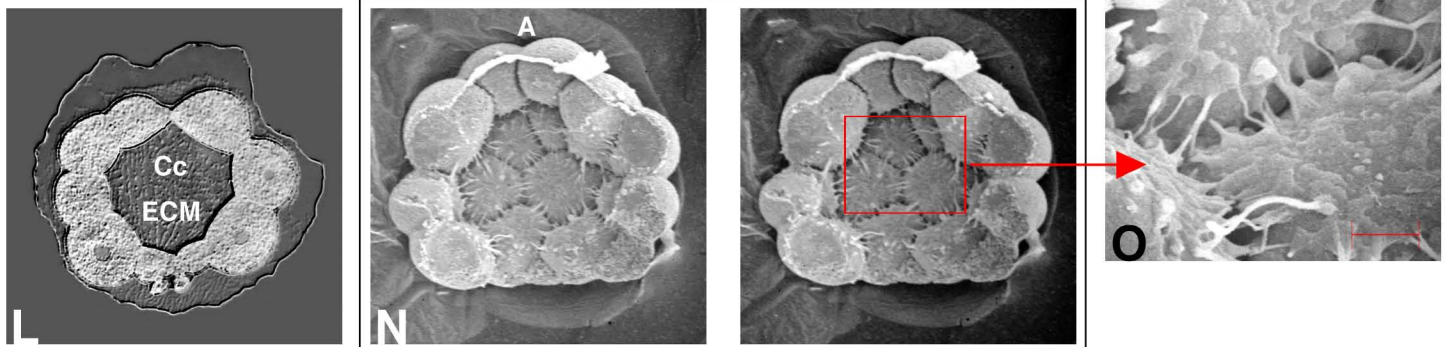
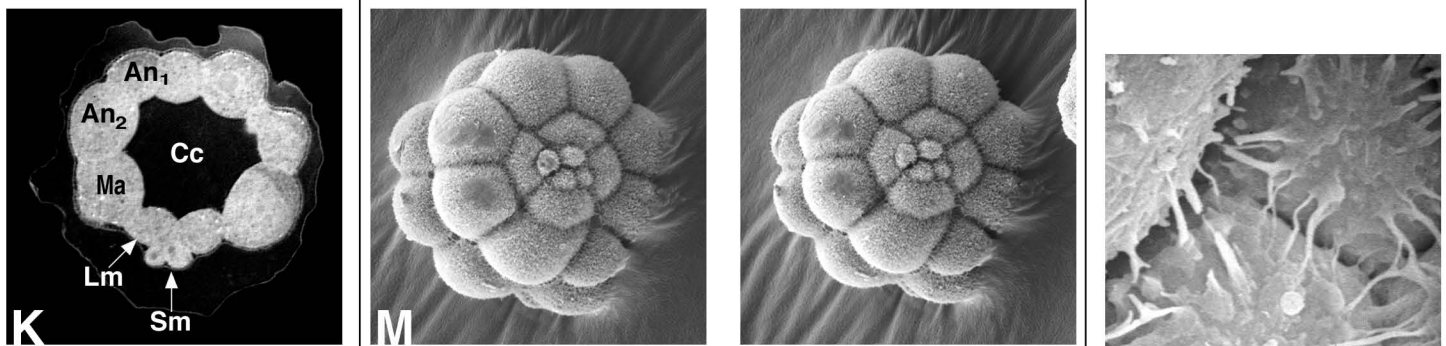
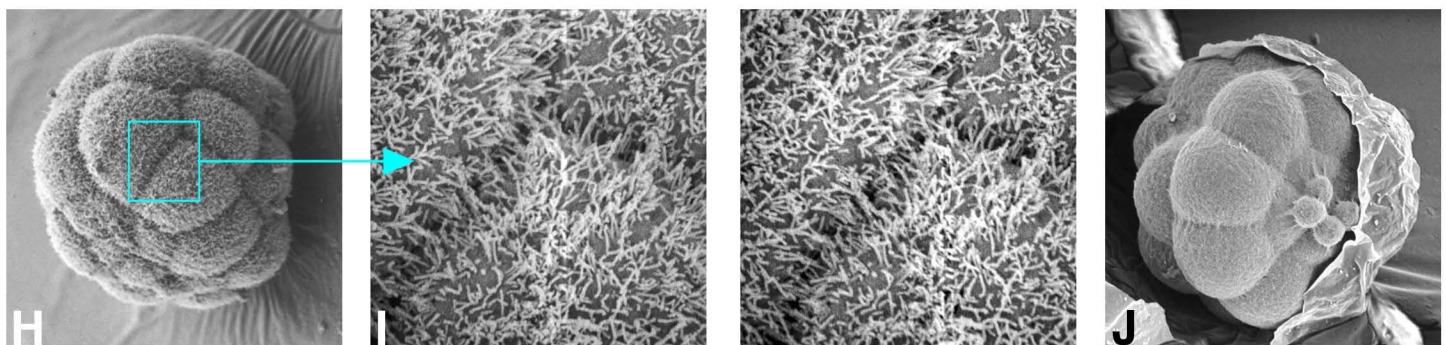
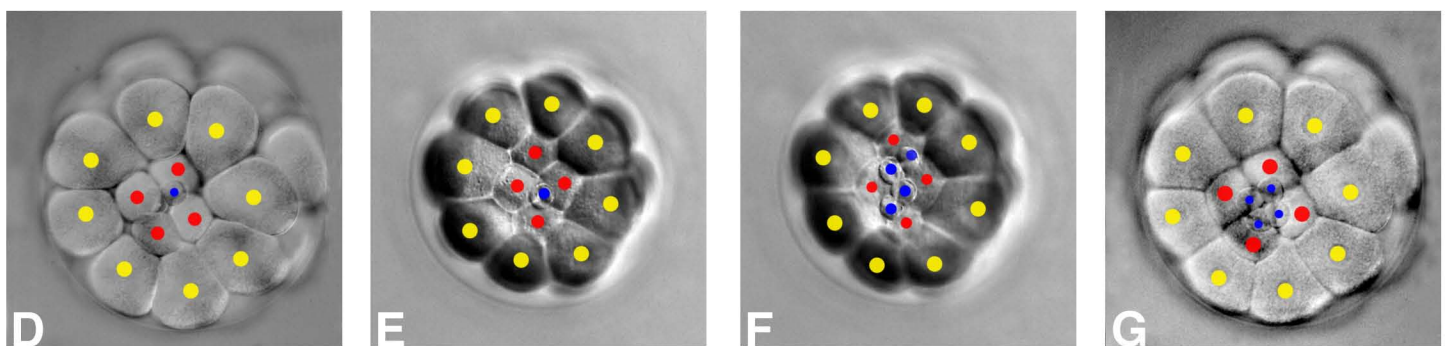
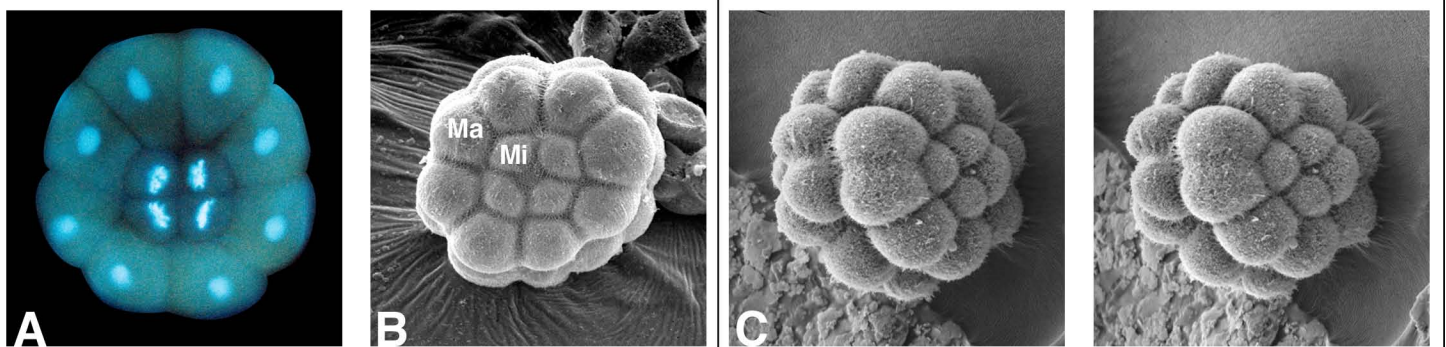


PLATE 12

Sixth Cleavage

60-Cell Stage

- A. Vegetal pole view of sixth cleavage stage egg showing nuclei of macromeres and mesomeres dividing and interphase nuclei of the four central small micromeres and four large micromeres.
- B. Lateral view of DIC light micrograph of a 56-cell stage embryo.
- C. SEM of a 56-cell stage embryo.
- D. False colored SEM of a 56-cell stage embryo. Yellow dashed line marks interface of mesomeres and macromeres.
- E-H. Parasynchronous division of nuclei of large micromeres during 6th cleavage cycle (vegetal pole view).
- I. Vegetal pole view of 60-cell stage embryo showing four small micromere nuclei surrounded by eight large micromere nuclei.
- J. Stereopair SEM of vegetal pole of a 60-cell stage embryo.
- K. SEM of 60-cell stage embryo (lateral view).
- L. SEM of fractured 60-cell stage showing cleavage cavity sides of blastomeres. Small white arrows, intercellular connections.
- M. Enlarged boxed area in L. Bar, 10 μm .
- N. Enlarged boxed area in M shows connection processes between cells. Bar, 0.1 μm .
- O. Light micrograph of thick section of resin embedded 60-cell stage embryo (glutaraldehyde-osmium fixative) shows cleavage cavity (Cc). Extracellular matrix not visible. A, animal pole. V, vegetal pole.
- P. Light micrograph of thick section of resin embedded 60-cell stage embryo (FSF fixation) shows preservation of cleavage cavity and perivitelline space extracellular matrices. A, animal pole. V, vegetal pole. Fe, fertilization envelope. Pv, perivitelline space.
- Q. SEM micrograph of vegetal pole of a fractured 60-cell stage embryo shows the four small micromeres surrounded by the eight large micromeres.
- R. Boxed area in Q enlarged to show the four micromeres and cytoplasmic protrusions (arrows) of the large micromeres.

PLATE 12

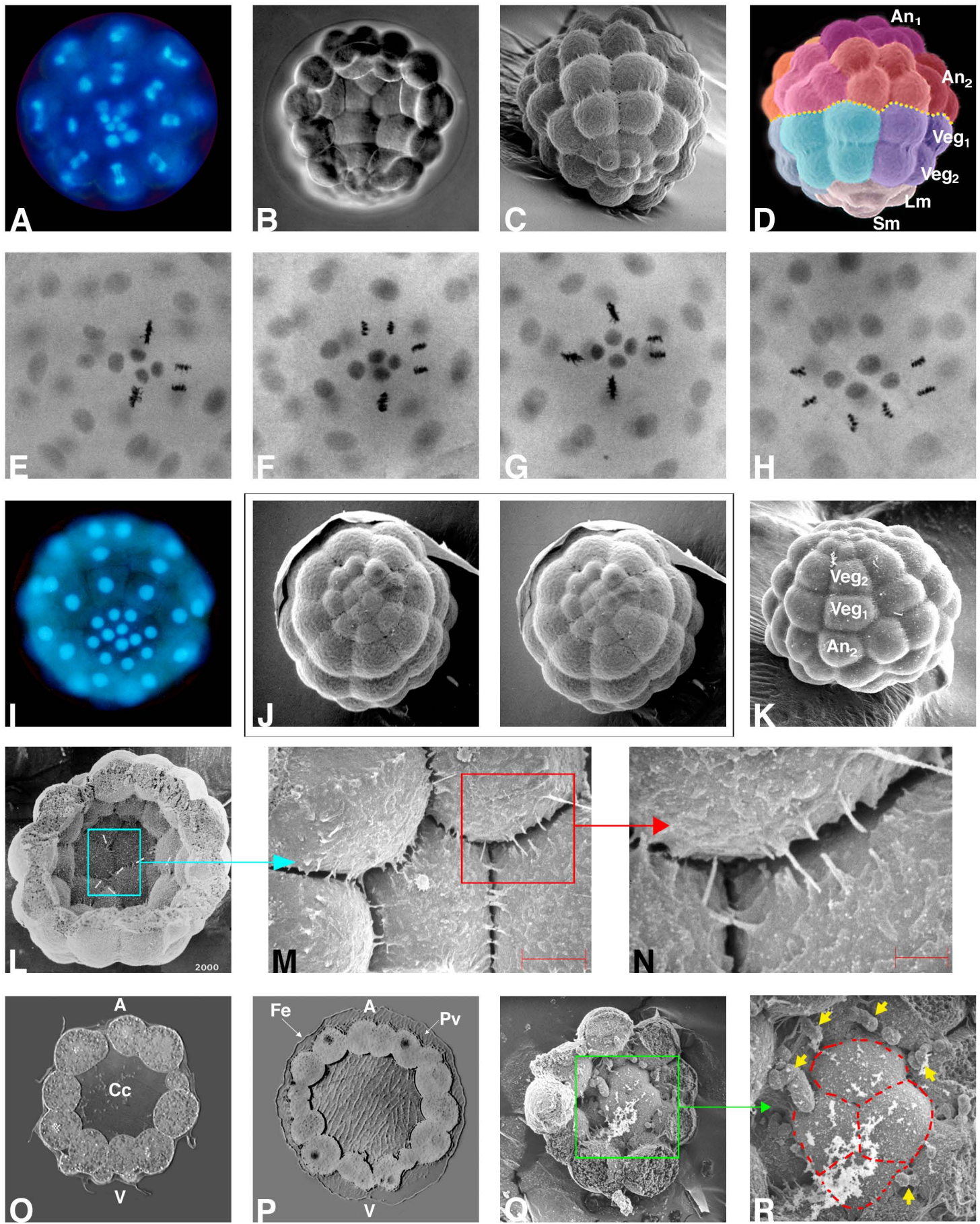


PLATE 13

Seventh Cleavage

Early Blastula

- A. Light micrograph of 7th cleavage embryo (lateral view).
- B. Light micrograph of vegetal pole of early 7th cleavage with four small micromeres and eight large micromeres surrounded by 14 Veg₂ macromeres.
- C-F. Four diagrams show the parasynchronous division of the large micromeres (Lm) during 7th cleavage.
 - C) All shaded Lms are in interphase at 3:30 post fertilization (pf). D) Four Lms (dotted) begin mitosis at 3:40 pf.. E) Dotted Lms have cleaved; shaded Lms have begun mitoses at 3:45 Pf. F) At end of 7th cleavage (3:50 pf) all Lms have cleaved to form two tiers of cells surrounding the four small micromeres.
- G. Fluorescent image of nuclei at the vegetal end of an embryo early 7th cleavage. Macromeres undergoing mitosis.
- H. Fluorescent image of nuclei of a 7th cleavage embryo shows orientations of anaphase spindles of the vegetal 1 and 2 tiers of macromeres and animal 2 tier of mesomeres.
- I-J. Stereo confocal scanning laser micrographs of nuclei of an early seventh cleavage embryo (3:24 hrs p.f.). I) Vegetal hemisphere view of micromeres and the two tiers of macromeres in anaphase. K) Animal hemisphere view of mesomeres with a dashed line marking the anaphase spindles along what maybe the interface between the future oral-aboral ectodermal regions.
- K-L. Stereocon stereographs of nuclei in vegetal (K) and animal (L) hemispheres of figures I and J. Pink, micromere nuclei. Blue, macromere nuclei. Green, mesomere nuclei.
- M. Stereo pair SEM of 7th cleavage, 96-cell stage embryo before division of micromeres (vegetal pole view).
- N. SEM of 7th cleavage stage embryo (lateral view).
- O. SEM of animal pole view of embryo in figure N shows arrangements of fifteen blastomeres (pink dots) derived from the four An₁₁ tier of cells at the 32-cell stage.

PLATE 13

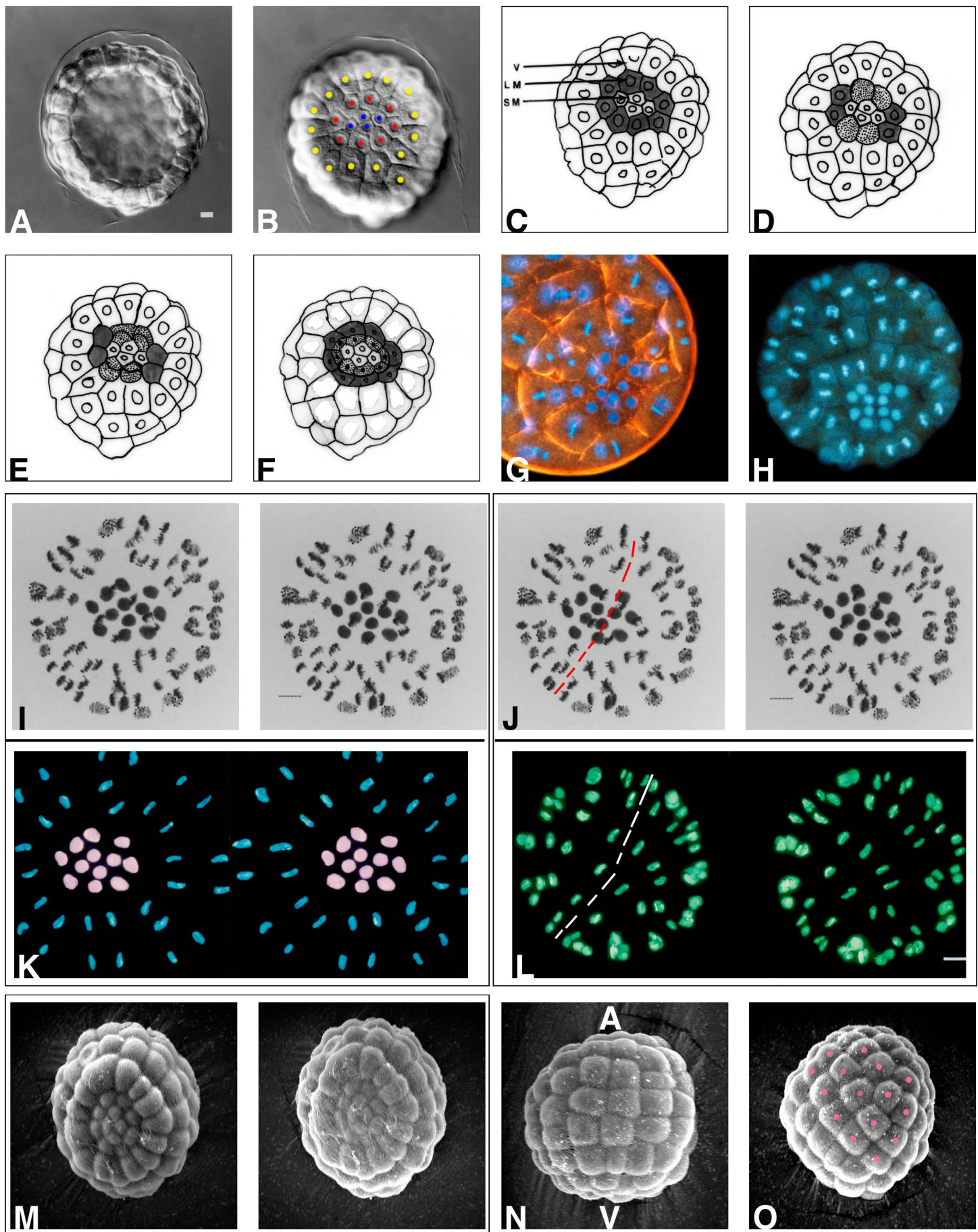
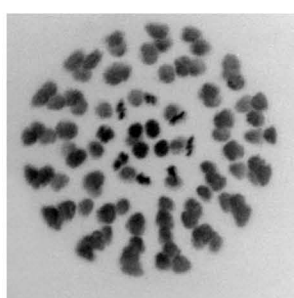
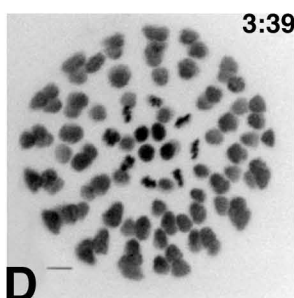
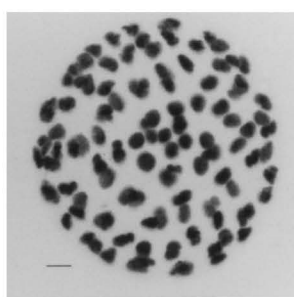
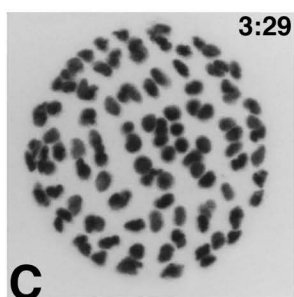
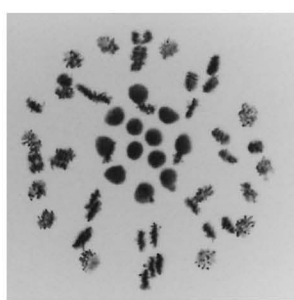
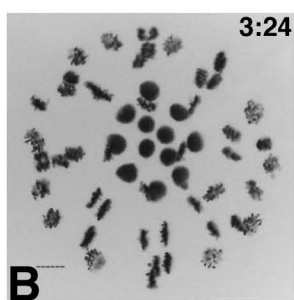
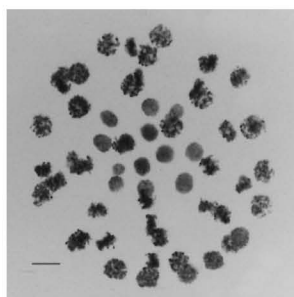
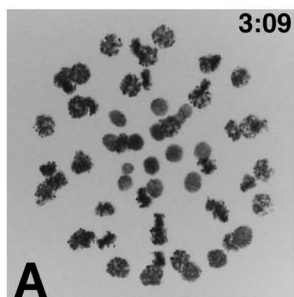


PLATE 14
Stereo Pair Confocal Images of Nuclei
of Seventh Cleavage Embryos

- A, A₁ Early 7th cleavage (3:09 hrs. p.f.). Micromeres in interphase. Macromeres in mid-metaphase. Mesomeres in prophase and early metaphase.
- B, B₁ Mid 7th cleavage (3:24 hrs. p.f.). Micromeres in interphase. Macromeres in metaphase and early prophase. Mesomeres in metaphase.
- C, C₁ Late 7th cleavage (96 cells, 3:29 hrs. p.f.). All nuclei in interphase. The eight large micromeres in this embryo have not entered mitosis.
- D, D₁ End of 7th cleavage (104 cells, 3:39 hrs. p.f.). Seven large micromeres in metaphase. Macromeres and mesomeres in interphase.
- E-G. Diagrams of division patterns of An₁ mesomere derivatives in three embryos. Short bold lines denote nearly latitudinally dividing mesomeres. Thin lines divide the animal hemisphere of each embryo into four quadrants with eight mesomeres in each quadrant. Small micromeres at the vegetal pole are denoted by a small cross with double head arrows indicating the cross furrows of the four small micromeres.

PLATE 14

Vegetal Pole View



Animal Pole View

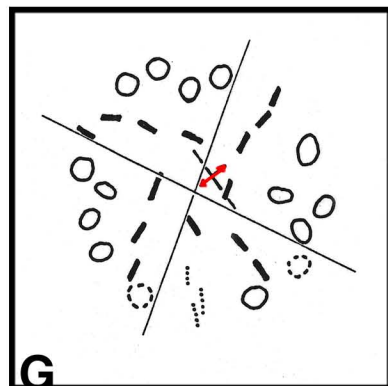
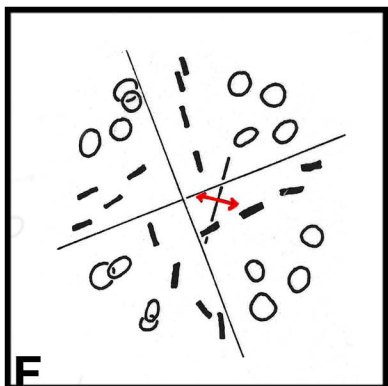
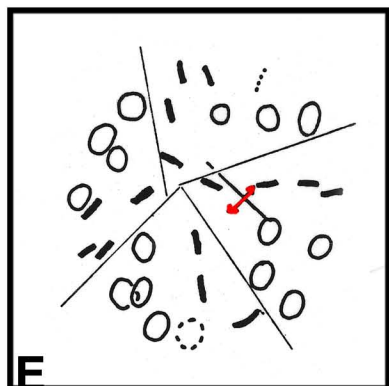
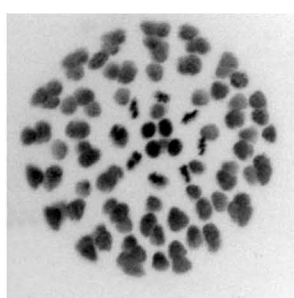
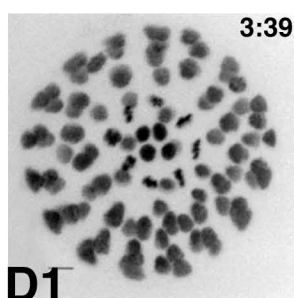
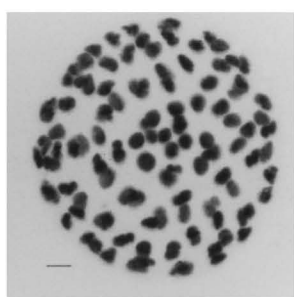
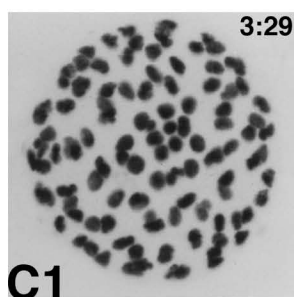
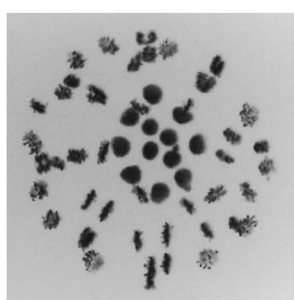
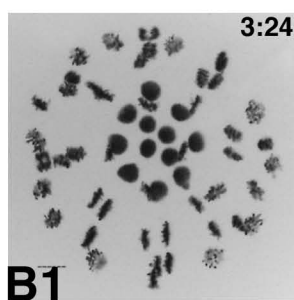
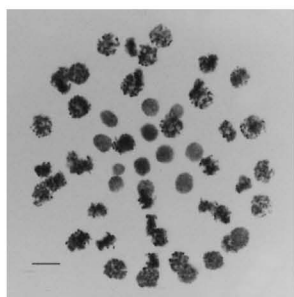
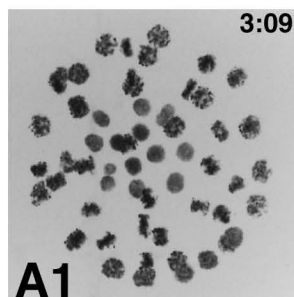
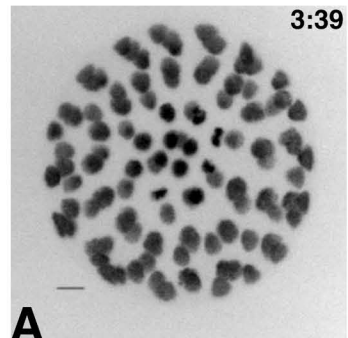


PLATE 15
Stereo Pair Confocal Images of Nuclei of Eighth Cleavage Embryos

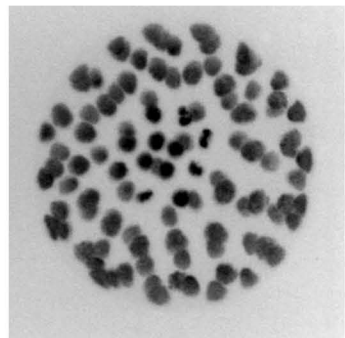
- A, A₁. End of 7th cleavage and start of eighth cleavage (3:39 hrs. p.f.). Nuclei of four of the eight large micromeres dividing.
- B, B₁. Mid 8th cleavage (126 cells, 3:44 hrs. p.f.). Macromeres in telophase. Mesomeres in anaphase and telophase.
- C, C₁. Late 8th cleavage (3:44 hr. p.f.). Parasynchronous mitoses in mesomeres.
- D-F. SEMs of an 8th cleavage embryo. D) Vegetal pole view. E) Lateral view. F) Animal pole view.

PLATE 15

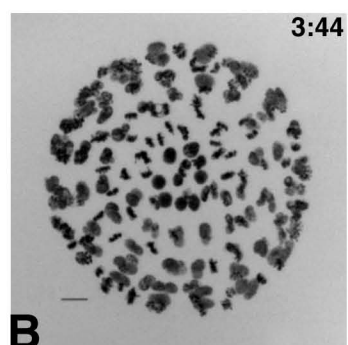
Vegetal Pole View



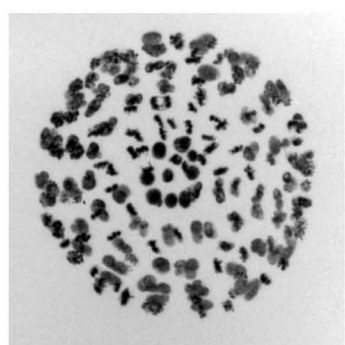
A



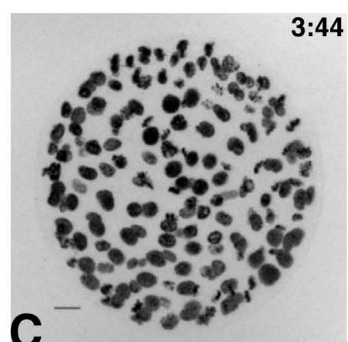
A1



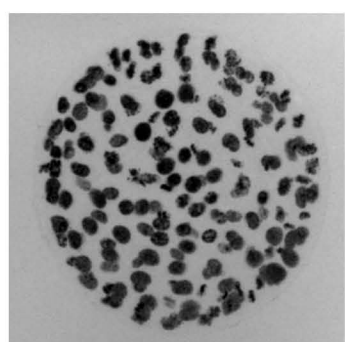
B



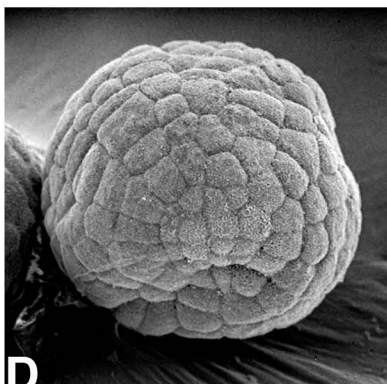
B1



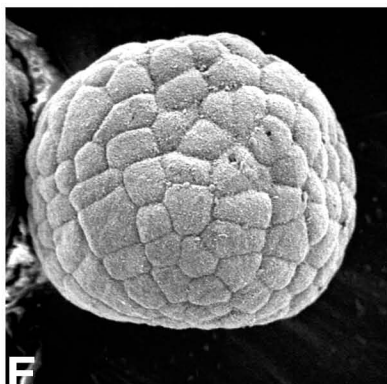
C



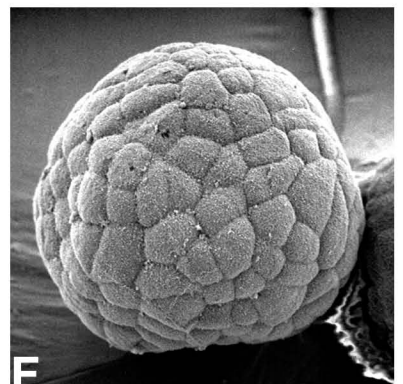
C1



D



E



F

Animal Pole View

PLATE 16

Ninth Cleavage

Prehatched Blastula

- A-C₁ Stereopair images from confocal optical sections of three prehatched blastulae (A, B, C, 5hrs. p.f.) show the absence of synchronous and parasynchronous mitosis in mesomeres and macromeres. A) Animal hemisphere. A1) Vegetal hemisphere. B) Lateral view of one half of embryo. B1) Lateral view of other half. C) Vegetal hemisphere. C1) Animal Hemisphere. A, animal pole. V, vegetal pole.
- D-F Three views of SEM images of a prehatched blastula (5hrs. p.f.) D) Vegetal pole view with area of micromeres within dashed line. E) Lateral view. F) Animal pole view.
- G. Stereopair SEM of interior of animal pole region of an embryo (5 hrs. p.f.) Green dots, descendants of An₁ tier of mesomeres.
- H. SEM of vegetal pole of a fractured embryo (5 hrs. p.f.) shows large micromeres extending toward the central region of small micromeres.

PLATE 16

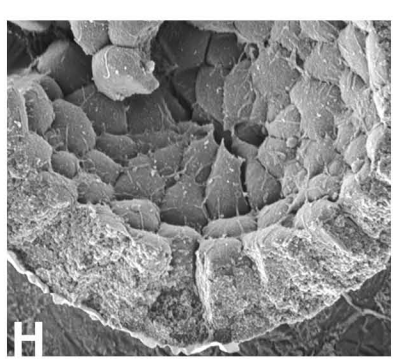
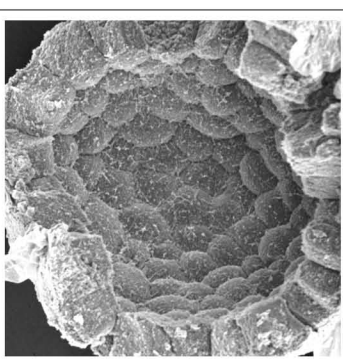
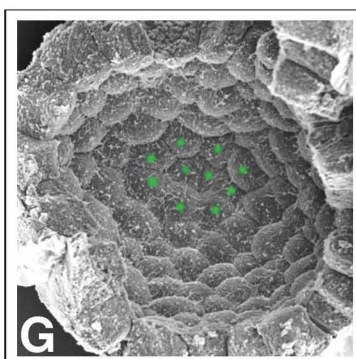
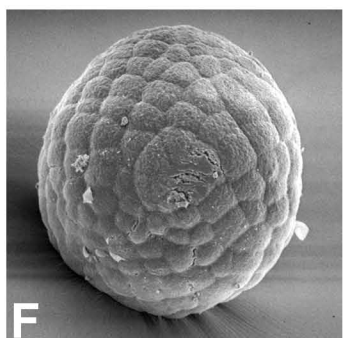
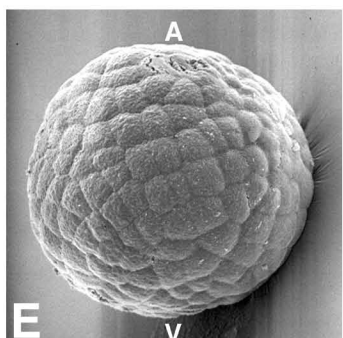
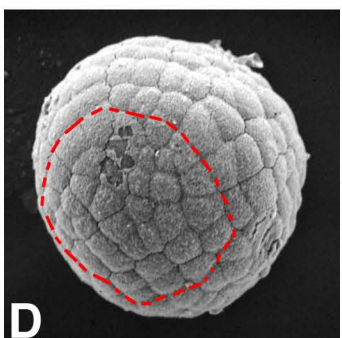
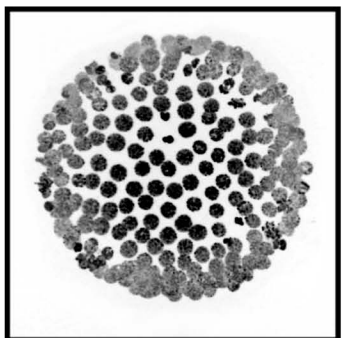
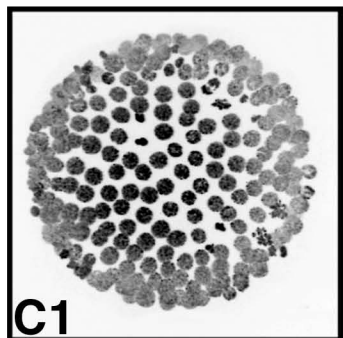
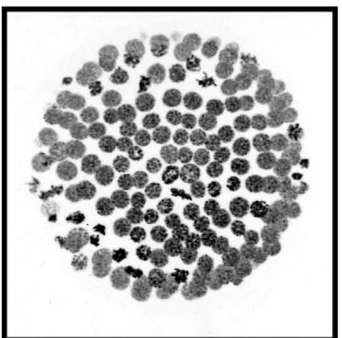
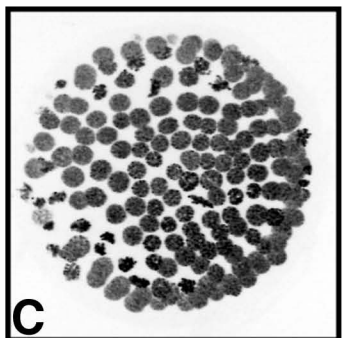
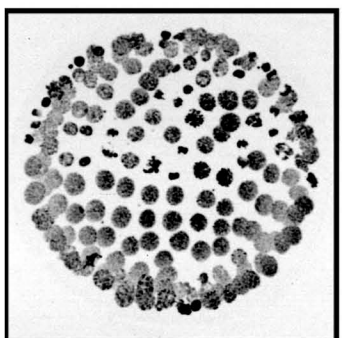
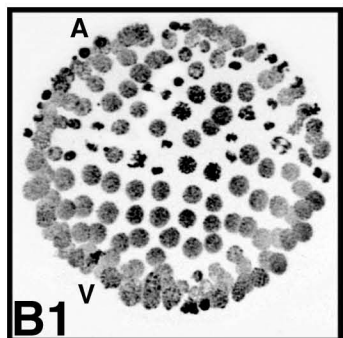
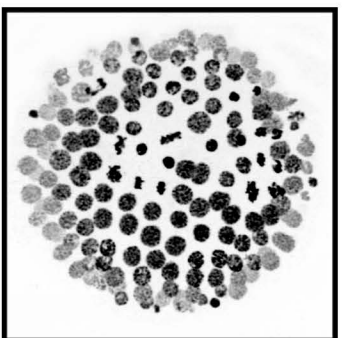
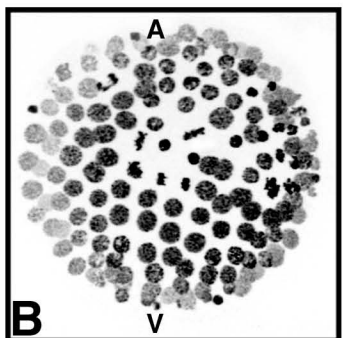
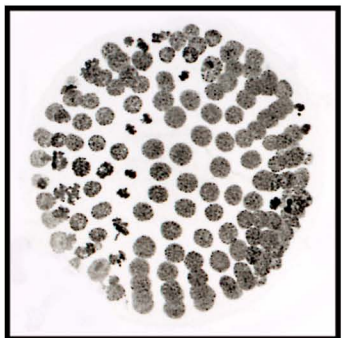
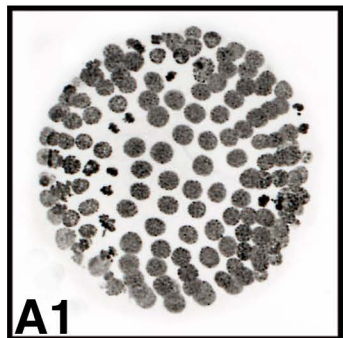
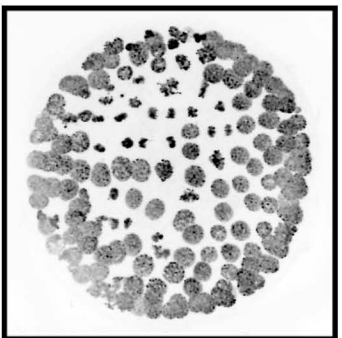
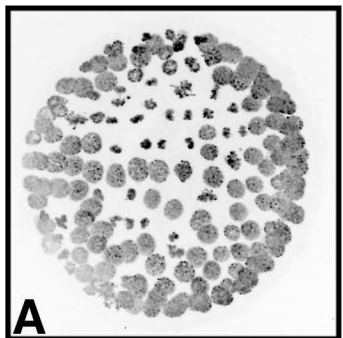
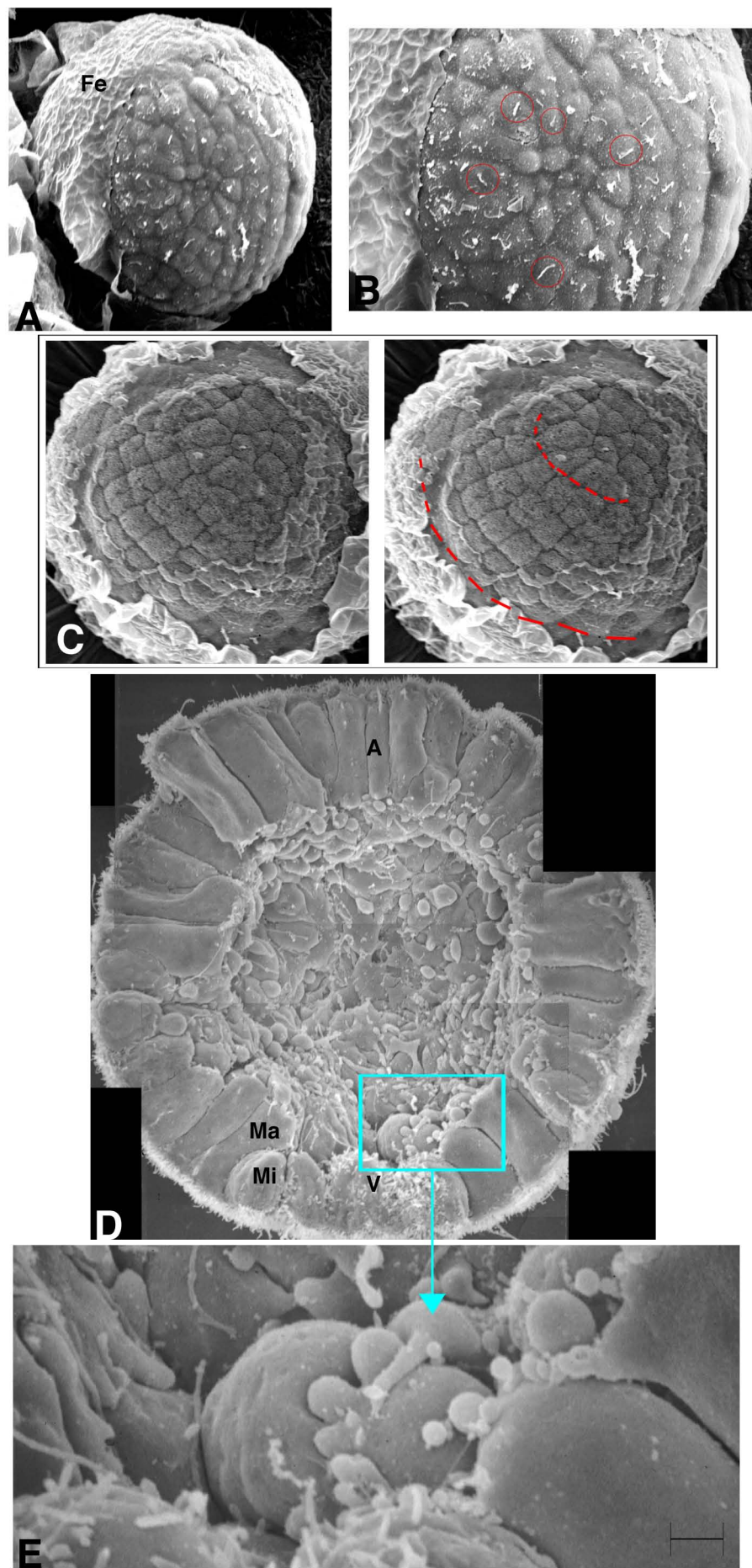


PLATE 17
Pre Hatched Blastula (5.5 Hr. P.F.)

- A- SEM vegetal pole view of embryo shows convergence of large micromeres around the eight small micromeres. Cilia (circles) are present on the large micromeres and adjoining macromeres but are absent on the surface of the small micromeres. Fe, Fertilization envelope.
- C. SEM stereo pair of vegetal region of an embryo with the fertilization envelope and hyaline layer removed by plucking with sticky tape. Dashed lines marks the boundary of large micromeres and four visible tiers of macromeres (Veg_{11} , Veg_{12} , Veg_{21} , and Veg_{22}).
- D. SEM of embryo dry fractured along the animal-vegetal axis with basal ends of cells forming globular cytoplasmic protrusions that may or may not be fixation artifacts. A, animal pole. V, vegetal pole. Mi, micromeres. Ma, macromeres.
- E. Enlarged image of boxed area in D of cells with protrusions of different sizes. Bar, 1 μm .

PLATE 17



Section 5:

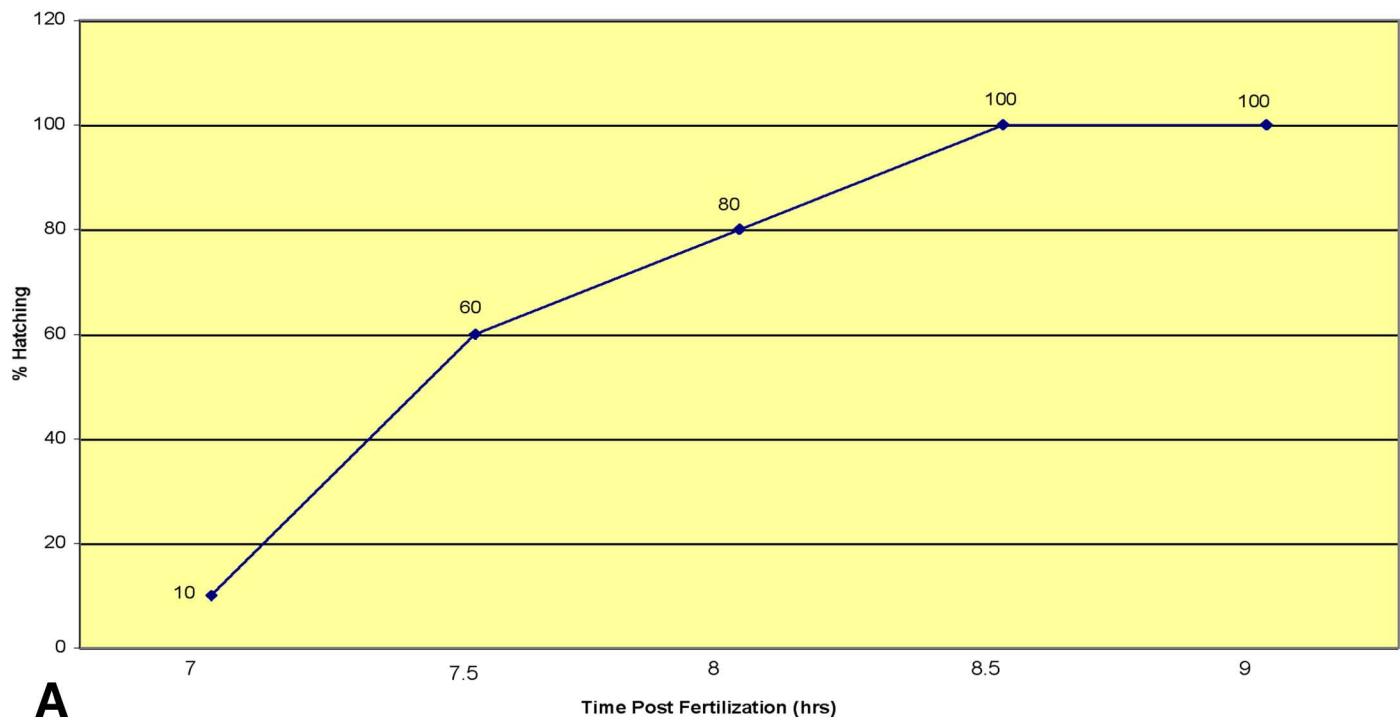
Hatched Blastulae

PLATE 18
Hatched Blastula

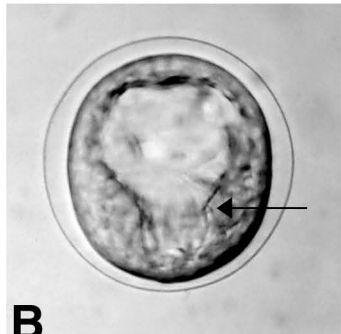
- A. Embryos cultured at 25°C begin to hatch from their fertilization envelopes at 6-7 hours post fertilization. This time table shows the hatching period lasts 90 minutes.
- B-C. Prehatched blastula at a “key hole” stage where there is a sharp boundary (arrows) between vegetal macromeres and ectodermal mesomeres.
- D-G. Time-lapse photos of a blastula hatching from the fertilization envelope. Arrow, ruptured fertilization envelope.
- H. Spherical hatched blastula.
- E. Ovoid hatched blastula.
- J-K. SEMs of fractured hatched blastulae show the overlapping extensions of the lateral ectodermal wall cells.

PLATE 18

Timetable of Hatching (22.5°C)



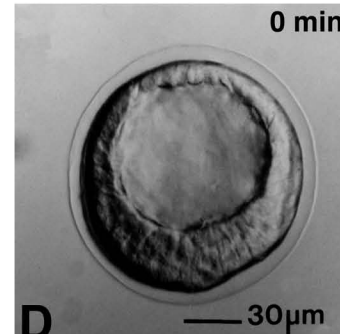
A



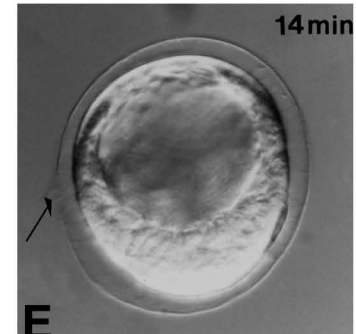
B



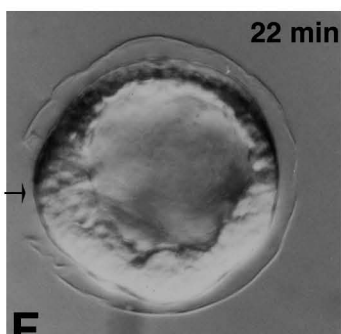
C



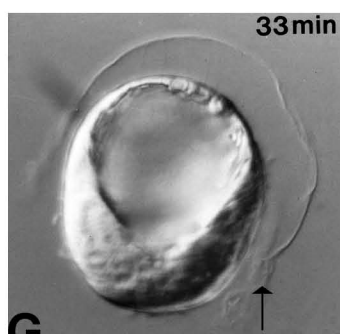
D



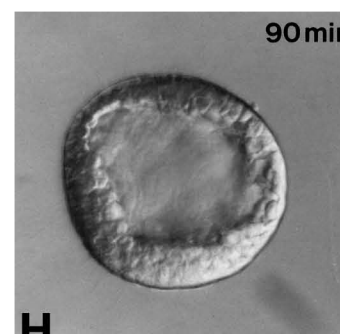
E



F



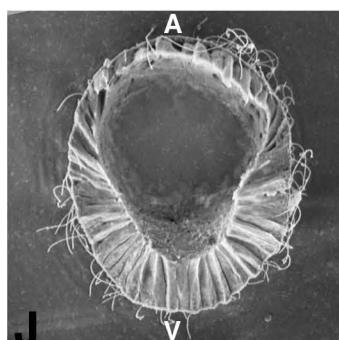
G



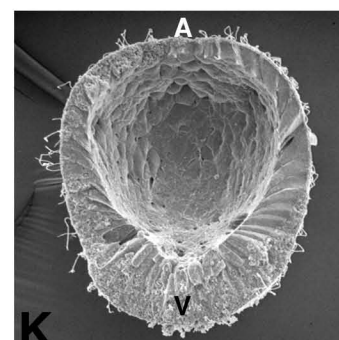
H



I



J



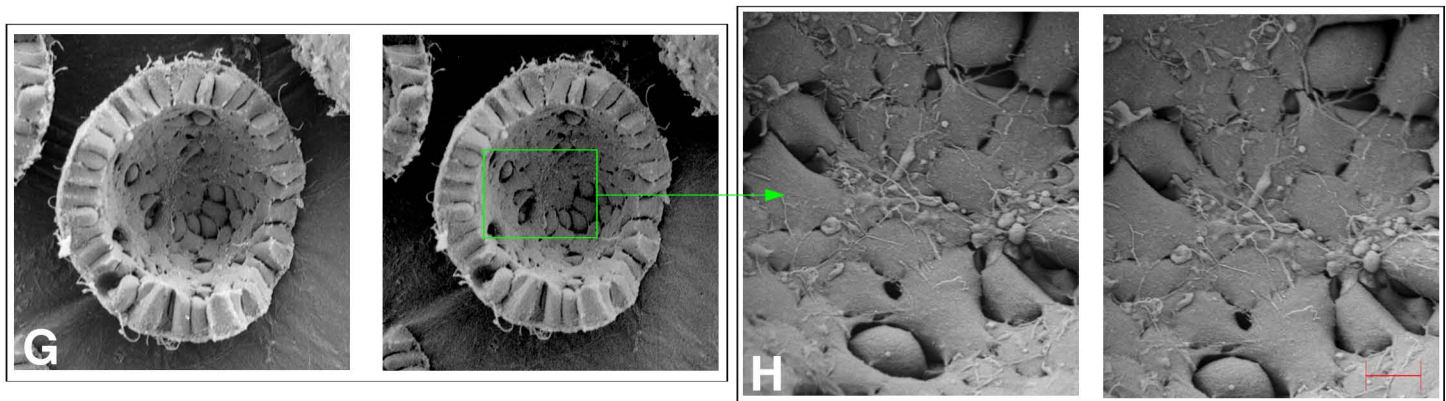
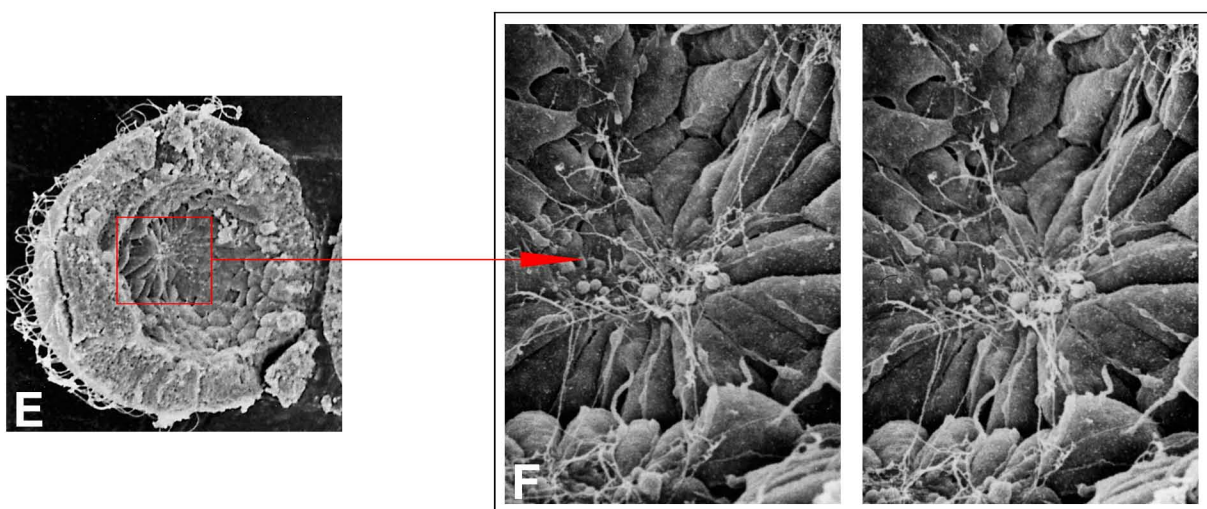
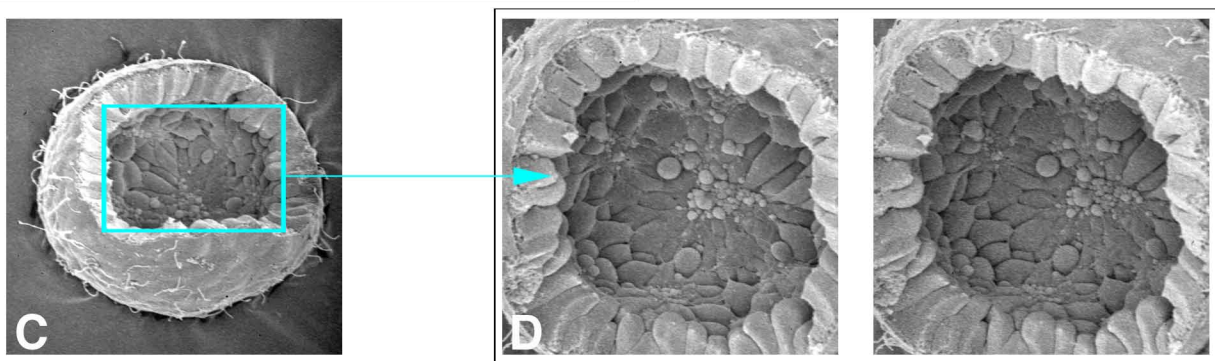
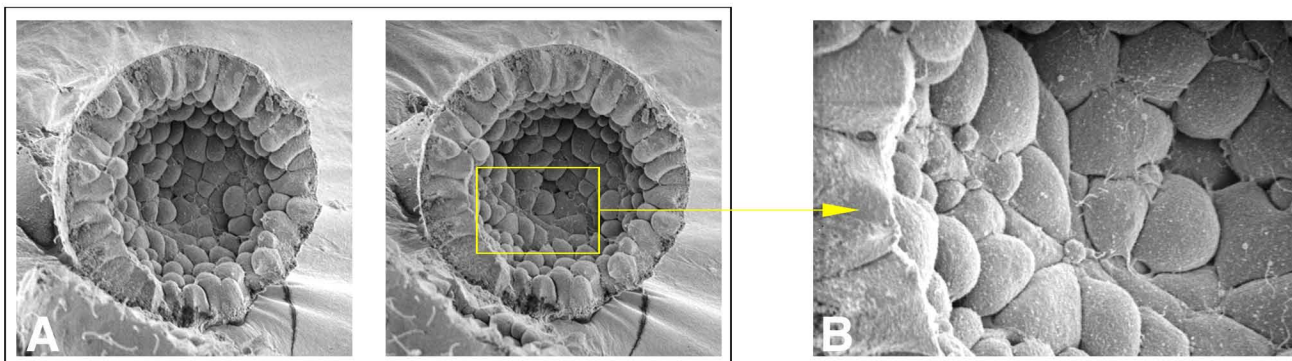
K

PLATE 19
Hatched Blastulae - Inner Views of Vegetal Pole

- A. Stereopair SEM of vegetal half of blastula.
- B. Boxed area in (A) shows convergent micromeres with cell processes connecting cells.
- C. Fractured blastula shows convergent cells around the vegetal pole.
- D. Stereopair of boxed area in (C) shows numerous cytoplasmic blebs and cytoplasts on the small micromeres at the vegetal pole.
- E. Fractured blastula shows convergent cells at vegetal pole.
- F. Stereopair of SEM boxed area in (E) shows large micromeres converging on small micromeres. Cytoplasmic blebs and extracellular matrix fibers present.
- G. Stereopair SEM of vegetal region with several large micromeres preparing to divide surrounded by spaces between them and non-dividing cells.
- H. Stereopair SEM of boxed area in (G) shows spaces between dividing and non-dividing micromeres and cellular processes attaching cells to one another.

Bar, 1.0 μ m.

PLATE 19



Section 6:

Mesenchyme Blastula

PLATE 20
Mesenchyme Blastula-Primary Mesenchyme Cell Ingression

- A. LM of ovoid, early mesenchyme blastula. Red arrow points to the eight small micromeres bulging outward at the vegetal pole.
- B. SEM of early mesenchyme blastula. Green arrow points to the small micromeres at the vegetal pole.
- C. Stereopair view of vegetal pole with the eight small micromeres surrounded by large micromere descendants, the primary mesenchyme cells (PMCs) that have shorter cilia compared to those of other epithelial cells.
- D,E. SEM of early PMC ingression in two embryos.
- F. Stereopair SEM of early PMC ingression shows polygonal shapes in PMCs. At this stage there are a total of 28-32 PMCs.
- G. LM of ingressing PMCs.
- H. TEM montage of ingressing PMCs during early PMC ingression. Bar, 10 μm .
- I. LM of late PMC ingression. At this stage there are 30-60 PMCs in the blastocoel. Note the flattening of the vegetal pole end of the blastula that now may be called the vegetal plate of the blastula and gastrula.
- J. TEM montage of late PMC ingression. Presumptive secondary mesenchyme cells (SMCs) surround the ingressing PMCs and the small micromere descendants (SMDs). S, small micromere descendant. Bar, 10 μm .

PLATE 20

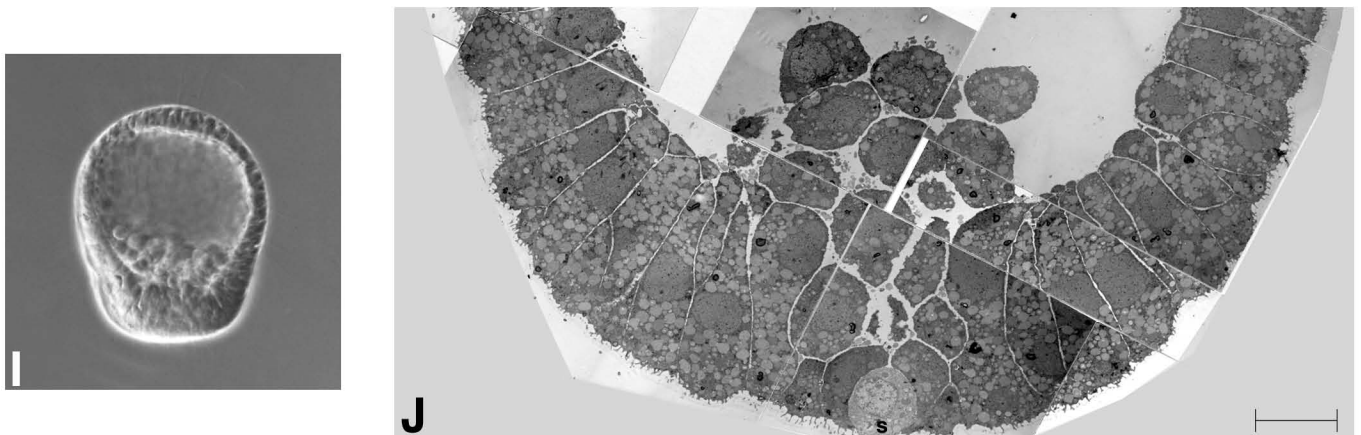
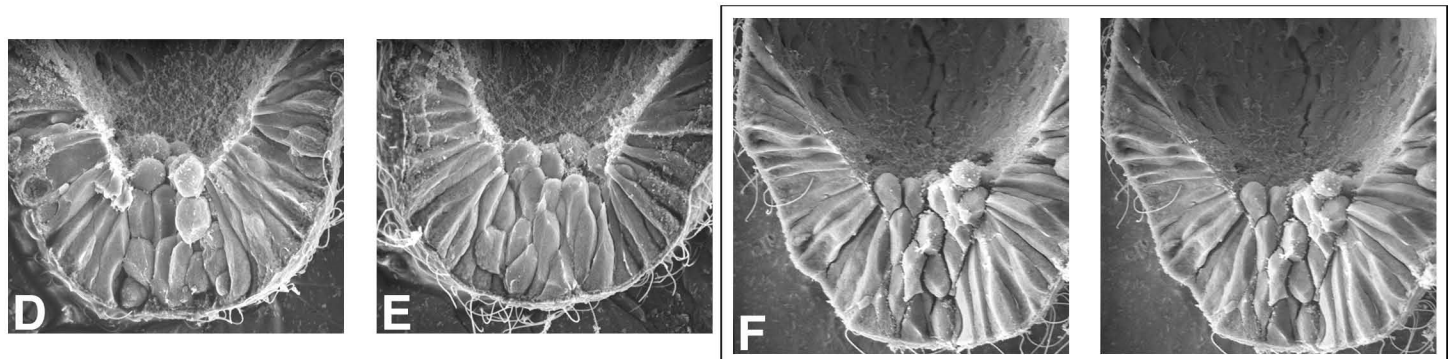
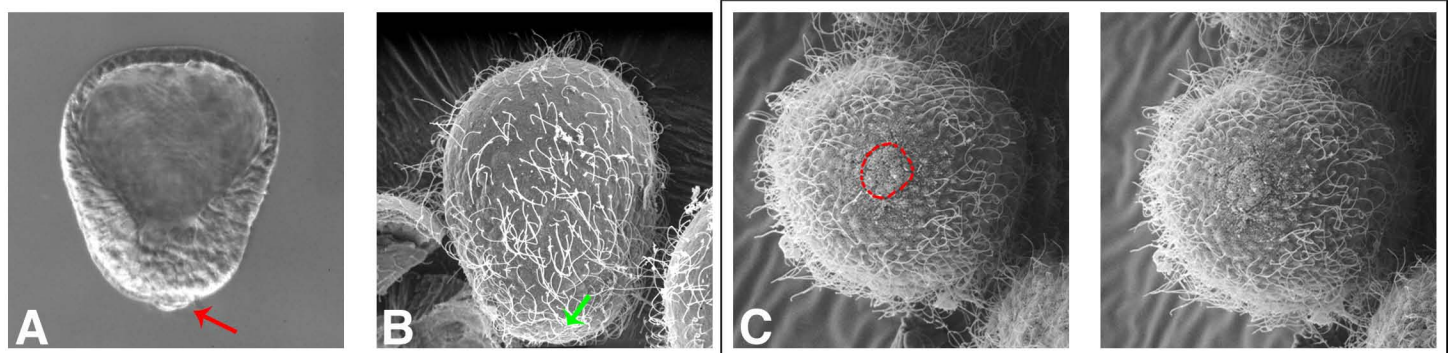


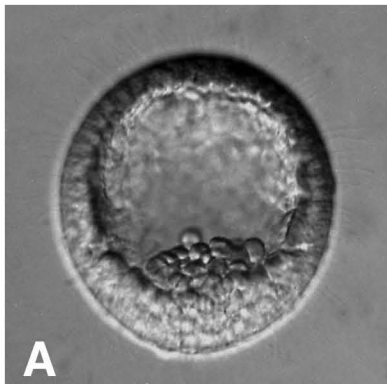
PLATE 21
Mid - Mesenchyme Blastula

- A,B. LM (A) and confocal optical section (B) of a mesenchyme blastula.
- C. Stereopair images of a short stack of optical sections.
- D. Stereopair images of a short stack of optical sections of one side of the embryo.
- E. Stereopair images of a short stack of optical sections of the other side of the embryo.

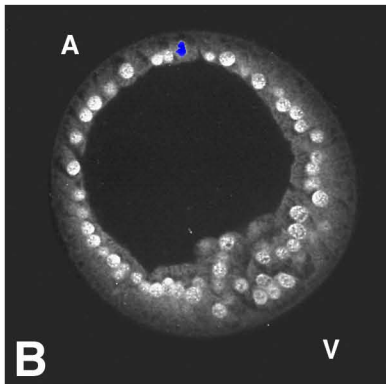
Note: Nuclei of dividing cells are colored blue. One or two PMC nuclei may be dividing. Stereo pairs D and E represent the aboral and oral ectoderm sides respectively.

PLATE 21

Optical Sections #

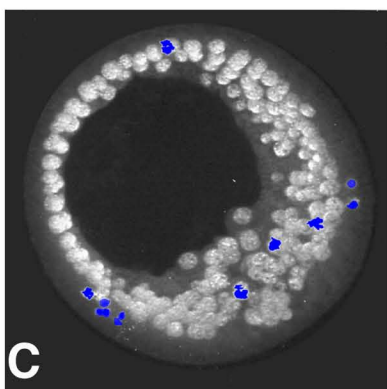


A

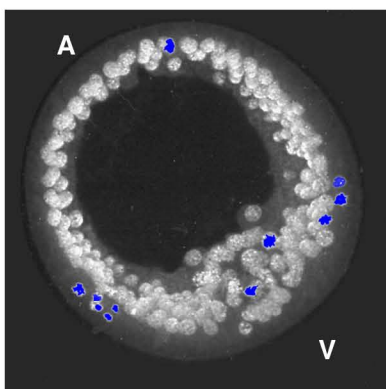


B

103

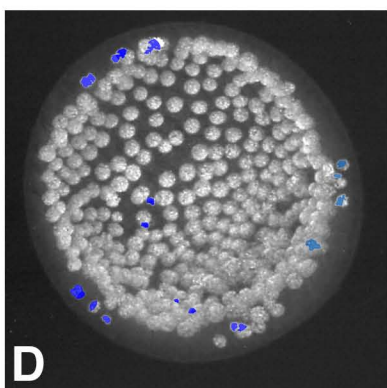


C

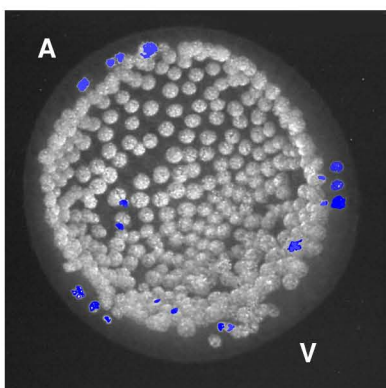


V

87-117

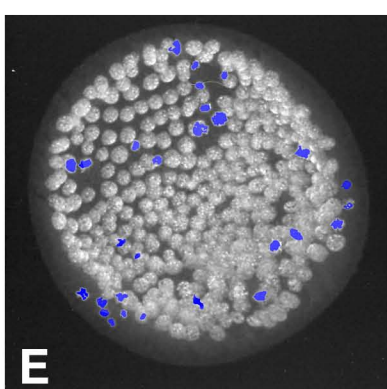


D

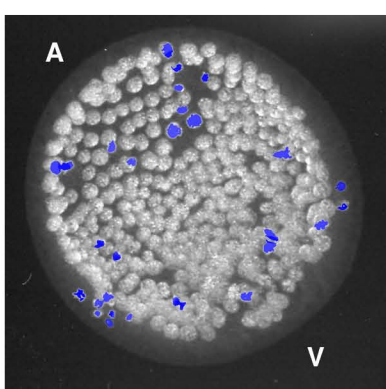


V

87-173



E



V

1-86

PLATE 22
SEM Views of Morphological Features of Mesenchyme Blastulae

- A. An early mesenchyme blastula fractured along the A-V axis shows the polarized elongations of lateral wall ectodermal cells toward the interface (black arrow) of the An_2 and Veg_1 descendants.
- B. Enlarged box area in (A) shows a mat-like array of fibers at the aforementioned interface. There are two of these convergence areas that indicate the loci of the PMC aggregation centers and reflect the bilateral symmetry of the embryo at this stage.
- C. Polarized elongation of lateral ectodermal cells in another early mesenchyme blastula.
- D. A-V fracture of vegetal region shows ingressing PMCs.
- E. High magnification of the yellow box in (D). Spherical PMCs along the epithelial wall and fibrous extracellular matrix are evident.
- F. High magnification of the blue box in (D). The red arrow points to long retraction process of one PMC. At the vegetal pole, one SMD is present and surrounded by SMCs.
- G. High magnification of the red box in (D). Two PMCs have retraction processes (yellow arrows) and extracellular cytoplasts.
- H. Enlarged boxed area in G shows the cytoplasts and ECM fibers at higher magnifications. Bar, 0.1 μm .
- I. View of cytoplasts and ECM fibers between a PMC and the basal lamina.
Bar, 0.1 μm .

PLATE 22

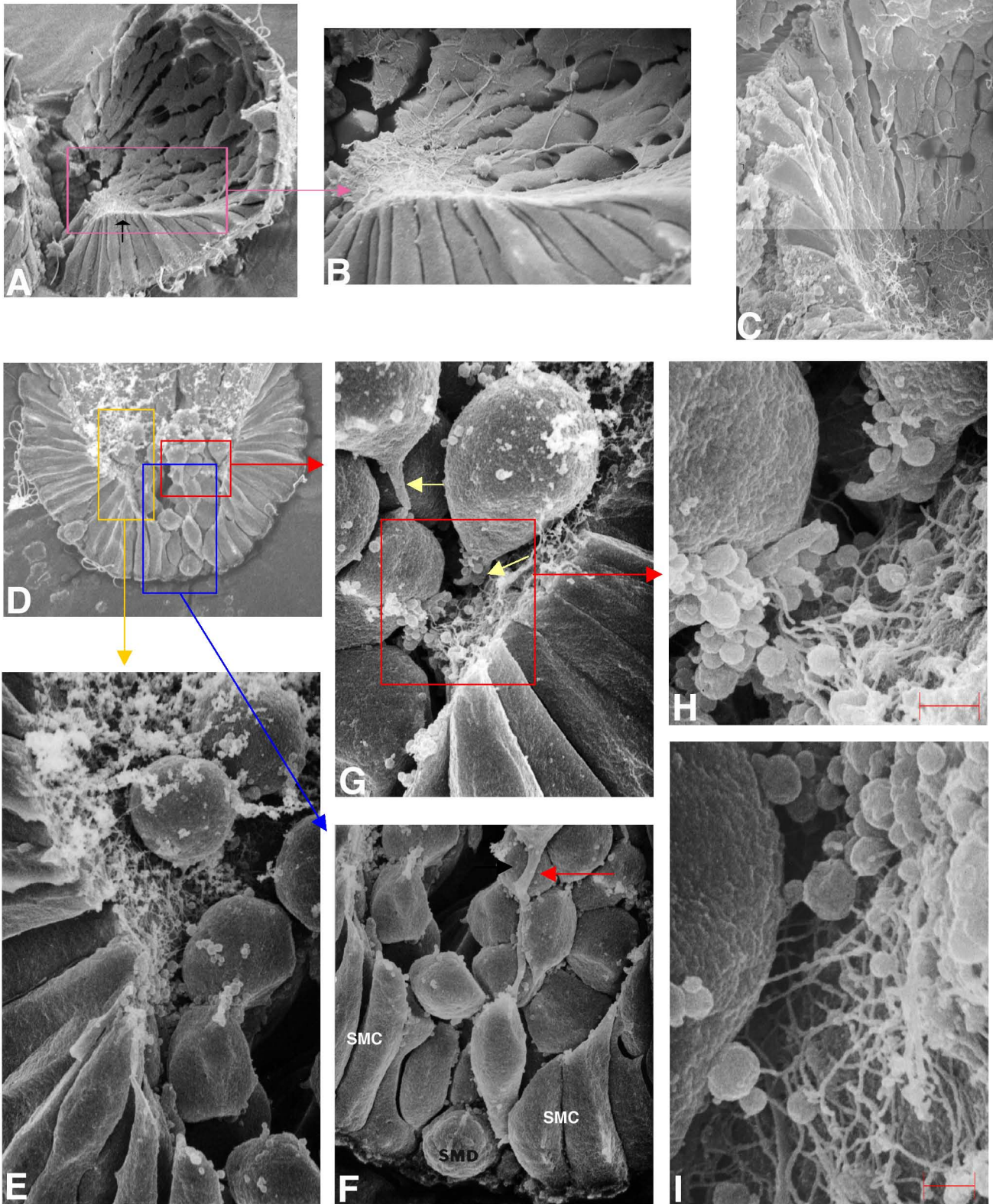
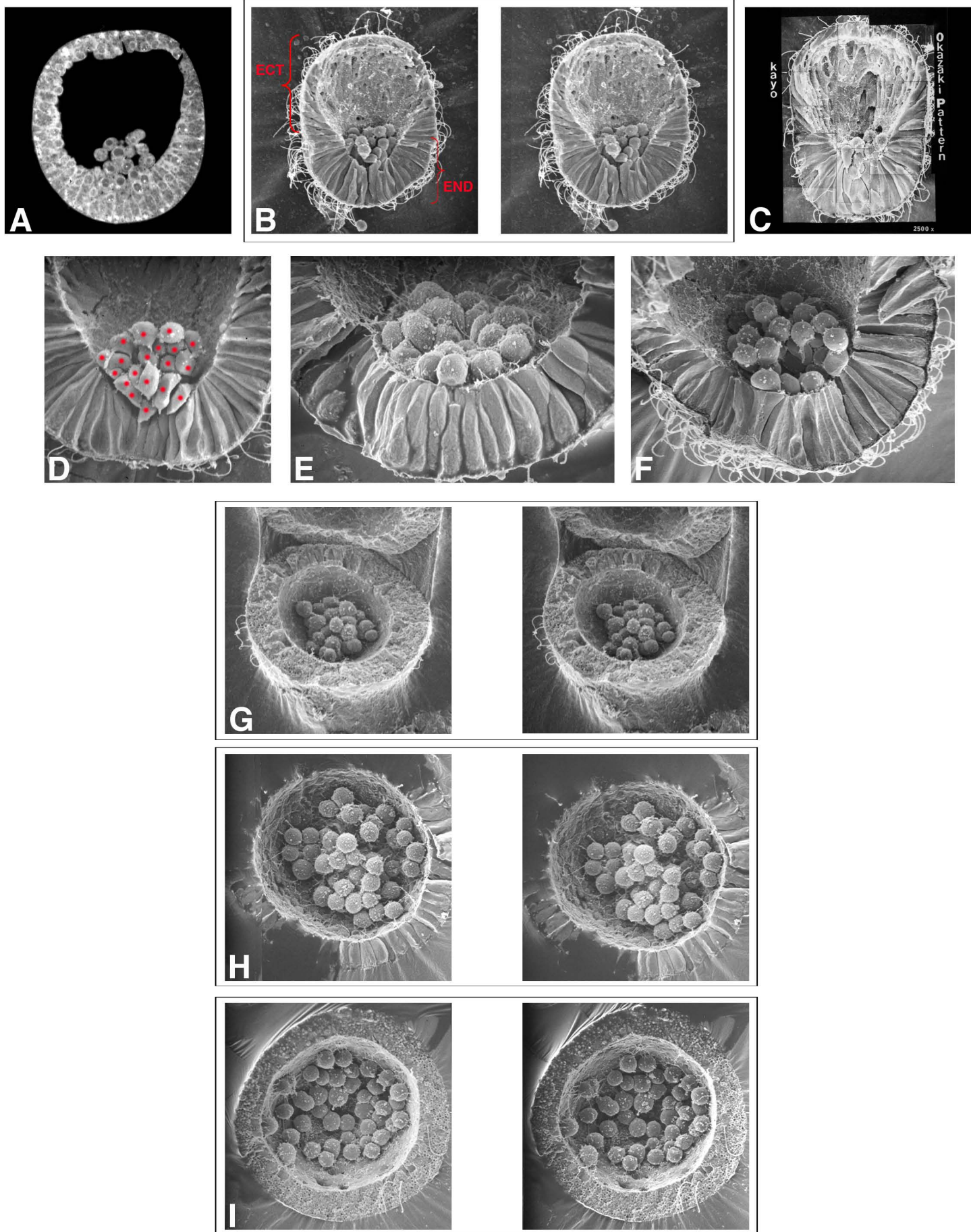


PLATE 23

Late Mesenchyme Blastula: End of PMC Ingression and Beginning of Primary Mesenchyme Migration

- A. Sagittal section of a mesenchyme blastula whose PMCs have completed their ingression.
- B. Stereopair SEM of a fractured mesenchyme blastula with seventeen PMCs visible.
Note the Okazaki patterns of the presumptive ectoderm (ECT) and endoderm (END) cells.
- C. Embryo fractured along the A-V axis to show the Kayo Okazaki pattern of cells of the blastular wall and convergence of ectodermal and endodermal cells in the region of the PMC aggregation centers.
- D. SEM of vegetal pole region of the mesenchyme blastula fractured along the animal-vegetal axis. Twenty PMCs are visible.
- E- SEM views of ingressed PMCs. (E) Twenty-one PMCs are visible (F) Thirty-one PMCs
F. are visible.
- G- Stereopair series of late mesenchyme blastulae show increases in numbers and dispersal
I. of PMCs. (G) Twenty two PMCs; (H) Forty PMCs; (I) Forty four PMCs.

PLATE 23



Section 7:

Primary Mesenchyme Cells from Late Mesenchyme Blastula to Late Gastrula

PLATE 24
Primary Mesenchyme Cell Migration from Late Mesenchyme Blastula
to Primary Invagination of Archenteron

- A-D. PMCs begin to migrate away from the vegetal pole shortly after ingressing (A). They continue to migrate primarily along or in the vicinity of the basal ends of the epithelial cells in the mid (B) and late (C) mesenchyme blastula until the beginning of primary invagination of the archenteron (D). Occasionally, PMCs migrate to the animal pole before returning to the vegetal half of the embryo (arrow, panel D).
- E. SEM of early mesenchyme blastula with PMCs spreading over the basal side of the vegetal plate. Arrow, long cilia of acron. Dashed lines mark peripheral margin of apical plate ectoderm.
- F. SEM of late mesenchyme blastula shows initial aggregation of PMCs on one side and migrating cells with long exploratory filopodia and retraction processes.
- G. Boxed area in (F) at higher magnification. F, exploratory filopodia of two PMCs (yellow). R, retraction process of one PMC (red). A, initial PMC aggregation center.
- H. SEM of late mesenchyme blastula/primary invagination transition shows migrating PMCs with exploratory filopodia and retraction fibers.
- I. Stereopair SEM of PMCs near end of migration phase at initial invagination of archenteron. Arrow points to the SMCs at the distal end of the invaginating archenteron.
- J. SEM of early primary invagination with PMCs beginning to aggregate and encircle the inner end (arrow) of the archenteron.
- K-M. Confocal optical sections of nuclei during primary invagination of the archenteron. (K) Mid sagittal section (average 11 sections). (L) Stereo pair of a short stack of sections 5-30. (M) Stereo pair of a stack of sections 5 to 42. By this stage PMCs are localized near the two bilaterally positioned PMC aggregation centers. PMCs of the lateral arm of the PMC syncitium are migrating toward the animal hemisphere.

PLATE 24

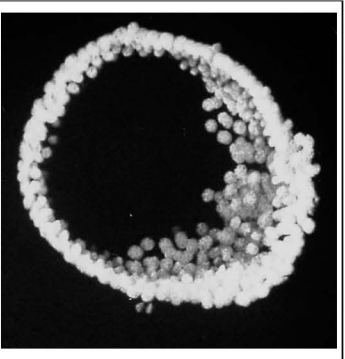
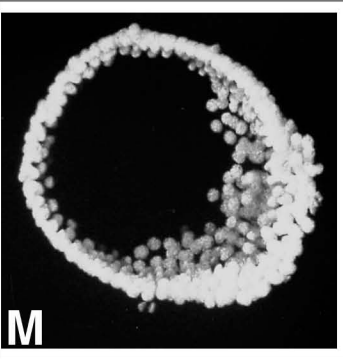
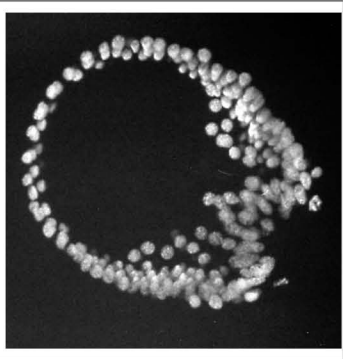
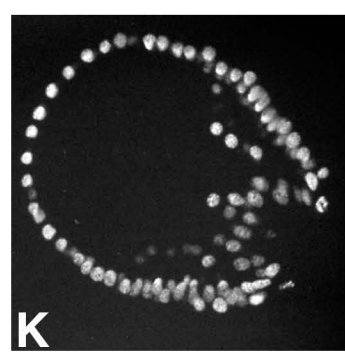
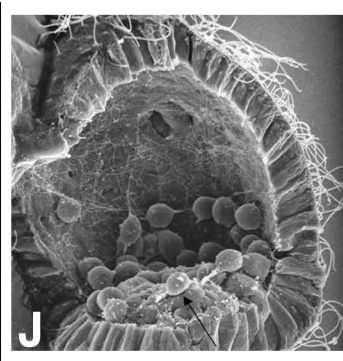
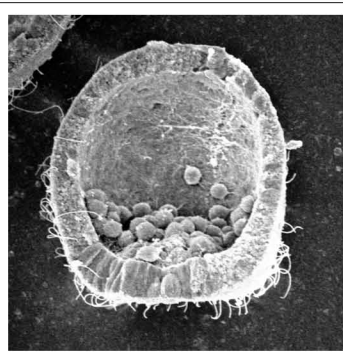
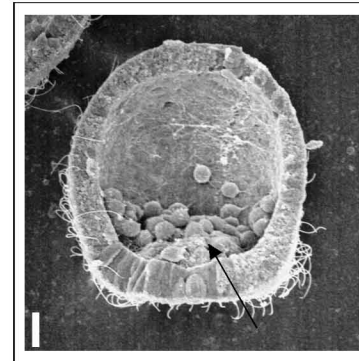
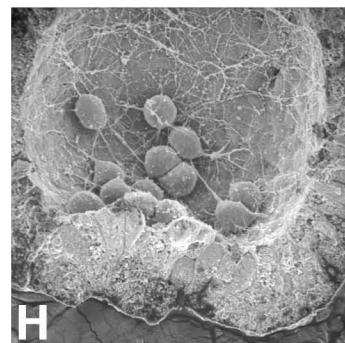
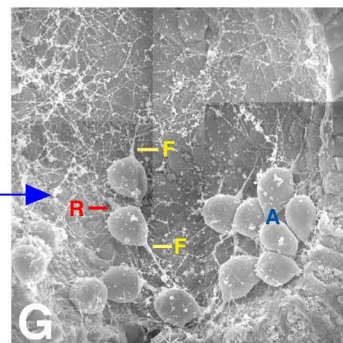
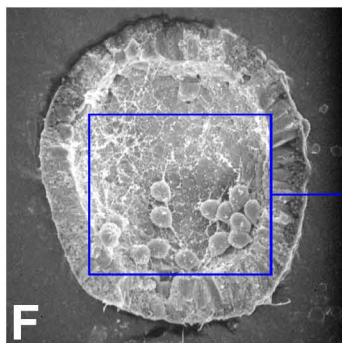
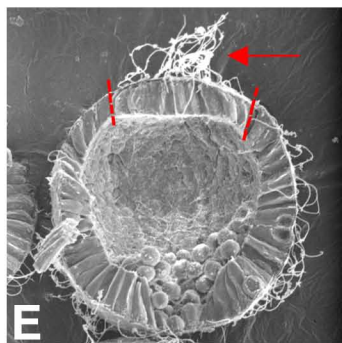
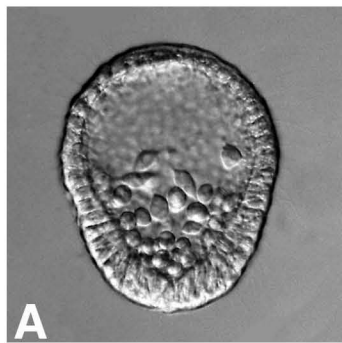


PLATE 25
SEM Views of Migrating Primary Mesenchyme Cells

- A. Fractured early gastrula with migrating PMCs.
- B. Boxed area in (A) at higher magnification showing PMCs with unbranched and branching cell processes.
- C. Fractured late mesenchyme blastula with PMCs beginning to migrate along the basal lamina side of the ectodermal wall.
- D. Boxed area in (C) at higher magnification.
- E. Stereopair of the tip of a PMC cell process with three filopodia, the branches extending over the surface of the basal lamina. Bar, 1 μ m.
- F. A single filopodia-like cell process with only the tip attached to the basal lamina. Bar, 1 μ m.
- G. A migrating PMC with a single cell process.
- H. Stereo pair of boxed area in (G) at higher magnification. Only the tip of the process is attached to the basal lamina. Bar, 1 μ m.

PLATE 25

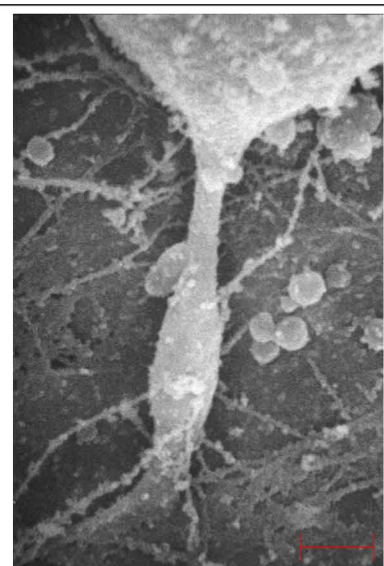
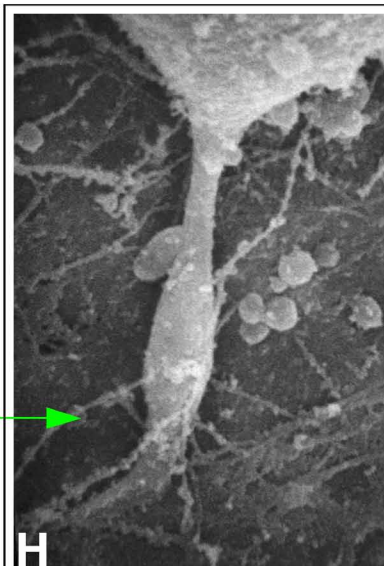
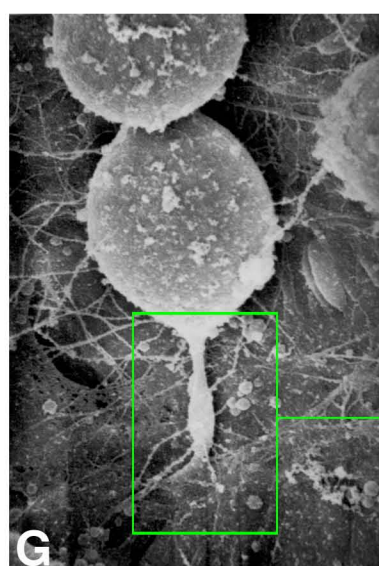
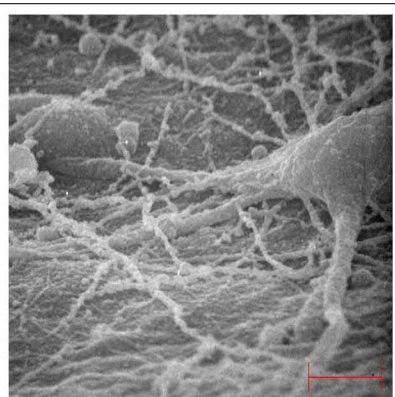
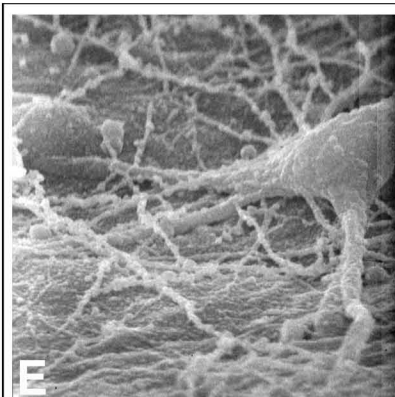
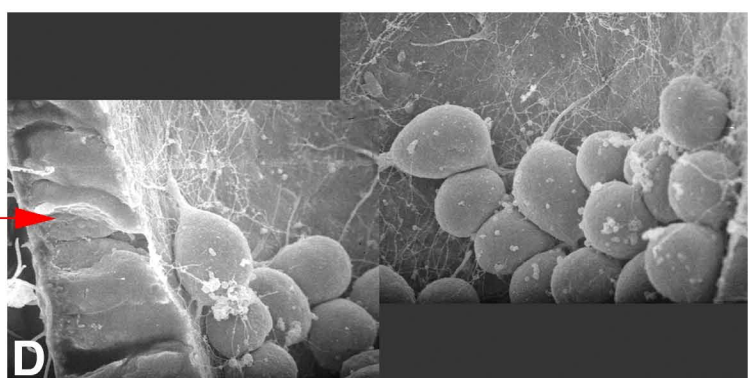
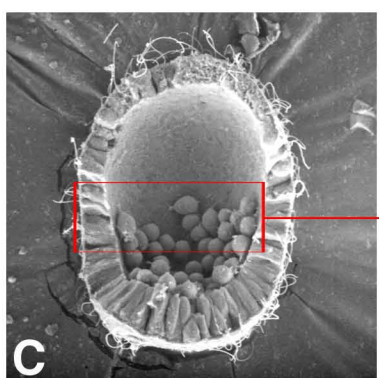
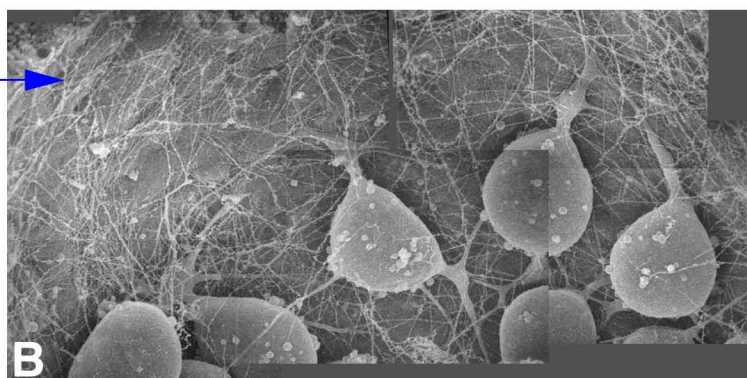
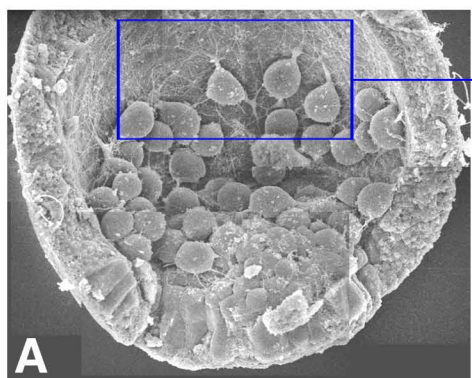


PLATE 26
TEM Views of Primary Mesenchyme Cells
and the PMC Cytoplasmic Syncytium

- A,B. Section of a spherical PMC in blastocoel. N, nucleus. Nu, nucleolus. Y, yolk platelet. Red arrow, rough endoplasmic reticulum. Bars: 1 μ m (A); 0.1 μ m (B).
- C. Section of a spherical PMC with protruding yolk platelets (blue arrows). Bar, 10 μ m.
- D. Section of a PMC with protoplasmic process. Yellow arrows point to extracellular cytoplasts in blastocoel. E, ectodermal wall. Bar, 10 μ m.
- E. Section of PMCs forming a portion of the PMC cytoplasmic syncytium.
- F. Section of lateral arm of PMC syncytium. Arrow points to the exploratory process of the distal cell of the lateral arm.
- G. Section of two PMC cell bodies attached to the common cytoplasmic syncytium (Cs) that is attached to the ectodermal wall (E) by short “anchoring” cell processes (blue arrows).
- H. Section of four adjoining PMC cell bodies and cytoplasmic syncytium (Cs) near but not in contact with the ectodermal wall (E). Bar, 1 μ m.

PLATE 26

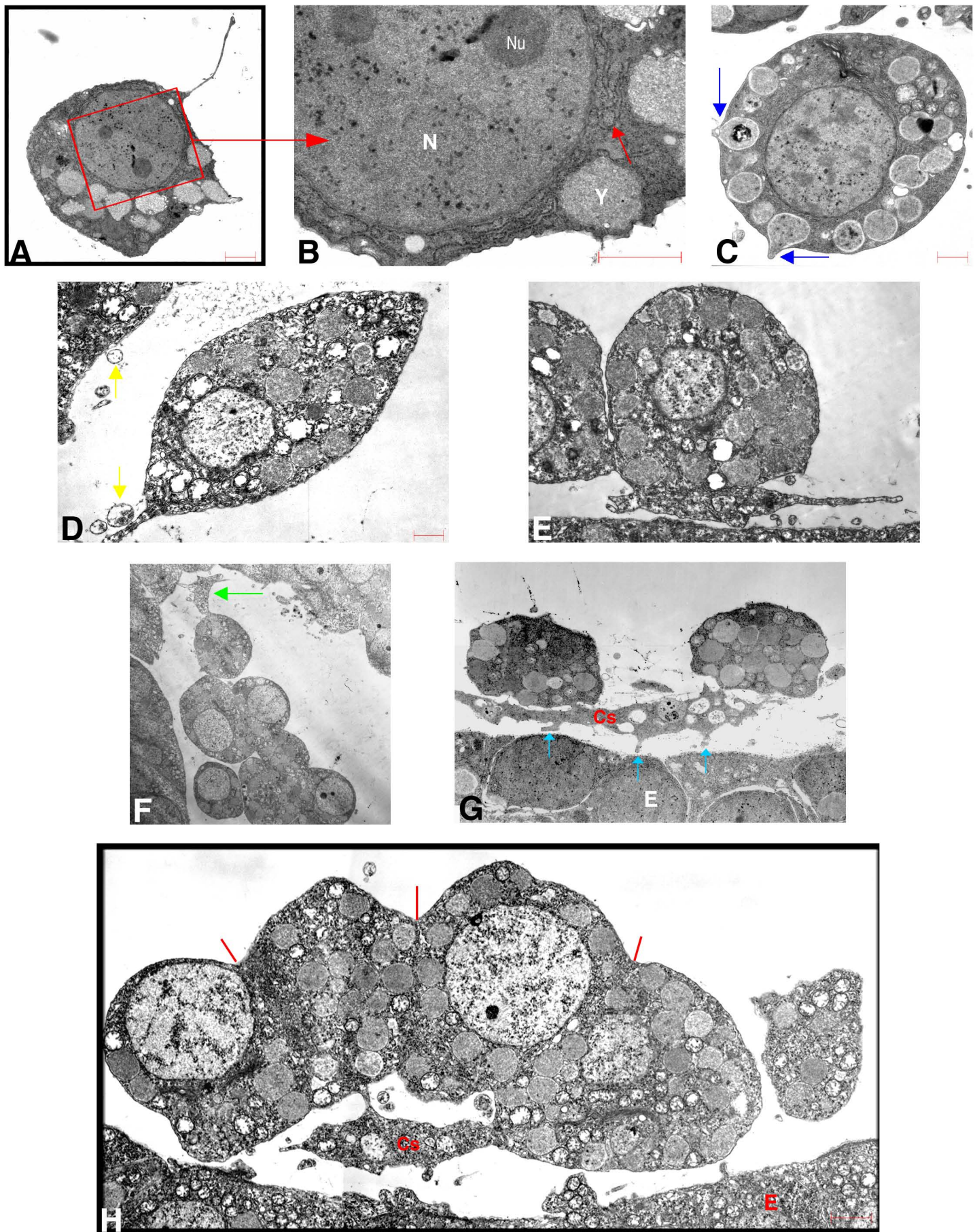


PLATE 27
SEM Views of a Migrating PMC and
Formation of the PMC Cytoplasmic Syncitium

- A-C. During the migration of PMCs, the two presumptive lead cells of the lateral arms of the PMC syncytium have a different morphology than other migrating cells as shown in panel A. (A). The PMC marked with a yellow asterisk is a presumptive lead PMC cell. (B) Stereo pair from panel A at a higher magnification shows that only the tips of the leading and trailing cell processes are in contact with the basal lamina of the ectodermal wall. (C) Side view of a leading cell process extending over the luminal surface for the basal lamina.
- D-F. An early gastrula with an initial PMC syncytium forming around the early primary invagination of archenteron. (D) Embryo oriented to show the basal lamina side of the syncytium and the dome-like cluster of the 8 small micromeres (blue arrow) in the center of the blastopore. (E and F) Enlargements of boxed area in panel D and E respectively showing numerous anchoring filopodia and the convergence of cell processes around the initial PMC aggregation center.
- G. Stereopair image of the basal lamina side of a PMC aggregation center before the cytoplasmic syncitium develops.
- H. Stereopair image of the basal lamina side of aggregated PMCs and a well developed triradiate cytoplasmic syncytium with numerous anchoring filopodia of a mid-gastrula stage embryo. Arrow points to tip of developing lateral arm of the syncytium.

PLATE 27

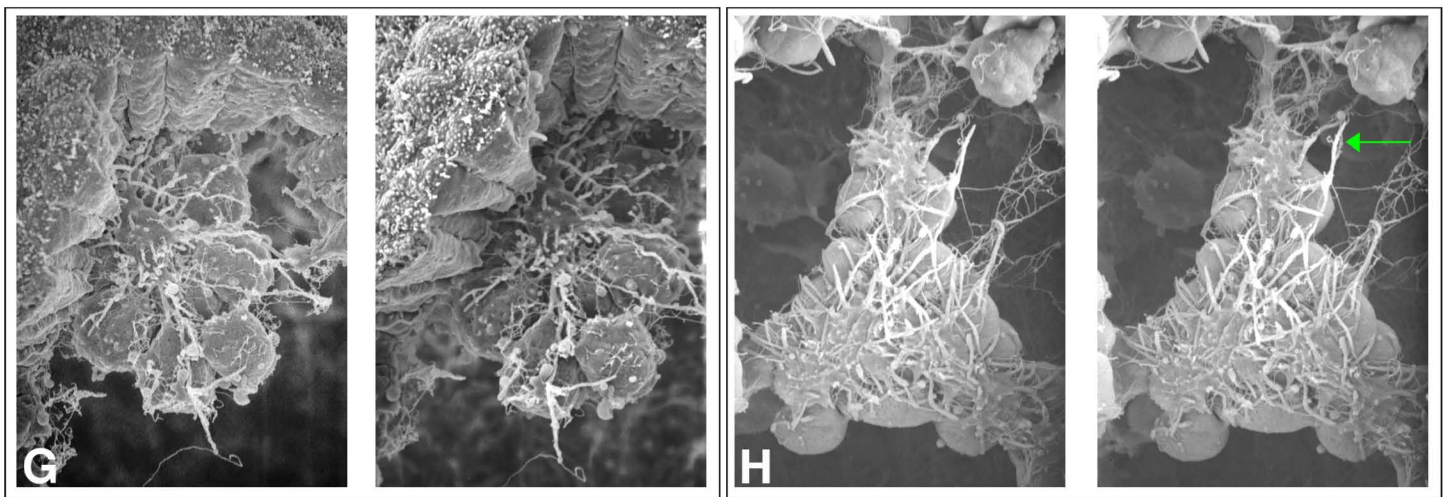
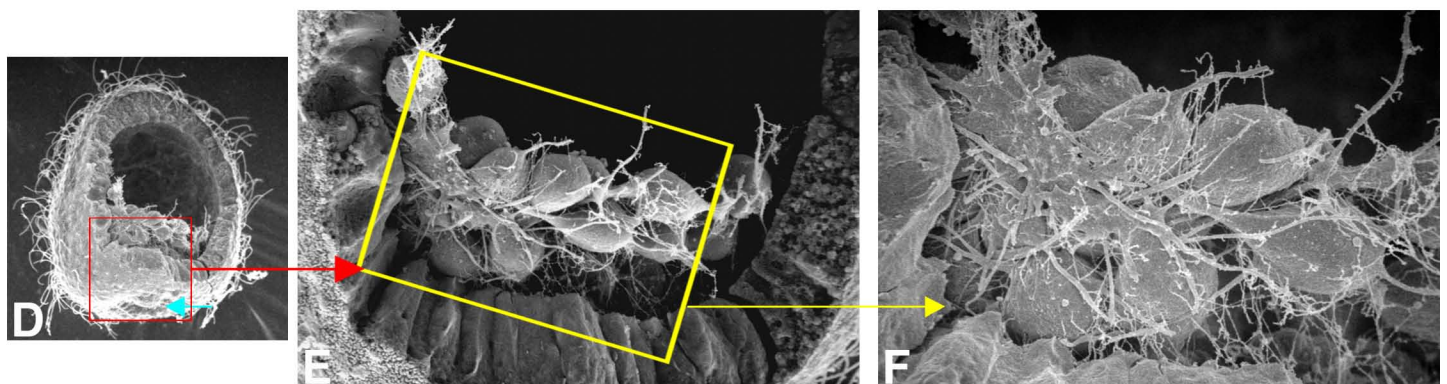
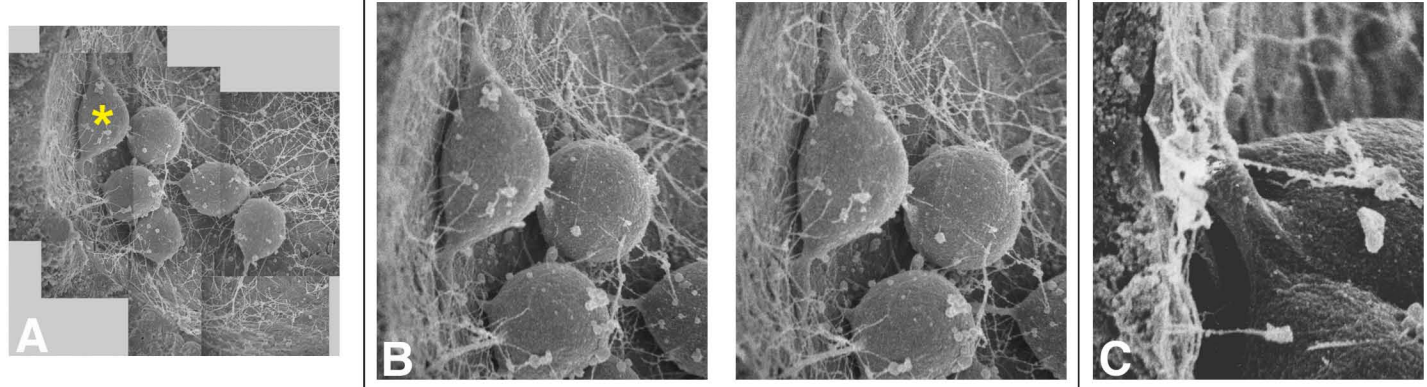


PLATE 28
SEM Views of the Ventrolateral Branch of Primary Mesenchyme Cells

- A. As early as the primary invagination of the archenteron, the ventrolateral branch of the PMC syncytium is present.
- B. Stereopair image of an early gastrula shows a side view of one ventrolateral arm of PMCs (blue arrow) extending toward the animal pole. Also note the cluster of secondary mesenchyme cells (S) at the tip of the archenteron wall.
- C. Stereopair of ventrolateral branch of PMCs in the blue-boxed area in panel B. Note the branching exploratory filopodial process at the tip of the lead cell.
- D. Stereopair image of a ventrolateral arm that typically consists of 18 to 20 cells.
- E. Stereopair image of a ventrolateral arm shows the leading cell of the arm with branching cell processes.
- F. Enlargement of boxed area in panel E.

PLATE 28

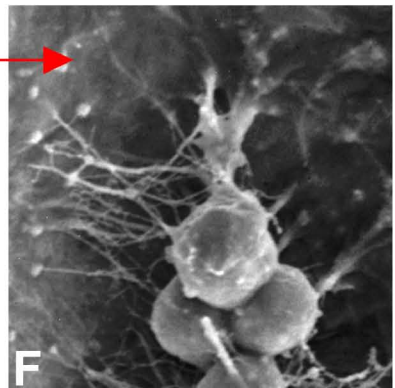
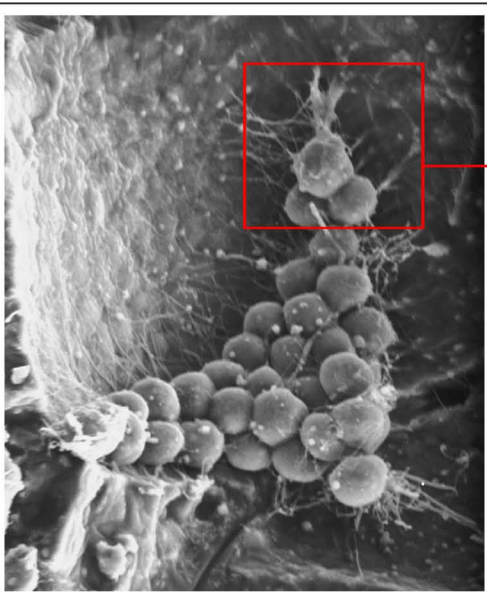
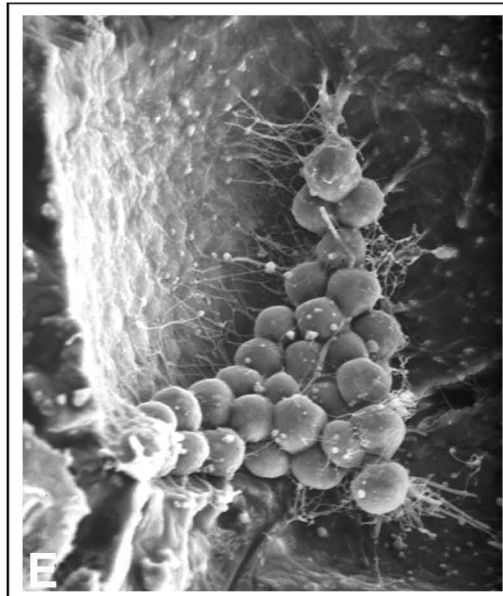
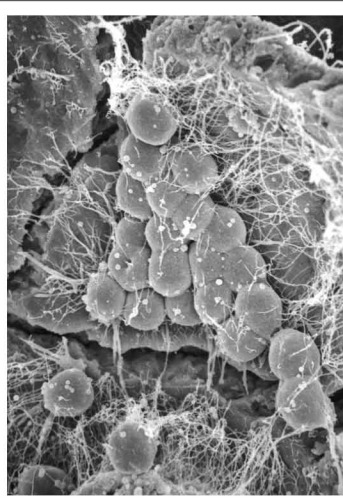
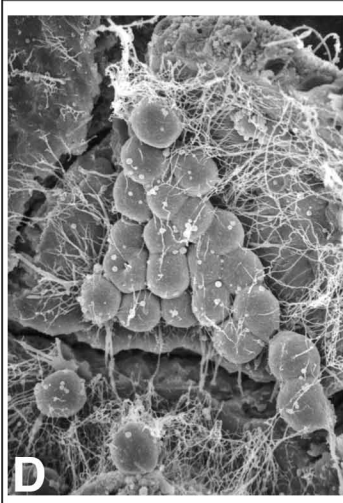
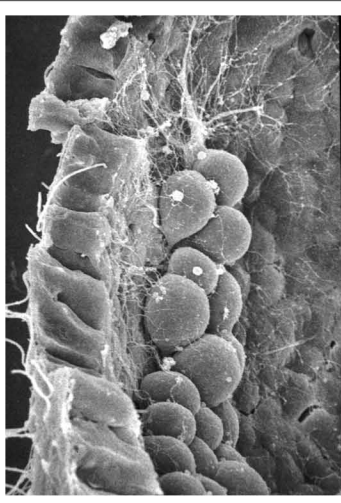
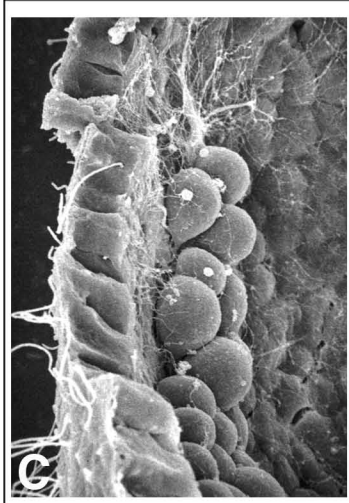
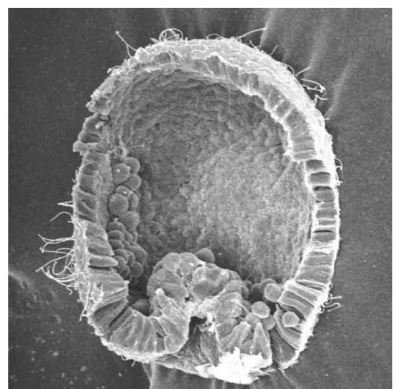
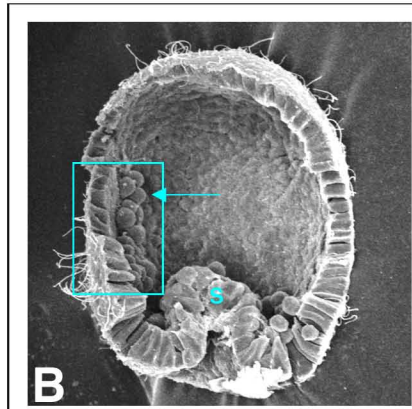
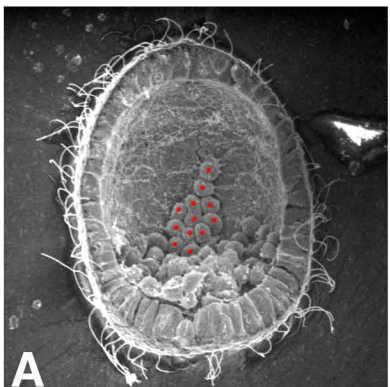


PLATE 29
Formation of Primary Mesenchyme Cell Syncytial Ring

- A. Oral view of a late gastrula with lateral arms on oral side of the PMC ring. Blue arrows point to the triradiate spicules.
- B. Cross-section of a mid-gastrula stage with one half the PMC ring forming and one PMC aggregation center. Or, oral side. Ab, aboral side.
- C. Cross section of mid-gastrula labeled for 15 minutes with H_3 thymidine. Black nuclei are in the s-phase of the cell cycle. Or, oral side. Ab, aboral side.
- D. Stereopair of a fractured mid-gastrula showing the two aggregation centers (A) with one half of the PMC ring completed and the other half of the PMC ring beginning to develop.
- E,F. The developing half of the PMC ring viewed at 0° tilt (E) and 45° tilt (F) angles. Note the long, anchoring filopodial processes of cells in the aggregation centers. A, PMC aggregation centers.
Bar, 10 μ m.

PLATE 29

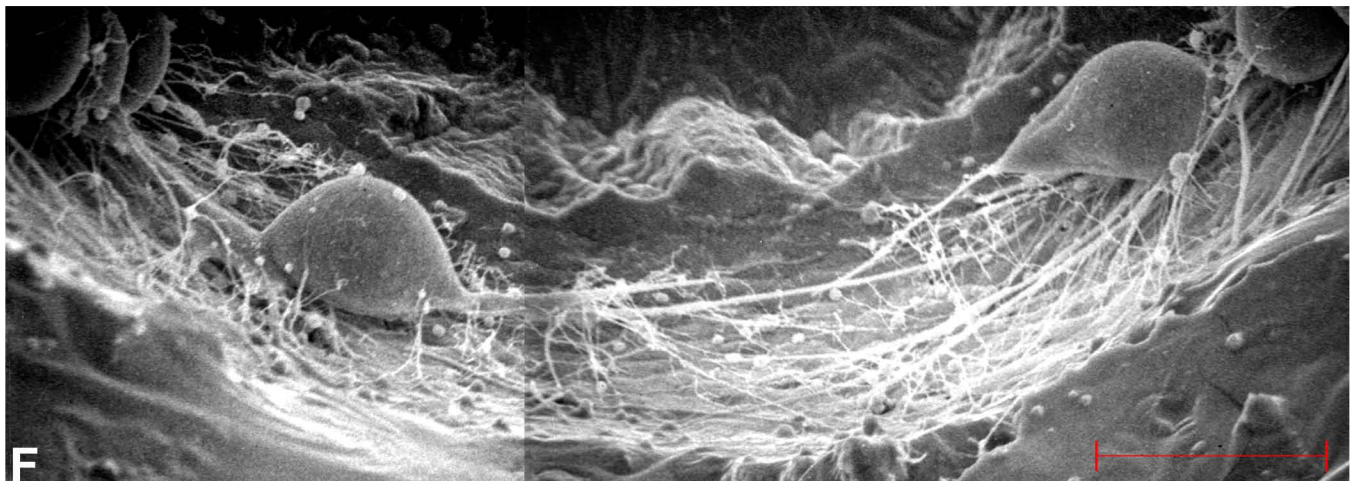
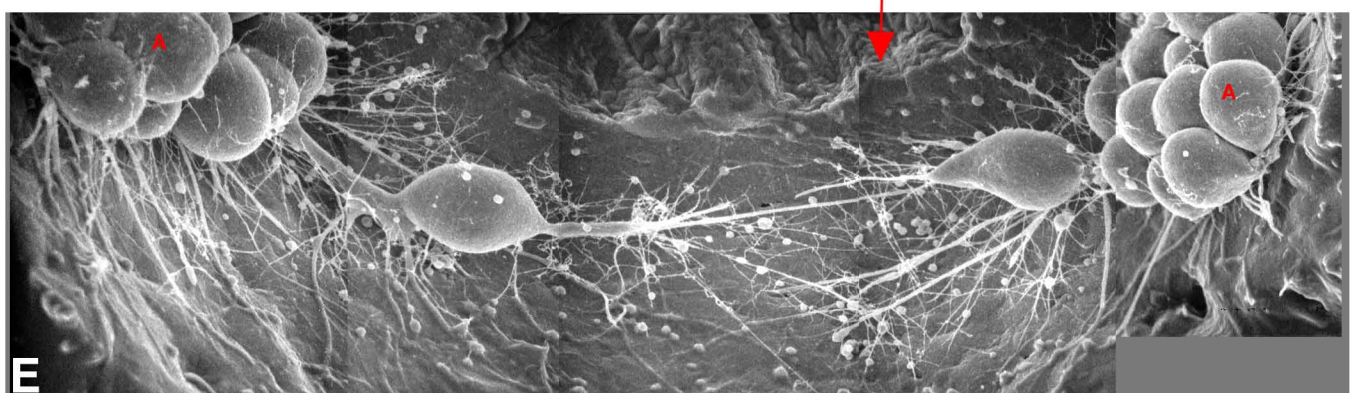
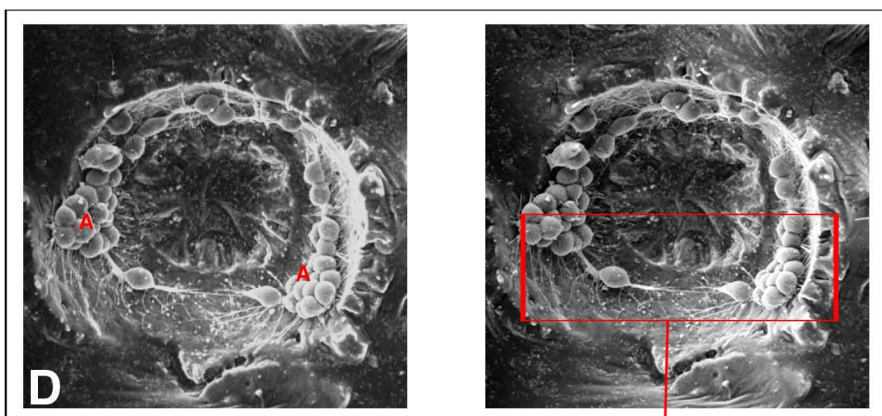
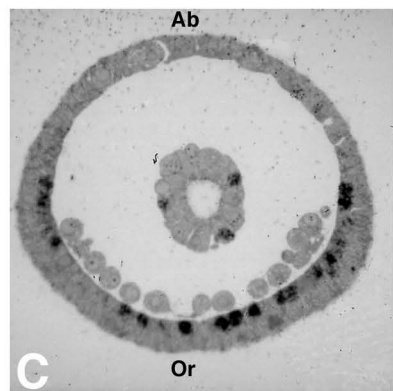
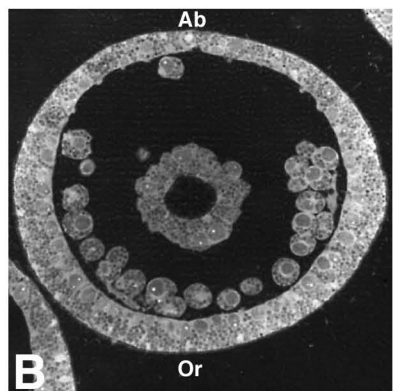
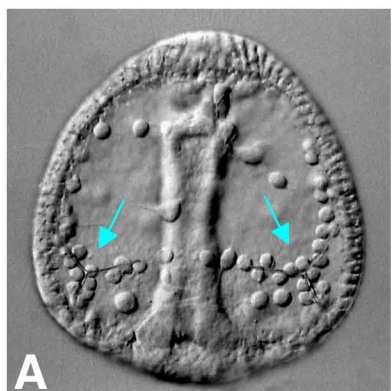
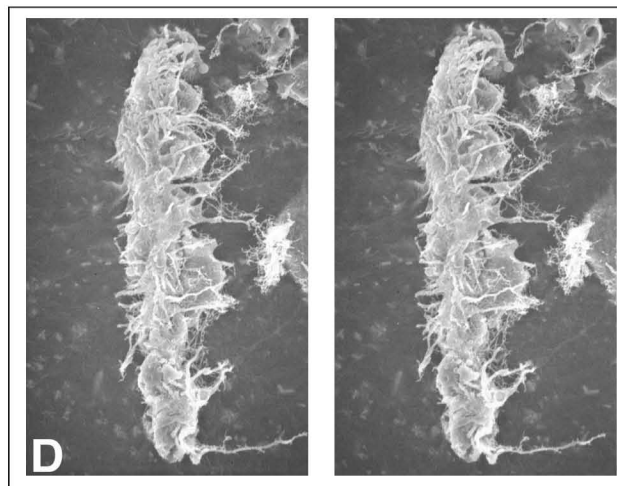
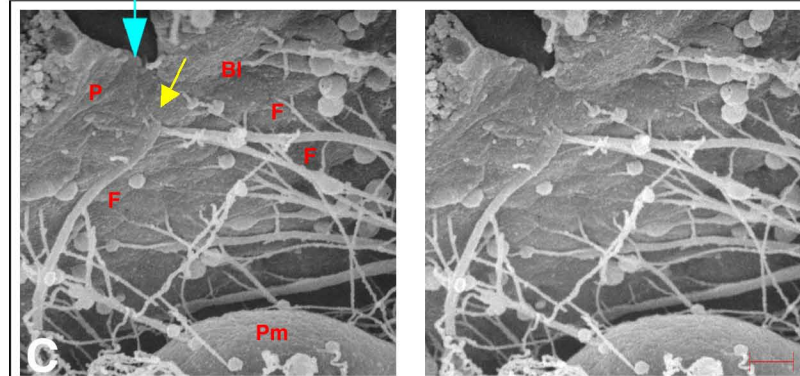
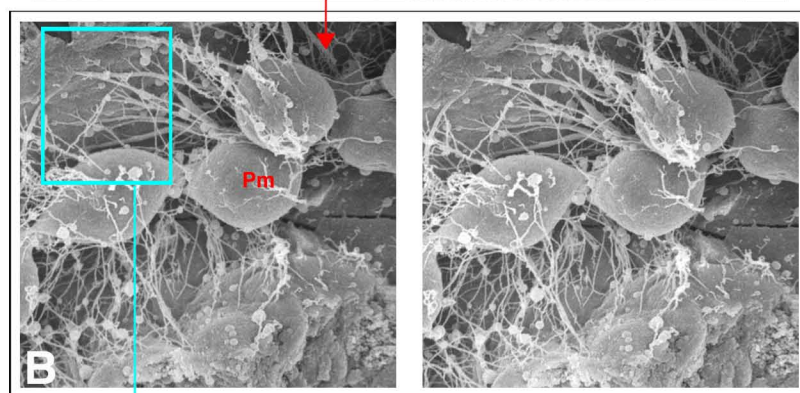
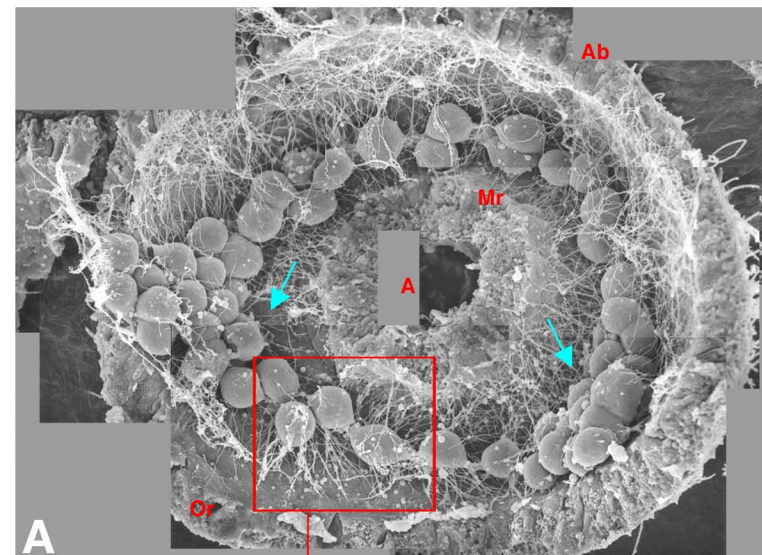


PLATE 30
Completed Primary Mesenchyme Syncytial Ring of the Late Gastrula

- A. Fractured late gastrula shows the bilateral symmetry of the PMC ring, the two ventrolateral branches and the oral (Or) and aboral (Ab) sides of the embryo. Fifty-one PMC are visible.
- B. Stereopair of PMCs of oral side of PMC ring attached to basal lamina of the ectodermal wall by anchoring cell processes.
- C. Stereopair of extracellular cytoplasts and tips of cell processes (F) extending through the basal lamina (B). Bar, 0.1 μ m.
- D. Stereopair view of the basal lamina side of a portion of the PMC ring syncytium.

PLATE 30



Section 8:

Archenteron Formation

PLATE 31

Initiation of Primary Invagination of the Archenteron of the Early Gastrula: Ingression of Secondary Mesenchyme Cells

- A. Initial ingression of SMCs around the eight SMDs (red arrow) that protrude at the vegetal pole.
This is the hemorrhoid phase of primary invagination.
- B. Sagittal section of vegetal plate. Approximate limit of SMCs shown by dashed lines.
- C,D. View of vegetal plate with hyaline layer removed. Remnant of the hyaline layer surrounds the eight SMDs.
- E. Stereopair of vegetal plate with hyaline layer removed. The eight SMDs here will be passively carried inside and form the blind end of the developing archenteron throughout the gastrula stage.
- F. Stereopair of an embryo with the hyaline layer and apical lamina removed shows arrangements of SMCs and endoderm cells in the vegetal plate region.
- G-J. Three views of an embryo undergoing early primary invagination. (G) External indentation of vegetal plate SMCs around the SMDs. (H) An oblique lateral view of the ingressing SMCs (red arrow) with PMCs in their migratory phase. (I) Ingressing SMCs viewed from a different stage tilt angle. (J) Stereopair shows the ingressing SMCs converging around the apical ends of the SMDs.
- K. Stereopair view of the tip of the archenteron with SMCs beginning to migrate from the tip.
Some SMCs have cell processes that converge upon the SMDs in the central region of the archenteron.
- L,M. Views of the vegetal plate of a late mesenchyme blastula after ingestion of the PMCs show arrangements of cells around the eight SMDs.
- N,O. Views of the vegetal plate displaying bilateral symmetry in the arrangement of cells around the initial blastopore. (B). Ab, aboral side. Or, oral side. R, right side. L, left side.

PLATE 31

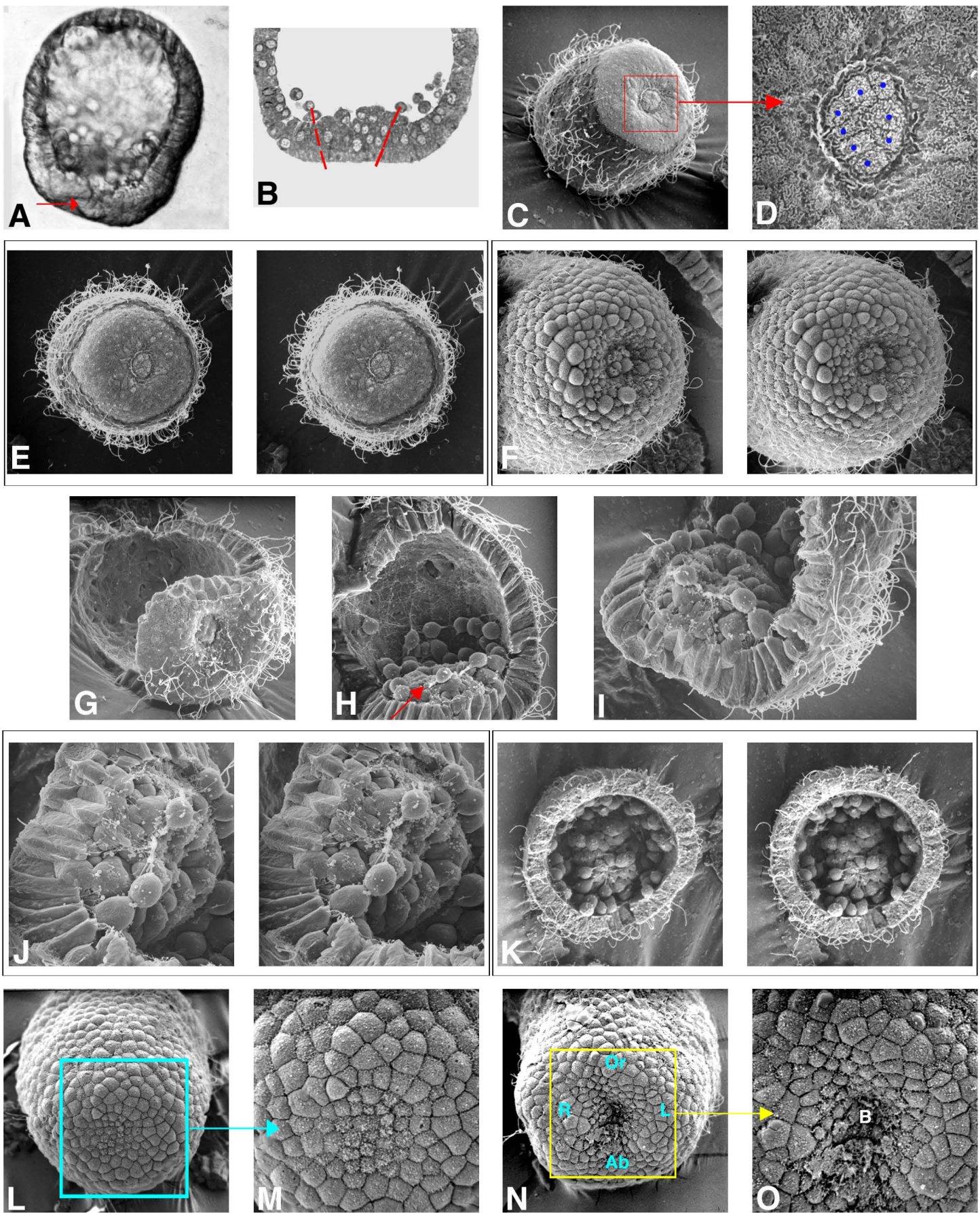


PLATE 32
Gastrula – Primary Invagination of Archenteron

- A. Longitudinal section of vegetal half of early primary invagination. Dashed lines mark limits of ingressing SMCs.
- B,C. Autoradiographs of early gastrulae incubated in ^3H -thymidine for 25 minutes. (B) Longitudinal section shows accumulation of labeled nuclei in the vegetal plate region. (C) Transverse section through the vegetal plate. Labeled cells encircle the vegetal plate surrounding the basal region of the archenteron.
- D,E. Oral side view of early gastrulae: note bilateral symmetry of the blastopore. (D) Ciliated embryo.
(E) Deciliated embryo.
- F. Stereopair view of ingressed SMCs.
- G. Polar view of ingressed SMCs at tip of invaginating archenteron before some of the SMCs begin to form extended cellular processes.
- H. Stereopair of luminal wall of the archenteron.
- I,J. Endoderm cells of archenteron wall with short, 2 μm long cilia (red arrows).
Bar, 1 μm .
- K,L. SEM of archenteron at the end of primary invagination and beginning of secondary elongation. SMCs have long exploratory processes. Bar, 10 μm .
- M. Stereopair of SMCs with 10 μm long cell processes at the distal end of the archenteron. A. PMC aggregation centers.

PLATE 32

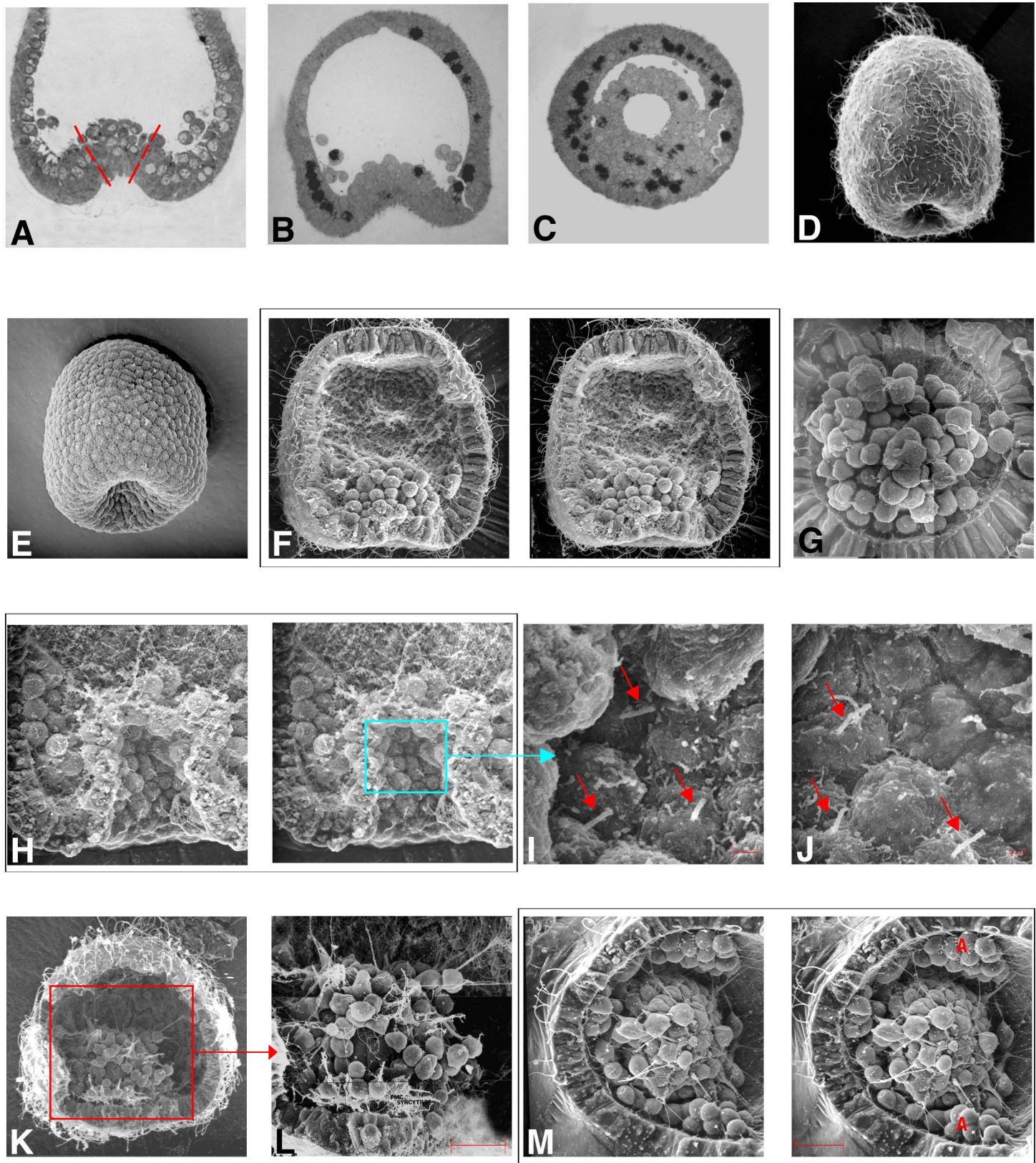


PLATE 33
Gastrula – Secondary Elongation of Archenteron

- A-G. Light micrographs of archenteron elongation. (A) Cross sectional view of archenteron and bilateral PMC aggregations. (B-F) Oral –aboral views of elongation of archenteron. (D-E) SMCs can be seen leaving the tip of the archenteron and migrating toward the acron region. (G) Lateral view of a late gastrula. The tip of the archenteron bends after attachment to the acron. Red arrow, triradiate spicules. Ab, aboral side. Or, oral side.
- H-K. SEMs of various morphologies of the SMCs at the beginning of secondary elongation in four different embryos.
- L-M. SEMs of archenteron extension. SMCs at the tip of the archenteron extend numerous thick filopodia toward the ectodermal wall. (L) Four tiers of endodermal cells. (M) Five tiers of endodermal cells.
- N-Q. Progression of elongation during the latter half of the gastrula stage. (N) Five tiers of endodermal cells. (O) Six tiers of endodermal cells. (P) Seven tiers of endodermal cells. (Q) Ten tiers of endoderm cells in the archenteron whose distal end is capped by at least 30 SMCs.
Bar, 10 μ m.

PLATE 33



A



B



C



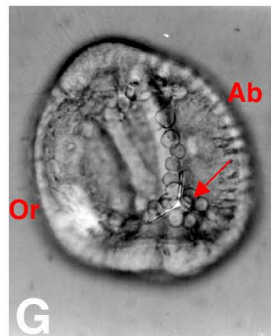
D



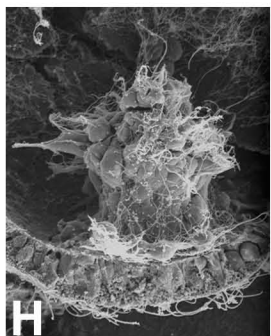
E



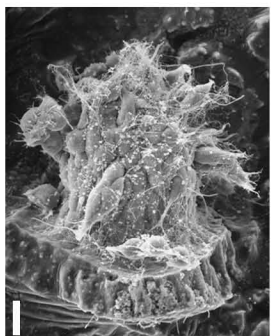
F



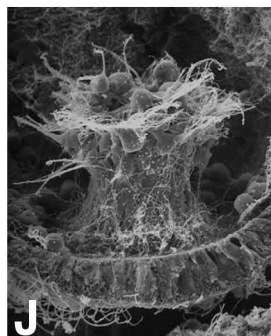
G



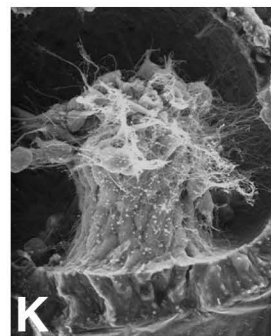
H



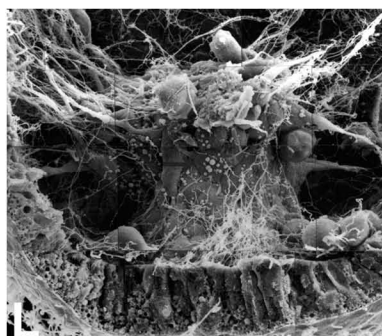
I



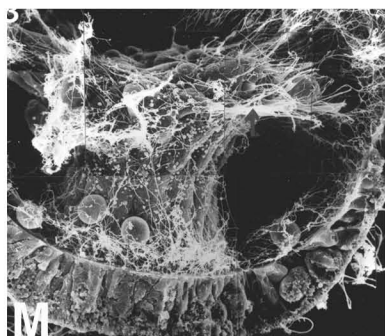
J



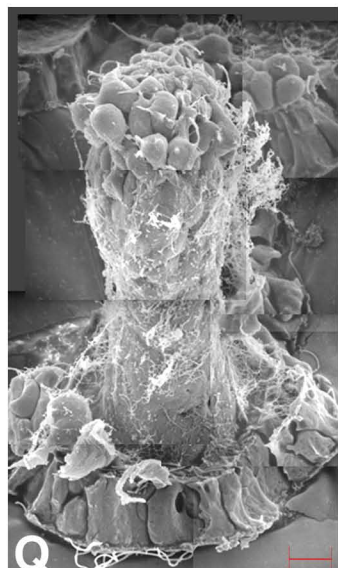
K



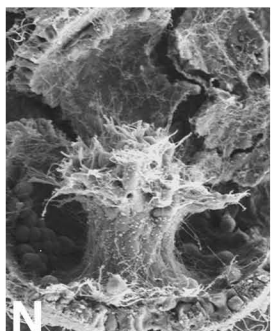
L



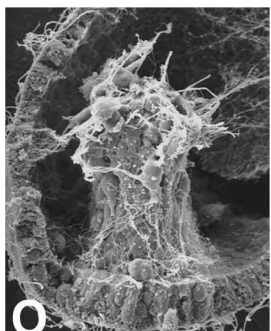
M



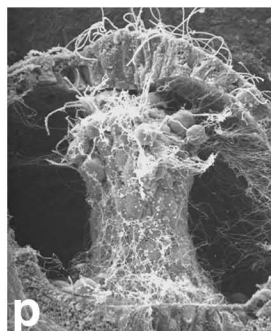
Q



N



O



P

PLATE 34
Gastrula – Confocal Images of Feulgen Stained Nuclei
of Gastrulae During Secondary Elongation of the Archenteron

The two left columns are stereo pair images of thirty nine to forty four 1 μ m optical sections. The images in the right column are short stacks of nineteen to twenty-seven 1 μ m optical sections. The arrows point to the nuclei of the SMD cells that form the distal end of the archenteron.

- A,A1. Beginning of secondary elongation with 43 endodermal nuclei and 38 SMC nuclei.
- B,B1. Midgastrula with SMCs migrating toward the animal pole. Archenteron with 39 endoderm nuclei.
- C,C1. Late gastrula near end of secondary elongation with 76 endodermal archenteron nuclei and 51 SMC nuclei.
- D,D1. Late gastrula at end of secondary elongation with 157 endodermal archenteron nuclei and 28 SMC nuclei at distal end of the archenteron.

PLATE 34

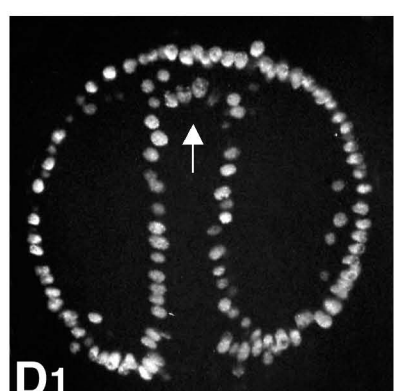
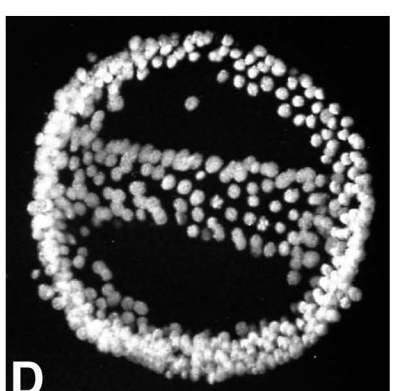
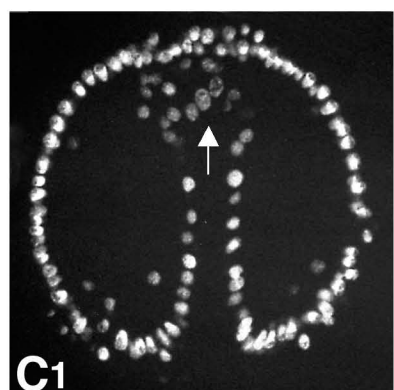
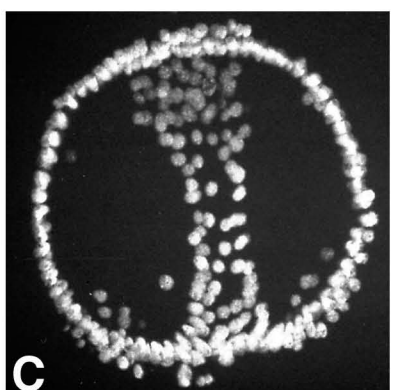
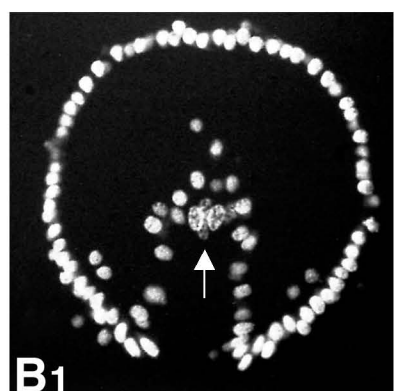
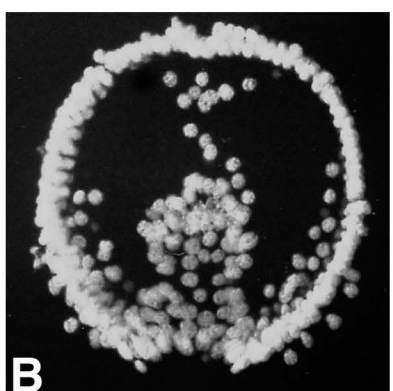
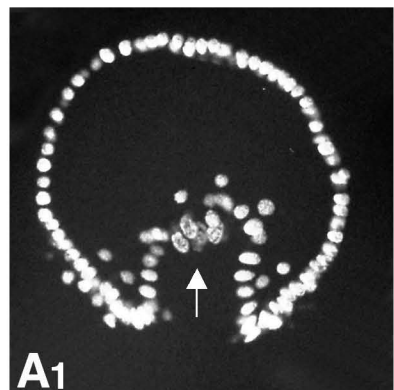
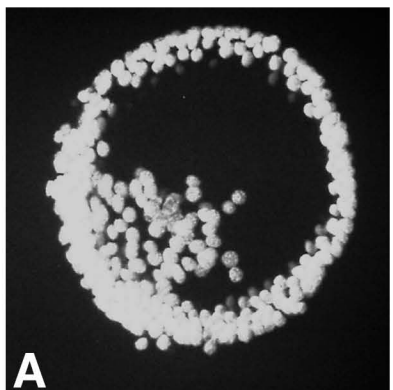


PLATE 35

Archenteron lengths and cell counts in the table and the diagram are from confocal stereo pair images of Fuelgen stained nuclei of gastrulae during the period of secondary elongation of the archenteron. Four of the embryos, with asterisks, in the table are shown on plate 33.

PLATE 35

Table : Archenteron Length and Cell Counts During Secondary Elongation Period (12-15 Hours Post Fertilization)

Hours Post Fertilization	Embryo	Archenteron Length (μm)	Total Number Endoderm Cells	Number of Dividing Cells
12	12A	10	22	0
	12B	25	31	0
	12C	14	40	0
	12D*	23	43	0
13	13A*	37	39	2
	13B	27	47	6
	13C	37	56	2
	13D	38	72	4
	13E	35	75	0
15	15A	67	76	0
	15B	61	84	3
	15C	64	86	5
	15D	69	102	6
	15E*	70	107	7
	15F	75	157	10

Archenteron Length Versus Number of Endodermal Nuclei

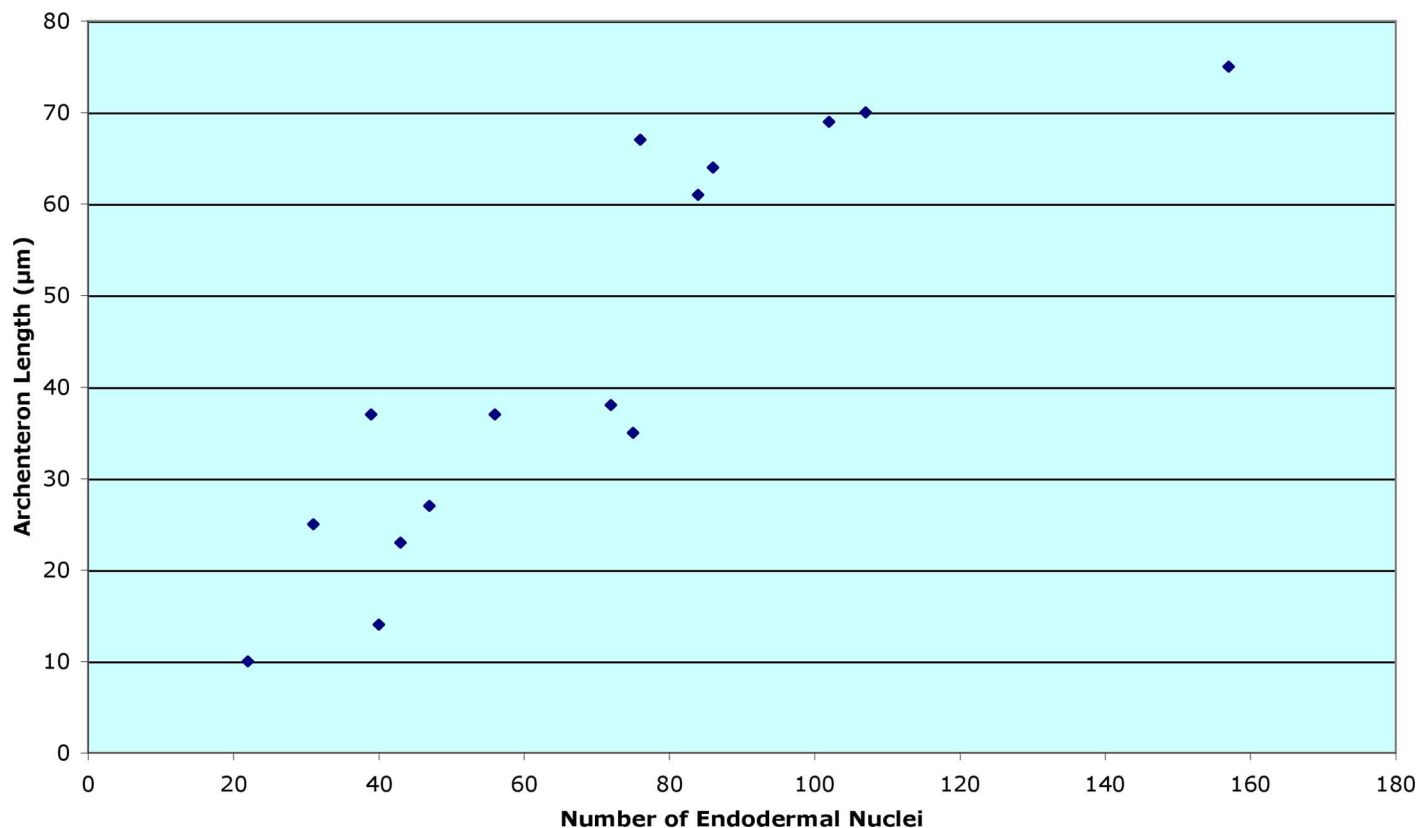


PLATE 36
TEM Views of the Archenteron During the Gastrula Phase of Gastrulation

- A. Photomontage of an A-V section of a gastrula near the end of primary invagination. Arrow points to SMCs at tip of archenteron.
- B. Photomontage of an A-V section of gastrula during secondary elongation. Arrow points to SMCs at tip of archenteron. L, lumen of archenteron filled with an ECM gel.
- C,D,E. Cross sections of the archenteron. (C) In an embryo fixed in gluteraldehyde (GA) and osmium tetroxide (OS) the archenteron ECM is not visible. (D) An embryo fixed in GA/OS plus ruthenium red and calcium. The archenteron ECM gel is preserved and distinct from the hyaline layer lining the luminal wall of the archenteron. (E) The archenteron gel of the archenteron at a higher magnification.
Bar, 1.0 μ m.
- F. An endoderm cell of the archenteron with a short cilium.
- G,H. Sections show possible exocytosis of a vesicle (arrows) into lumen of the archenteron and cellular connections between endodermal cells. Bars: 0.1 μ m.

PLATE 36

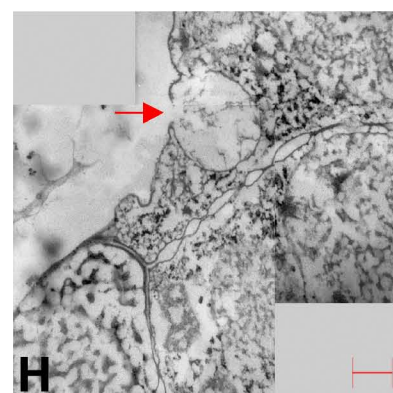
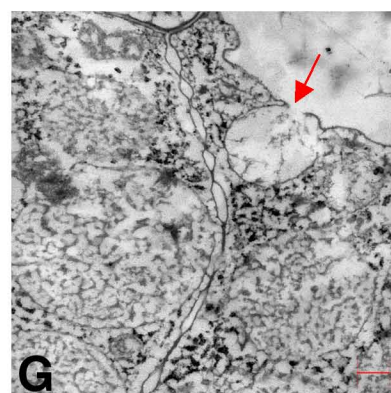
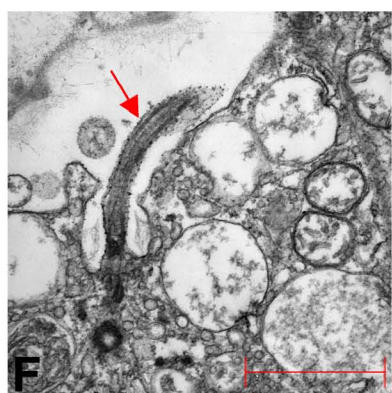
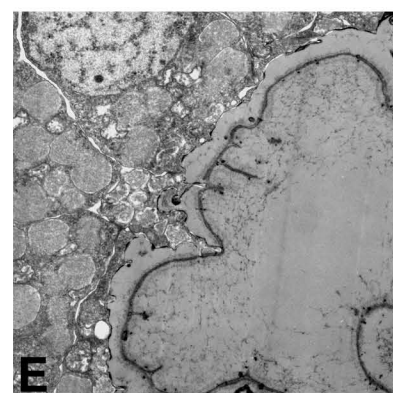
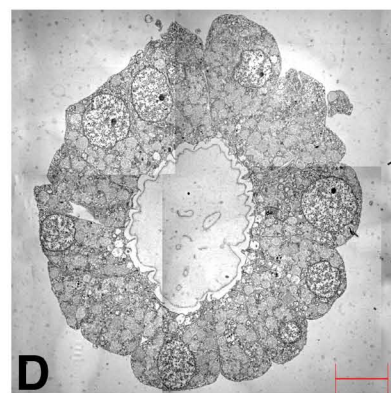
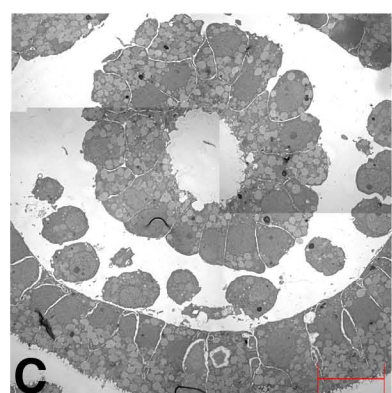
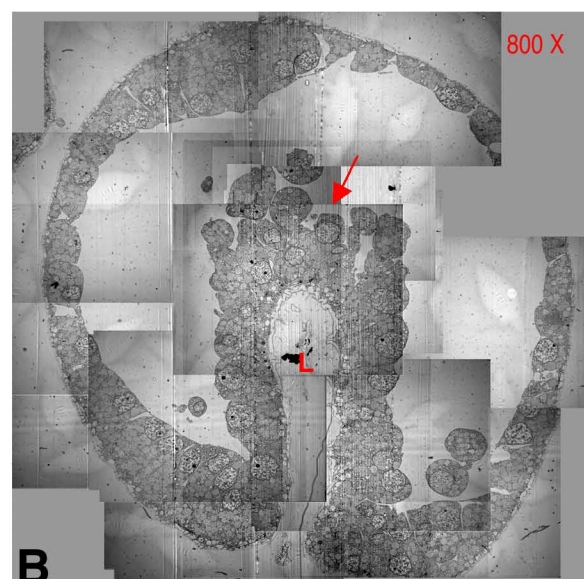
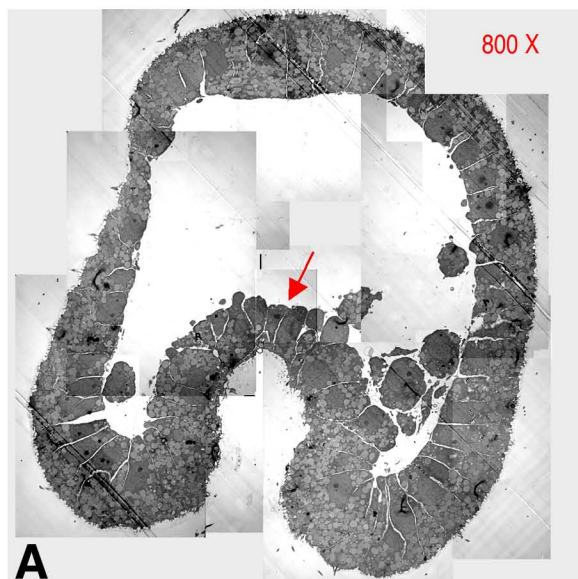
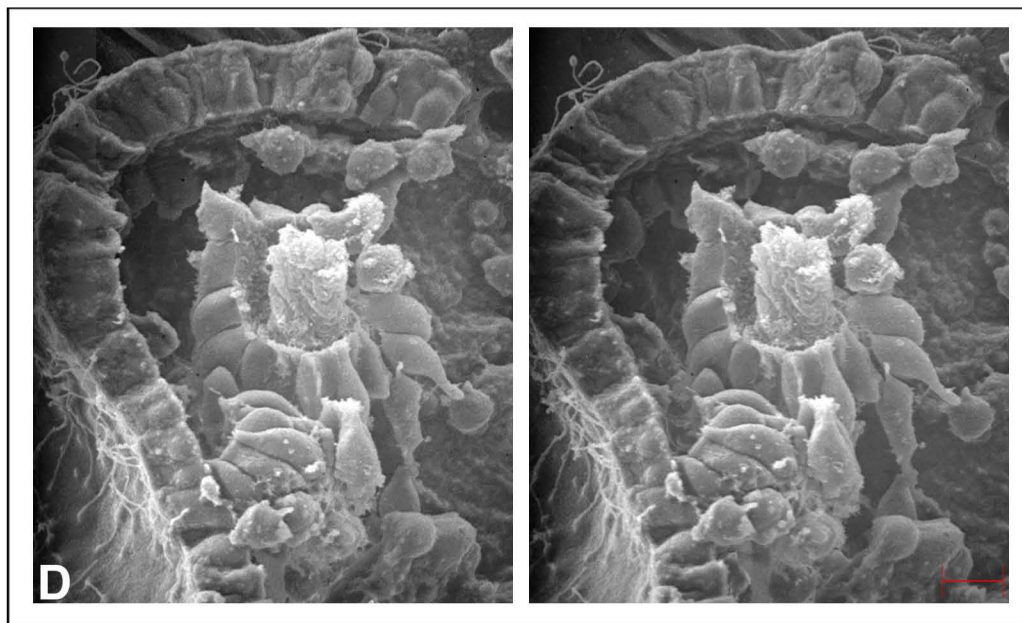
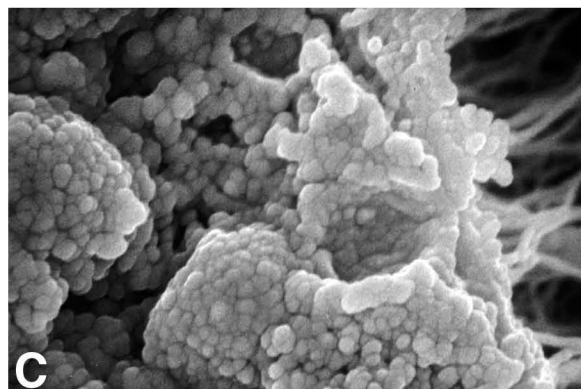
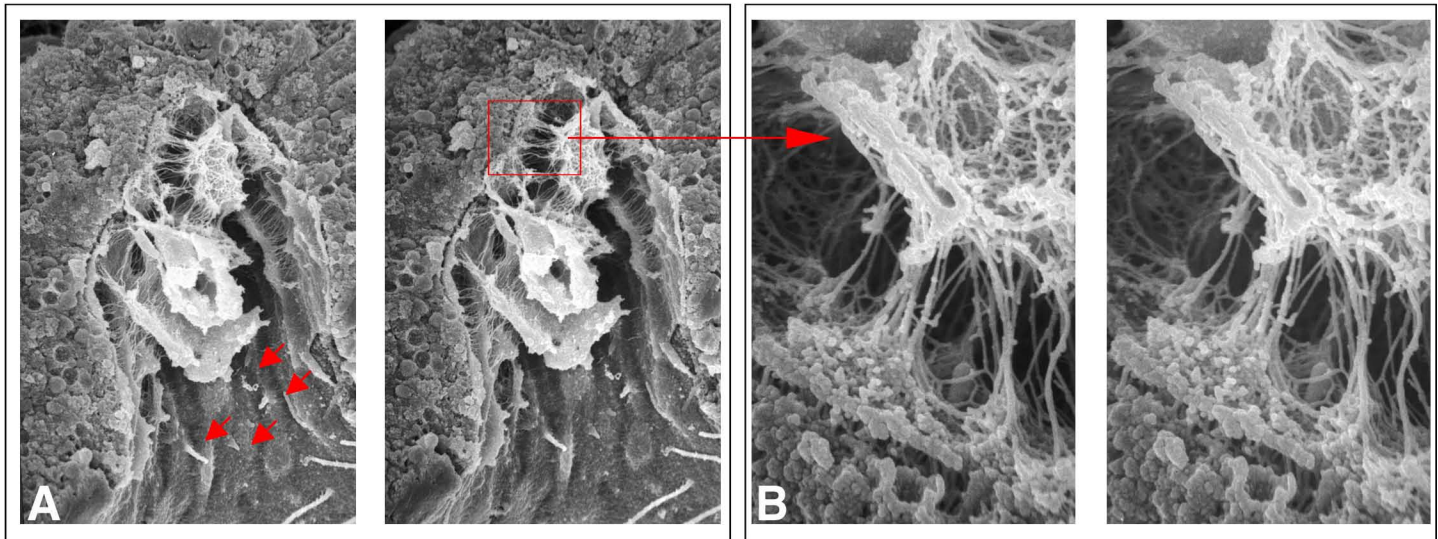


PLATE 37
SEM Views of Extracellular Matrix Gel in the Archenteron Lumen

- A. Stereopair of an archenteron of an early gastrula fractured along the A-V axis. The hyaline layer lines the luminal side of the endoderm cells. The ECM gel of the lumen appears coagulated but attached to the hyaline layer by fiberous strands. Arrows point to the endoderm cells with short cilia.
- B. Stereopair of boxed area in A at higher magnification.
- C. Surface of hyaline layer of wall of archenteron in A and B. The appearance of the hyaline layer is typical for embryos fixed in GA/Os/RR and calcium fixative.
- D. Stereopair of an early gastrula with the archenteron fractured near the blastopore. The coagulated archenteron gel appears as an ECM plug in the lumen of the archenteron. Bar, 10 μ m.

PLATE 37



Section 9:
Post Gastrula Prism
&
Pluteus Larva

PLATE 38
Prism Stage Larvae

- A. LM oblique, lateral view of an early prism larva focused on a fully developed triradiate spicule and PMC syncitium.
- B. LM lateral view of prism larva to show tilted, thickened apical plate (Ap), the oral (Or) and aboral (Ab) sides.
- C. Stereo pair view of ciliated prism larva.
- D. Prism larva with cilia regenerating 30 minutes post deciliation. Cells of ciliary band (Cb) regenerate faster than cells of the oral (Or) or anal plate (Ap) ectoderm.
- E. Prism larva with cilia of ciliary band (Cb), plucked off. Six to eight rows of ciliated cells form the ciliary band.
- F,G. LMs of a prism larva viewed from the aboral side (F) and oral side (G).
- H. Oblique lateral view of a ciliated prism larva.
- I,J. (I) Stereo pair of deciliated larva oriented as in H. (J) Larva oriented to show bilateral form of the blastopore. Ab, arm bud. Or, oral side.
- K. Aboral view of a stereo pair of a fractured early prism larva with fully elongated archenteron (A) covered with a basal lamina and apical tuft (At) of elongated cilia.
- L,M. Higher magnifications of the basal lamina of the elongated archenteron in (K).
Bar, 1.0µm.
- N,O,P. (N) Low magnification of three fractured larvae. Number 1 larva is shown at a higher magnification in the stereo pair (O). SMCs appear to migrate over the developing basal lamina shown in (O) and (P).
Bar, 10µm.

PLATE 38

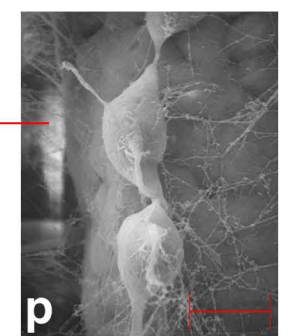
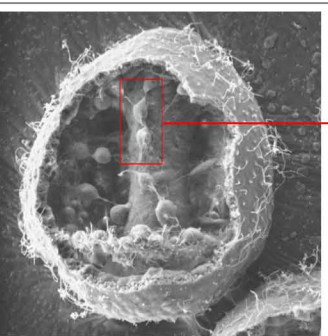
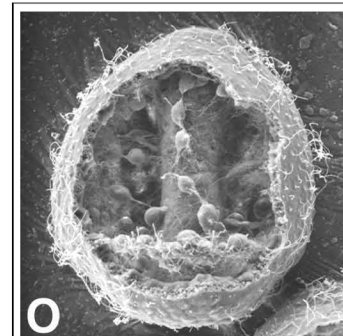
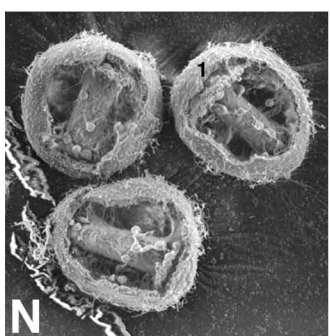
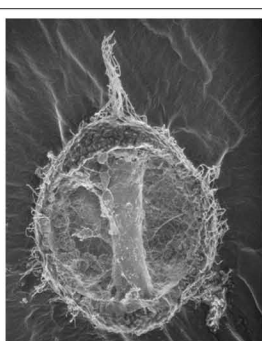
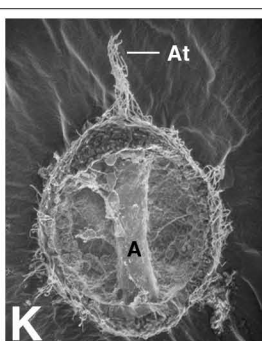
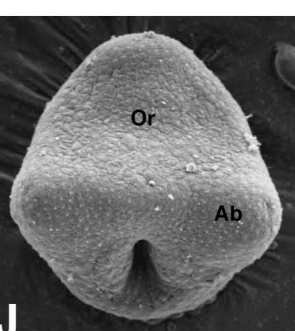
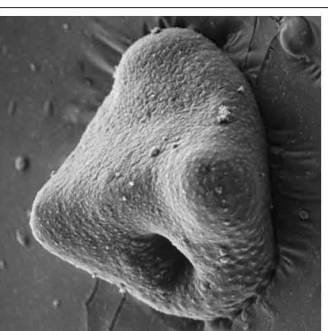
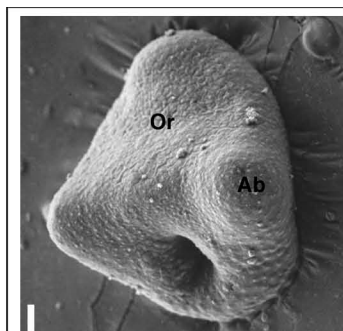
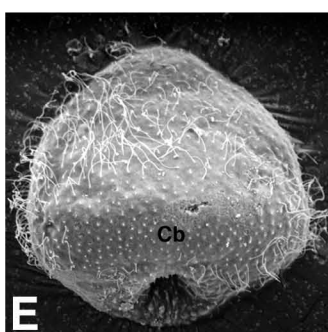
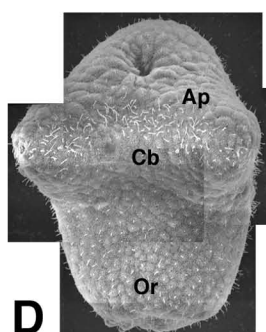
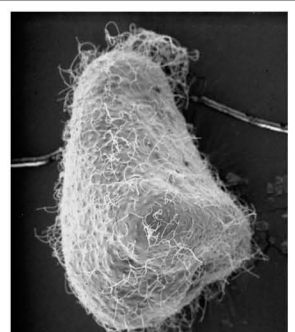
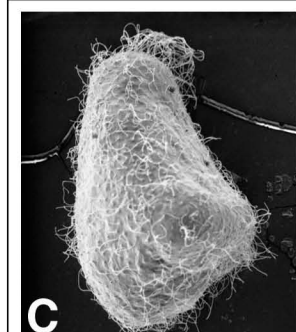
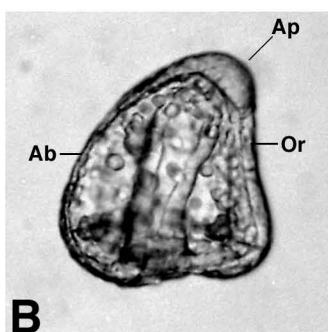


PLATE 39
Two Arm Pluteus Larvae

- A-C. Three views of early 2 arm plutei deciliated and dehyalinated and fixed for 30 min. post deciliation to show regeneration of ciliary band. (A) Lateral view. (B and C) Anal plate views.
- D, E. Anal plate view of early 2 arm pluteus. Note the rounded posterior end of the larva as compared to slightly older larvae in (F) and (G).
- F,G. Two arm plutei with squared off posterior ends.
- H-K. Fully developed 2-arm plutei. (H-J) Anal plate views. (K) Lateral view; arrows point to protrusion of body underlain by the developing recurrent rods of the larval skeleton.
- L-O. Four views of the fully developed 2-arm pluteus deciliated and dehyalinated (L) Anal or ventral view. (M) Aboral or dorsal view. (N and O) Lateral views. Note the delineation of the ciliary band cells of which there are six to eight rows of cells.
- P,Q. Deciliated, dehyalinated pluteus. (P) View of the ventral region of the ciliary band. (Q) The ciliary band consists of eight to nine rows of ciliated cells.
- R-S. Deciliated, dehyalinated larva shows the arrangements of cells of the ectodermal margin of the everted proctodeum.

PLATE 39

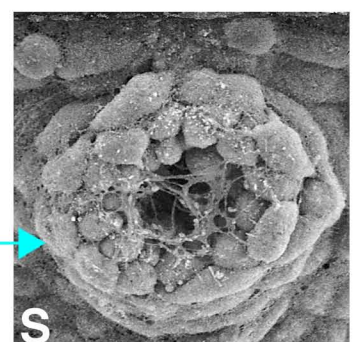
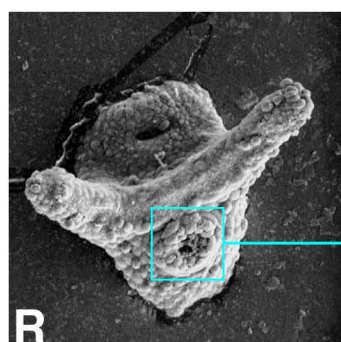
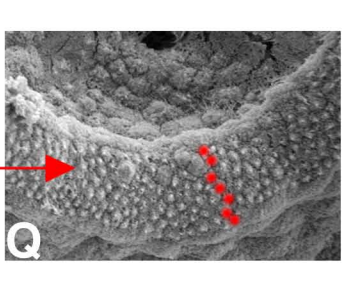
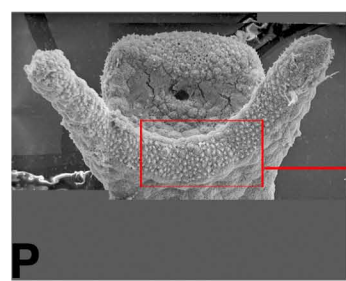
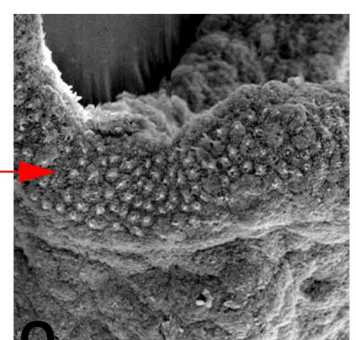
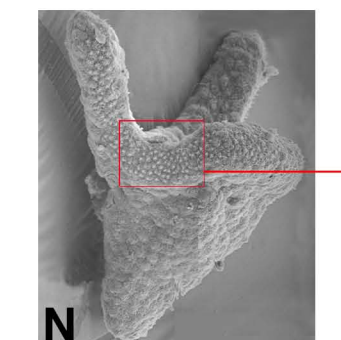
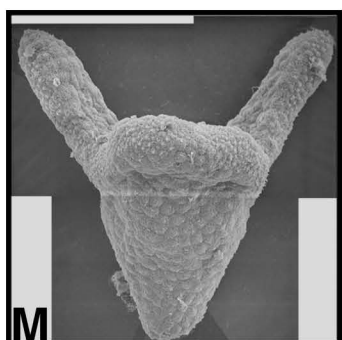
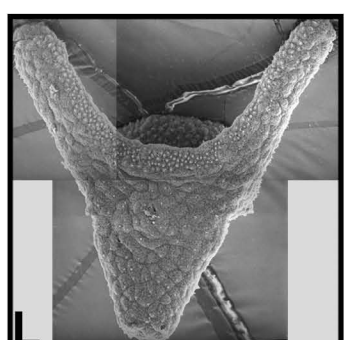
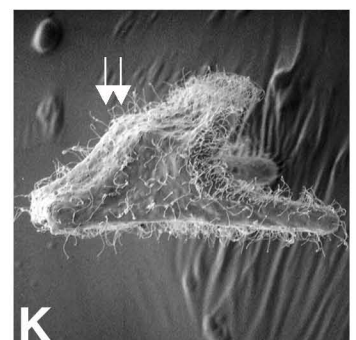
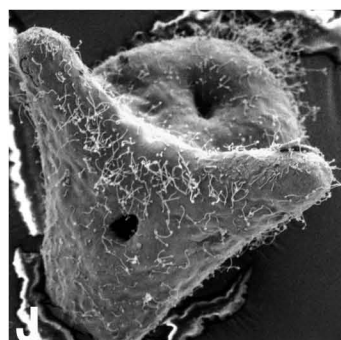
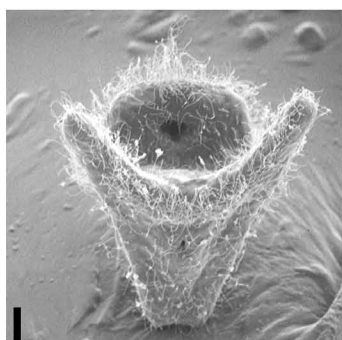
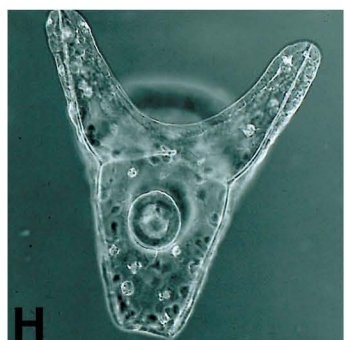
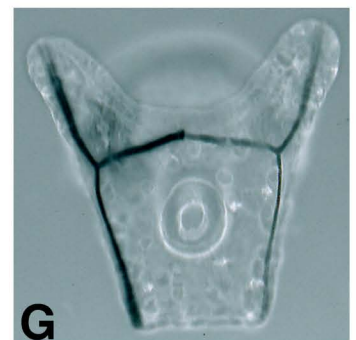
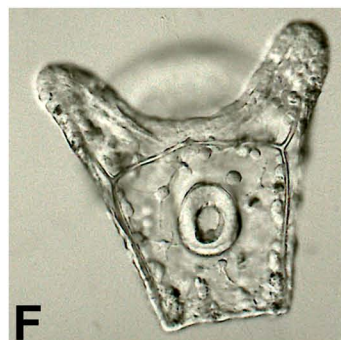
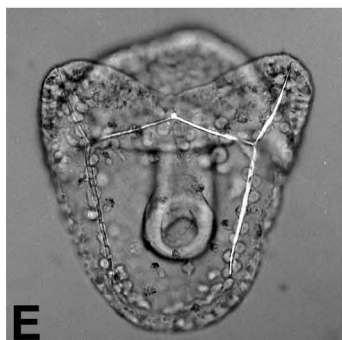
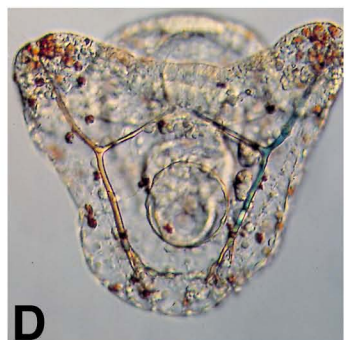
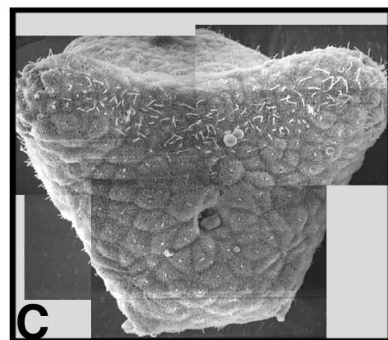
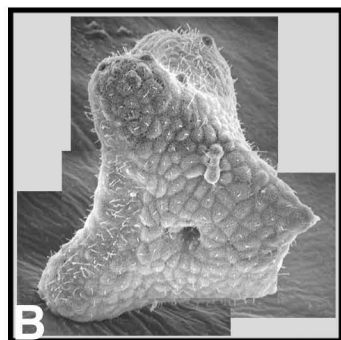
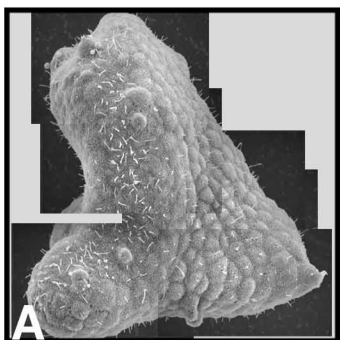


PLATE 40
Four Arm Pluteus Larvae

- A- Four arm pluteus larvae showing the distribution of red echinochrome pigment cells
- B. (echinophores). (A) Bright field (B) Partial polarized light to highlight larval skeleton.
- C- Dorsal (C) and ventral (D) views of the same pluteus larva with well developed oral and
- D. post anal arms and tripartite gut.
- E. Dorsal view of a pluteus larva.
- F. Ventral (anal) view of pluteus larva. Larval skeletal rods are birefringent in polarized light while the echinophores are black.

Key to labels in figures A-F

- Or. Oral arm
- Ab. Aboral arm
- m. midgut (stomach)
- e. foregut (esophagus)
- i. hindgut/anus (intestine/proctodeum)

PLATE 40

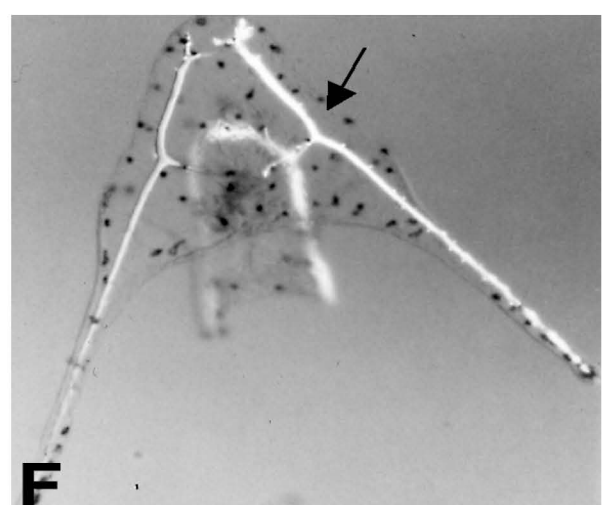
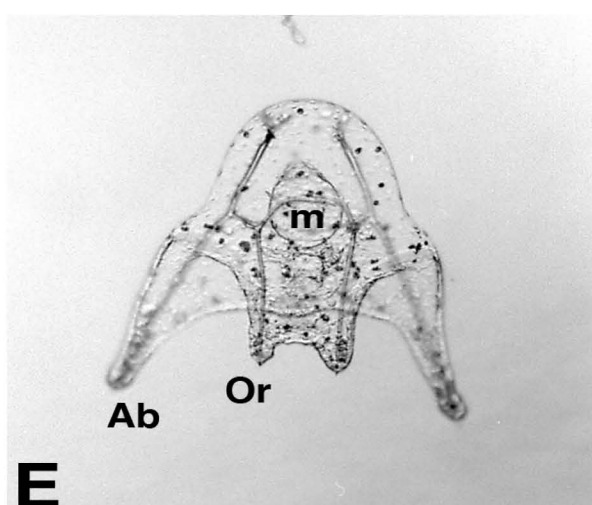
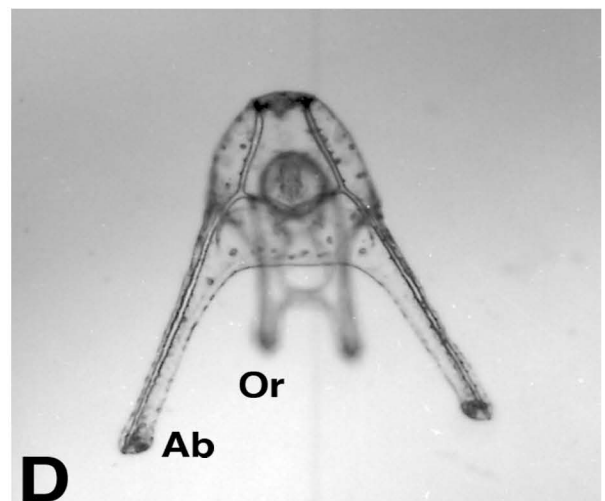
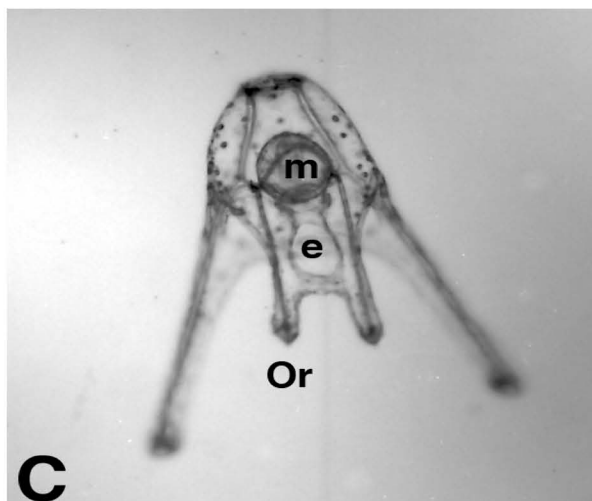
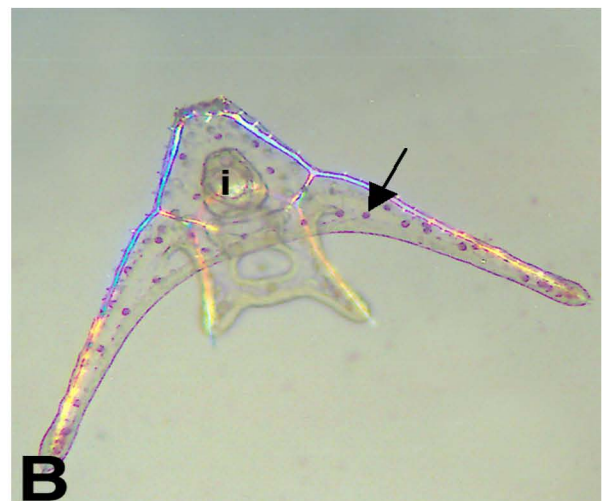
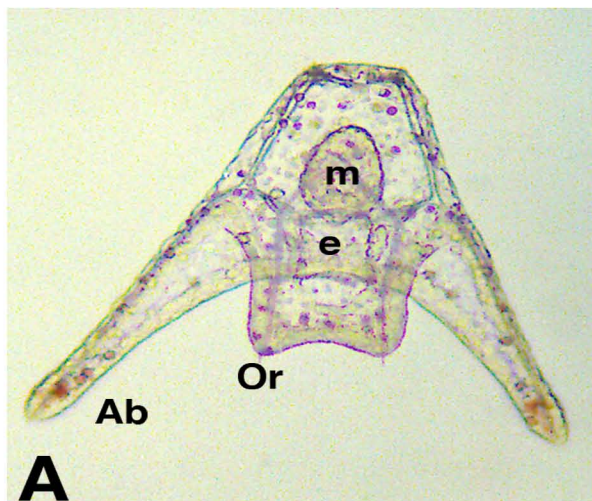
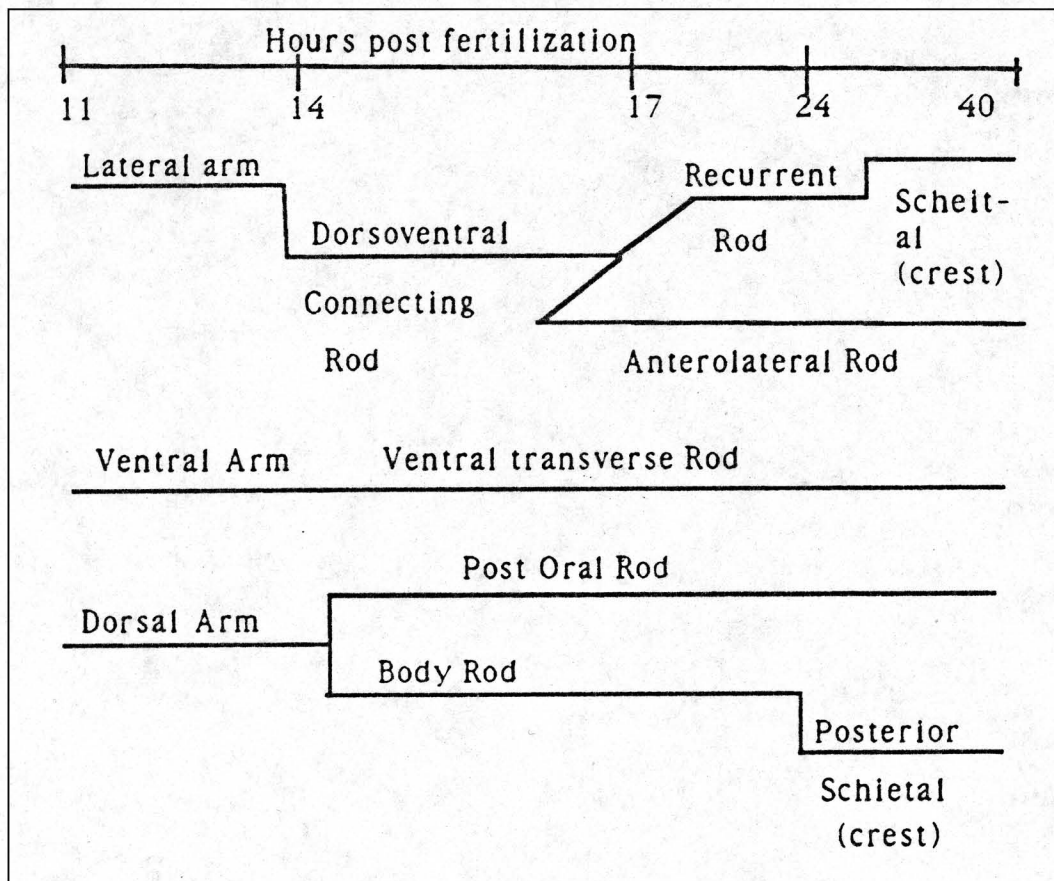


PLATE 41

Skeletal Rod Lengths (μms) from the Triradiate Spicule
Forming Center of Late Gastrula To 40 Hour Pluteus

STAGE	Late Gastrula	Late Prism	Short Arm Pluteus	Long Arm Pluteus
Hours Post Fertilization	14hrs	17hrs	24hrs	40hrs
LATERAL ARM	20			
DorsoVentral Connecting Rod		14	14	14
Anterolateral Rod			60	152
Recurrent Rod			42	42
Crest				17
VENTRAL ARM	17			
Ventral Transverse Rod		45	57	57
DORSAL ARM	17			
Post Oral Rod		17	175	266
Body Rod		46	133	133
Posterior Crest			30	121
Total Lengths	54	122	511	812
Growth Rate($\mu\text{m}/\text{hr}$)	18	41	73	51

Development of Larval Skeletal Rods from Triradiate Spicule Arms
from Early Gastrula to 40 Hours Post Fertilization



Section 10:

Development of Animal Pole Ectoderm

PLATE 42
Early Development of Animal Pole Ectoderm

- A-C. Animal pole views of three embryos during the 8th cleavage cycle. Cells with red and blue dots are descendants of the An₁ tier of mesomeres of the 5th cleavage.
- D. View of embryo in (C) enlarged to show the four cross cells (red dots) surrounded by ten other cells (blue dots).
- E. Blastocoelic side of the animal pole ectoderm forming the apical plate region of an early mesenchyme blastula. (E) Six cells (red dots) surrounded by eleven other cells (blue dots) form the central region of the acron. In this embryo there are a total of 84 cells in the apical plate.
- F,G. Blatocoelic side of the animal pole ectoderm of another early mesenchyme blastula. The central cells of the apical plate region have connecting cellular processes that distinguishes the apical plate from the cells of the lateral wall ectoderm. Of the 48 cells in the apical plate, the central 32 cells are from the An₁₁ tier of cells of the 7th cleavage.
- H. TEM montage of an A-V section of the animal half of a mesenchyme blastula. Dashed lines delineate peripheral limit of the apical plate. Short arrows point to overlapping basal ends of the lateral wall ectoderm cells.
- I. TEM montage of the apical plate region of an early gastrula. Dashed lines delineate periphery of the apical plate.
- J, K. Comparison of apical plate cells (J) with lateral with ectoderm cells (K) of the embryo in (I)).

PLATE 42

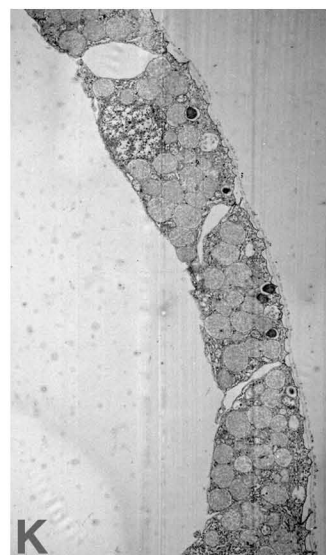
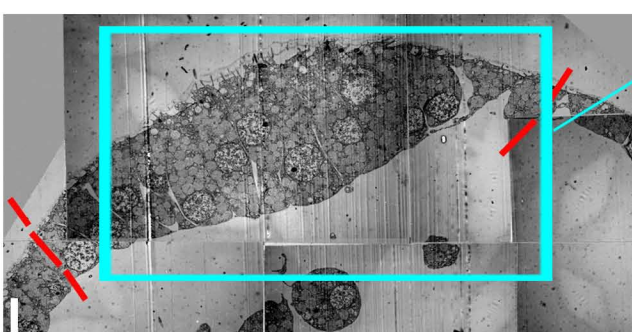
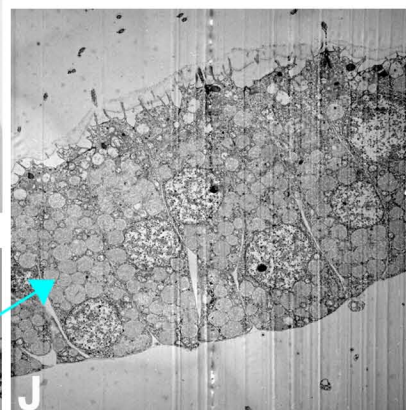
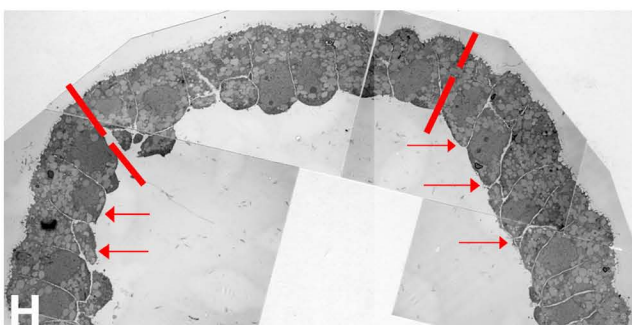
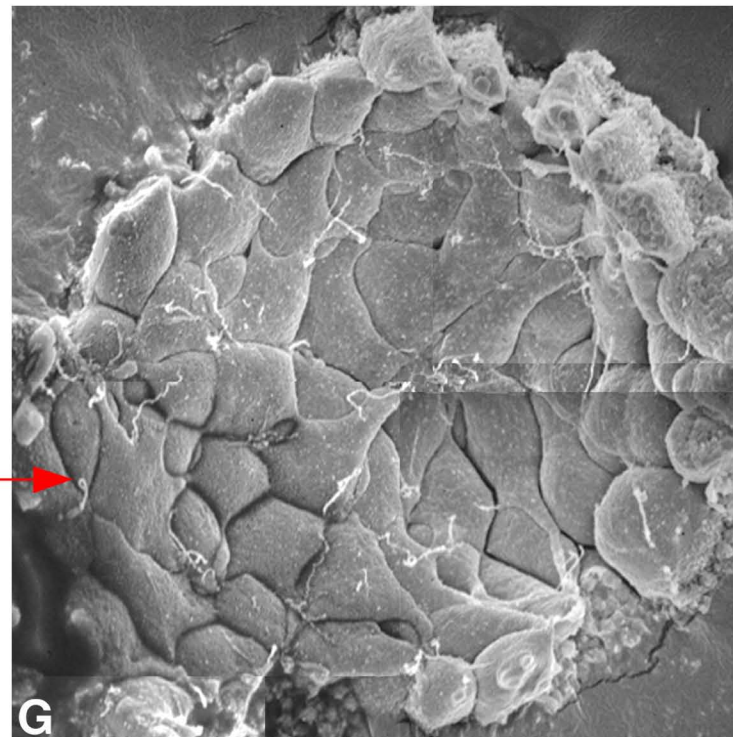
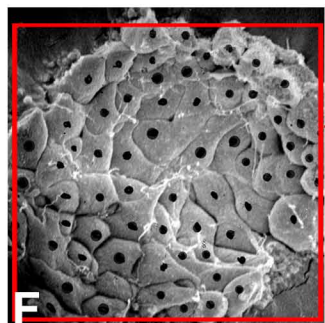
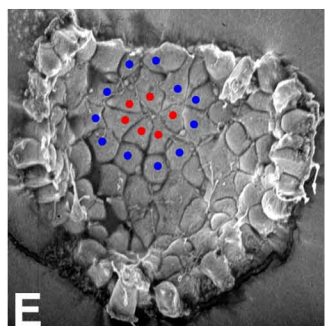
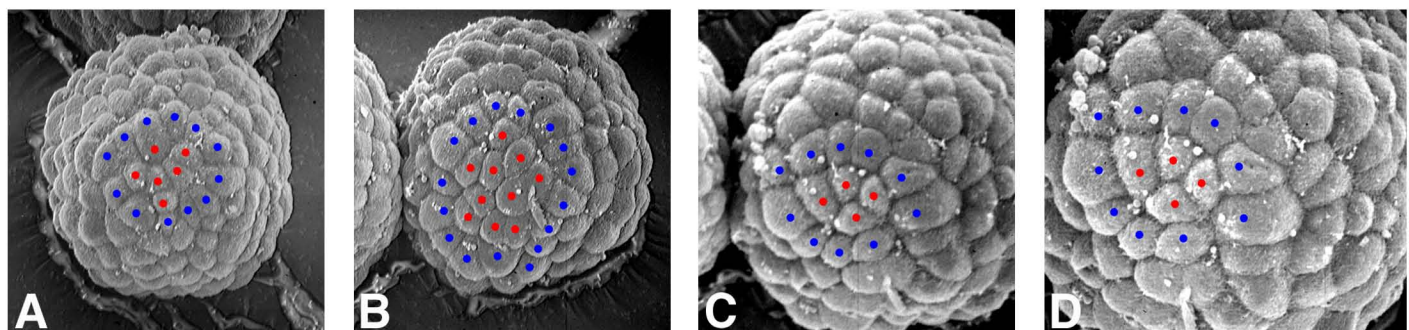
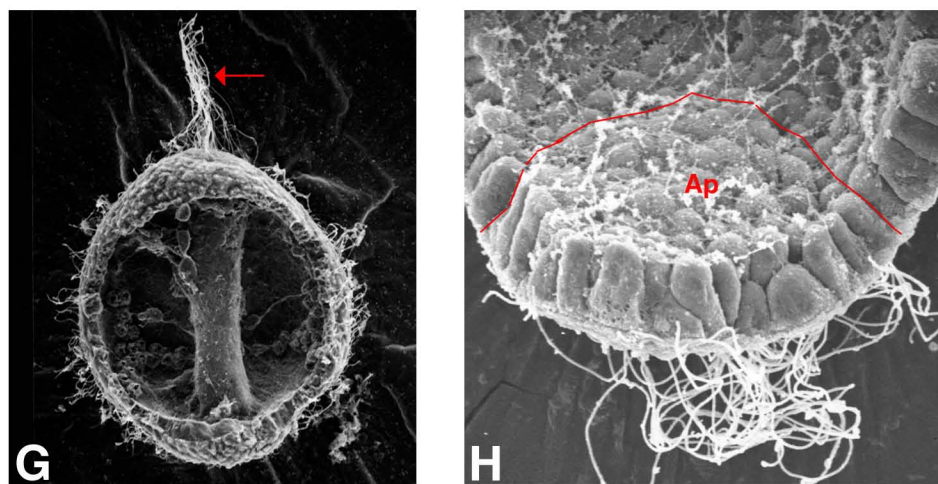
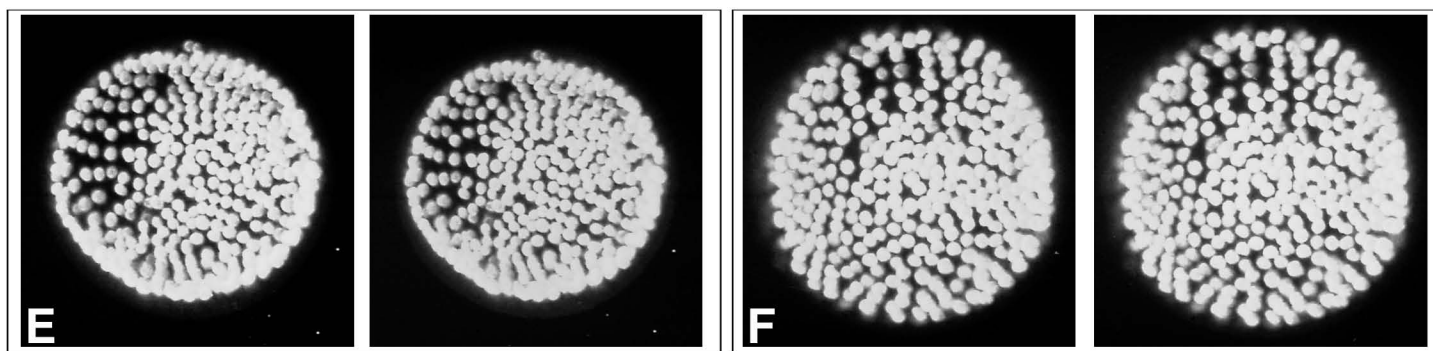
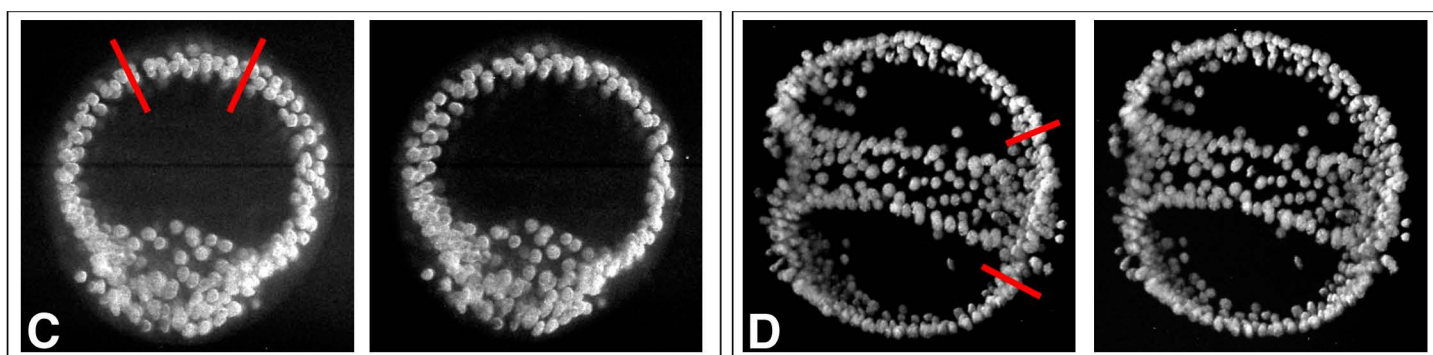
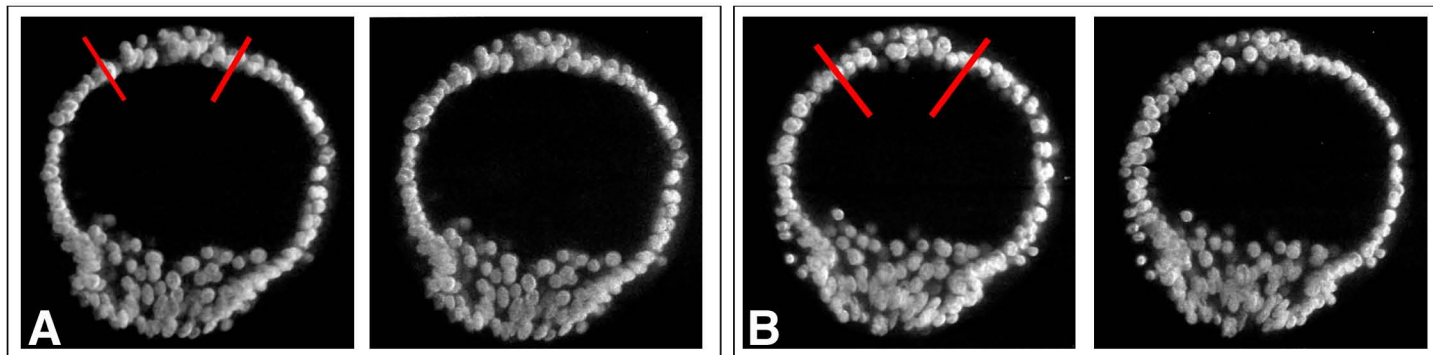


PLATE 43
Apical Plate Ectoderm of Mesenchyme Blastula and Late Gastrula

- A-C. Stereopair confocal images of Feulgen stained nuclei of a mesenchyme blastula. Each stereo pair is a short stack of four, 1 μm thick optical sections. The red lines mark the peripheral limits of the apical plate.
- D. Stereopair image of confocal image of Feulgen stained nuclei of a late gastrula. Red lines mark the peripheral limits of the apical plate.
- E, F. Stereopair confocal images of the nuclei of the animal hemisphere of two gastrulae.
- G. Fractured late gastrula with long acron cilia (arrow) at the center of the apical plate.
- H. Fractured late gastrula with the basal side of the apical plate (AP) delineated by a red line.

PLATE 43



Section 11:

Ectodermal Cilia

PLATE 44
SEM Views of Ectodermal Cilia

- A. Prehatched blastula (5:48 hr p.f.). Not all cells are ciliated. Embryo with hyaline layer
- B. Ciliated cells of embryo in A. Cilia are 8 to 10 μm long
- C. Cilium of prehatched blastula without hyaline layer. Cilium is 9 μm long.
- D-G. Mesenchyme blastula (9:20 hr. p.f.). There is a great variety in lengths of cilia associated in part with regionally dividing cells. (D) Whole embryo, lateral view. (E) Equatorial region with relatively short cilia (6-8 μm long), where cells are actively dividing. (F) Vegetal pole region with the SMDs surrounded by presumptive vegetal plate cells engaged in cell division. Beyond this zone is a region of presumptive endodermal cells with long cilia as well as cells that are dividing. (G) Ciliated cell with cilium 19 μm long. This is a “mature” ciliated, ectodermal cell.
- H-I. Vegetal plate region of a mesenchyme blastula (9:30 hr p.f.). (H) Low magnification of whole region. (I) Stereopair image of boxed area in (H) shows three cells with cilia 6-8 μm long and three cells with cilia less than 3 μm long.
- J. Photomontage of equatorial region of lateral ectoderm wall of a mesenchyme blastula. Arrows point to six cells that show initial formation of cilia. One cell has a cilium 38 μm long. Two other cells have cilia 7-8 μm long.
- K-M. (K) Lateral view of a late gastrula (13 hr. p.f.) without a hyaline layer. (L) Ciliated cells in equatorial region of the embryo with cilia that range in length from 5 μm to 18 μm . (M) High magnification of boxed area in (K) to show the base of the cilium's shaft surrounded by collar microvilli, the apical lamina and other cell surface microvilli.

PLATE 44

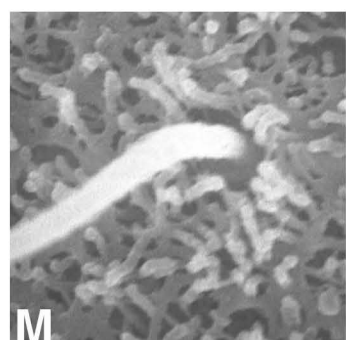
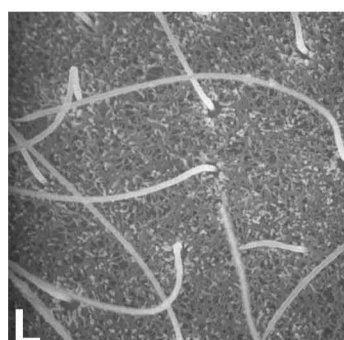
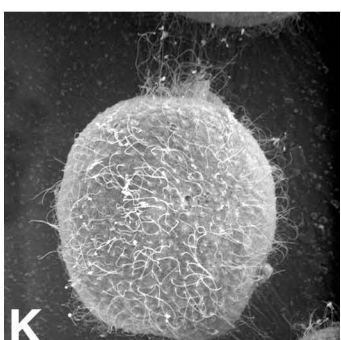
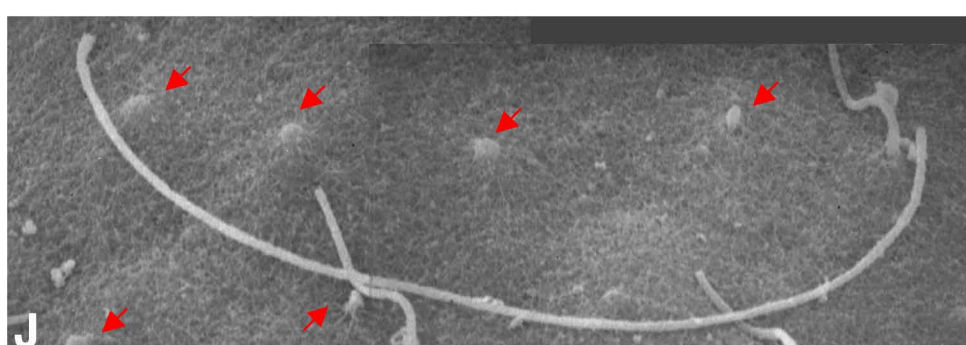
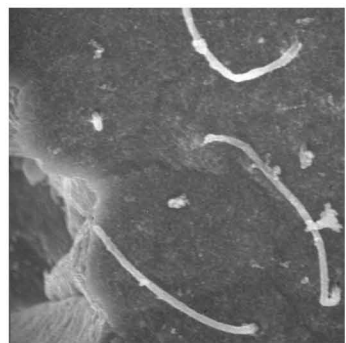
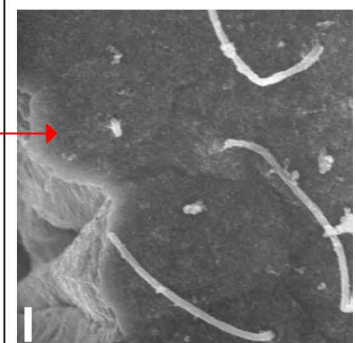
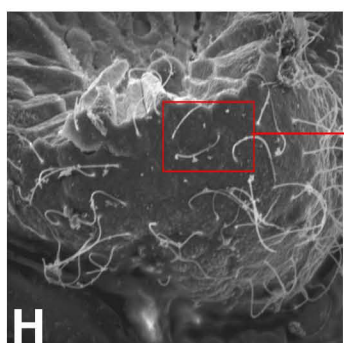
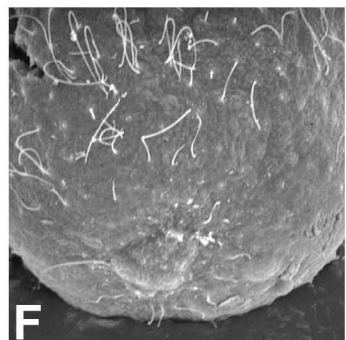
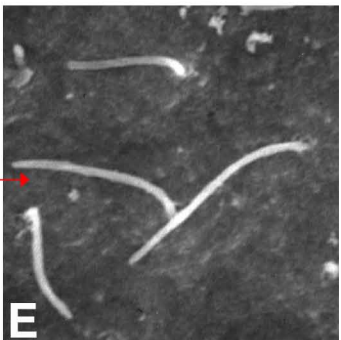
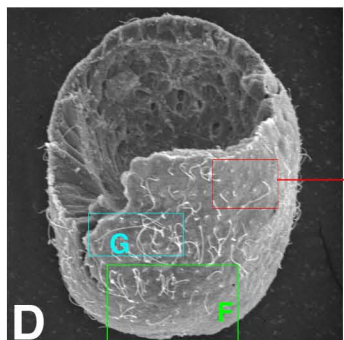
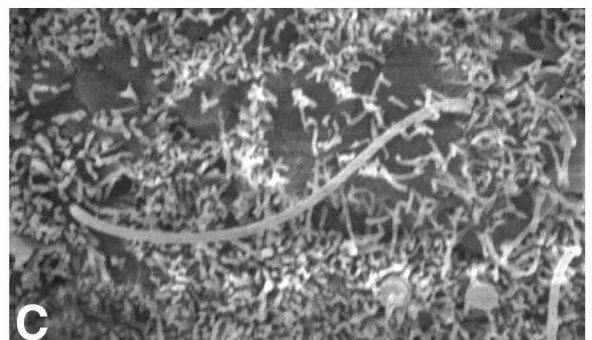
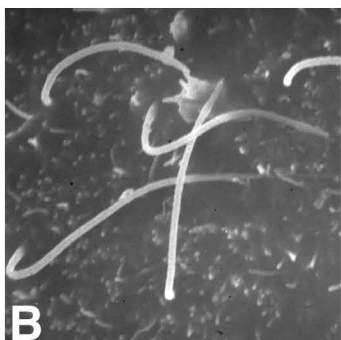
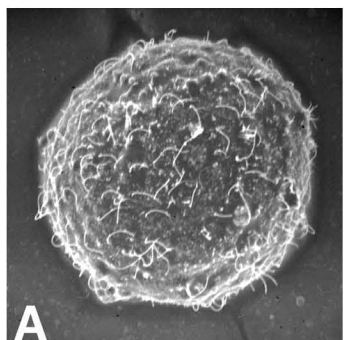


PLATE 45
SEM Views of Acron Cilia of Mesenchyme Blastula Stages

- A, B. (A) Early mesenchyme blastula (9:30 hr. p.f.) fractured along the A-V axis. (B) Stereopair image of the apical plate ectoderm and acron cilia in panel A.
- C, D. (C) Lateral view of apical plate area and long acron cilia. (D) Polar view of acron cilia and surrounding cells of apical plate with much shorter cilia. Some of these apical plate cells are entering or leaving the cell division cycle.
- E, F. (E) Polar view of animal hemisphere and acron cilia of a late mesenchyme blastula (10:30 hr p.f.) (F) Stereopair image of acron and apical plate in panel F at higher magnification.
- G, H. (G) Late mesenchyme blastula (10:30 hr p.f.) fractured along the A-V axis. (H) Stereopair image of acron region cilia in panel G.

PLATE 45

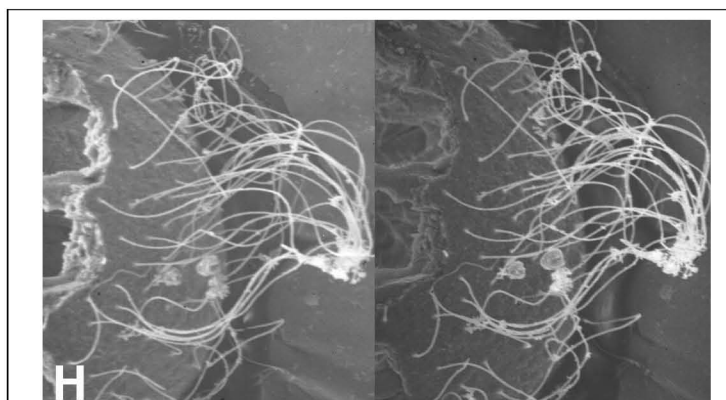
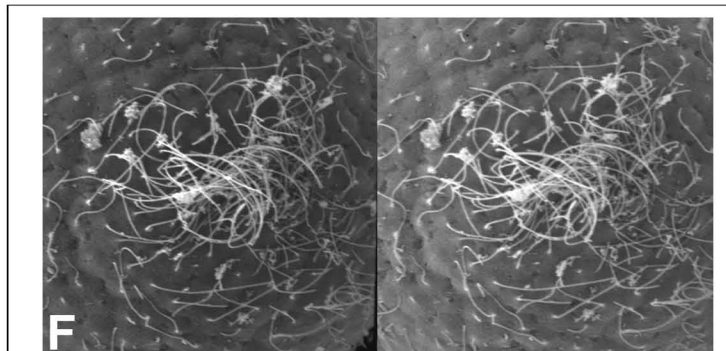
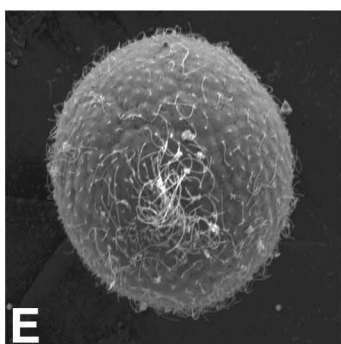
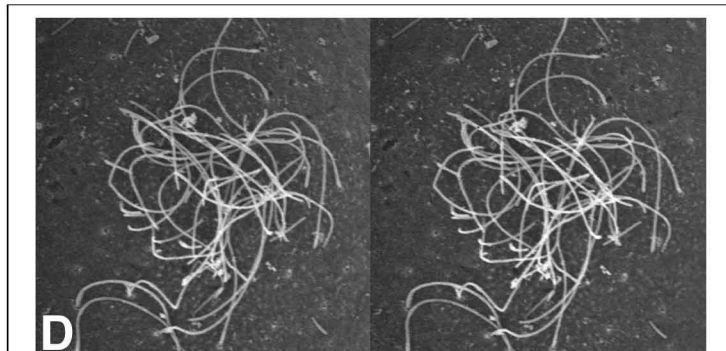
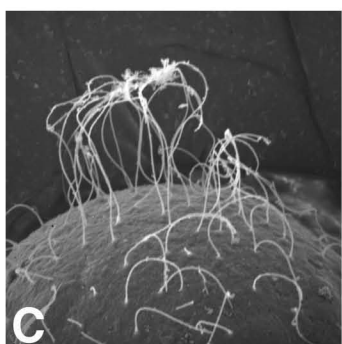
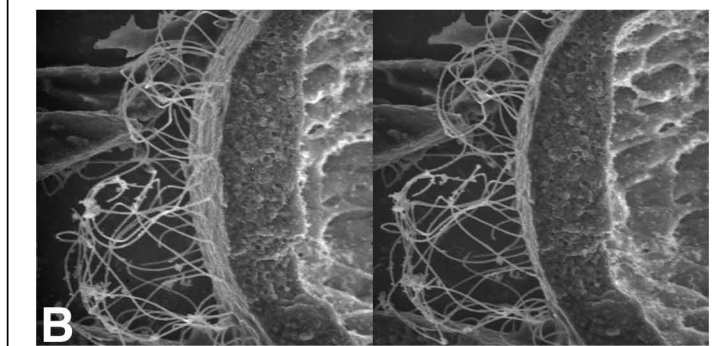
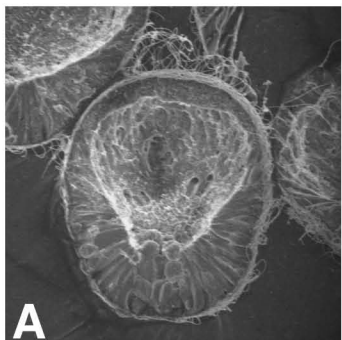


PLATE 46
SEMs of Acron Cilia of Late Gastrula and Prism Larva Stages

- A, B. (A) Stereopair image of a late gastrula (14 hr. p.f.) with long, entwined acron cilia. At this stage, acron cilia are 40-70 μm long. (B) Stereopair image of the acron cilia in panel A.
- C, D. (C) Prism stage larva with long entwined acron cilia. At this stage, acron cilia are 40 to 99 μm long. (D) Stereo pair image of the acron cilia. Presumptive stomodeal region with short cilia is outlined by a dashed line.

Table 1: Lengths of Cilia (μm) During Development at 20°C

Location	Hatched Blastula	Mesenchyme Blastula	Early Gastrula	Late Gastrula	Prism	2-Arm Larva	4-Arm Larva
Animal Plate/Acron	25-35	25-38	33-55	44-72	44-99	50-77	8-16
Equator	25-35	11	11	11	16-22		
Vegetal Pole		8-20		7-11			
Ciliary Band					16-22	16-22	

Table 2: Lengths (μm) and Number of Cilia in Acron Region of Animal Pole During Development at 20°C

Stage	Cilia	
	Lengths	Number
Hatched Blastula	25-35	6-8
Mesenchyme Blastula	25-38	24
Early Gastrula	33-55	18-50
Late Gastrula	44-55	20-50
Prism	44-99	20-53
4 Arm Larva	55-77	20

PLATE 46

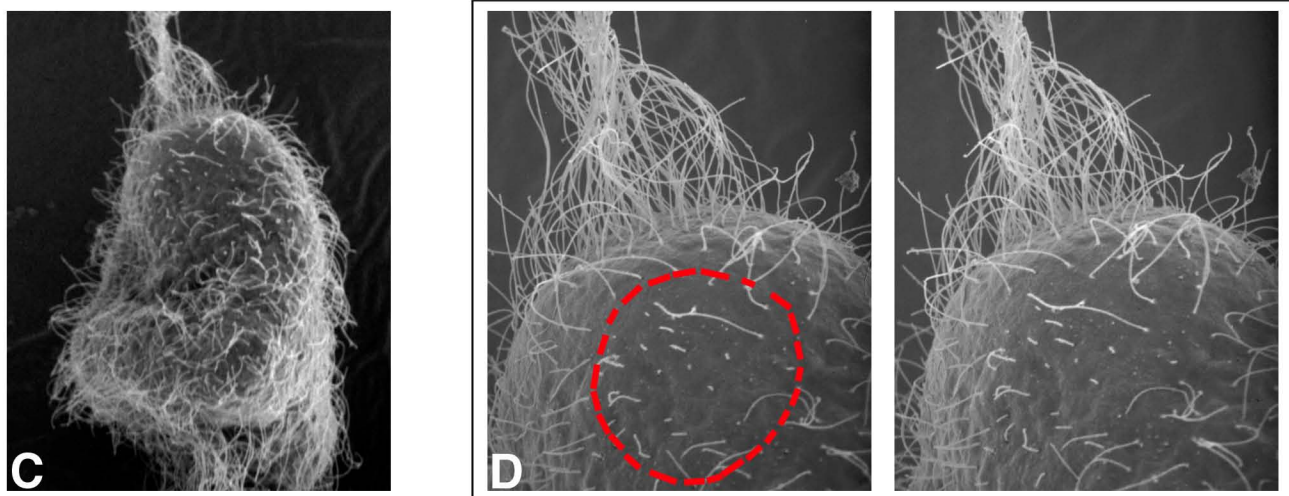
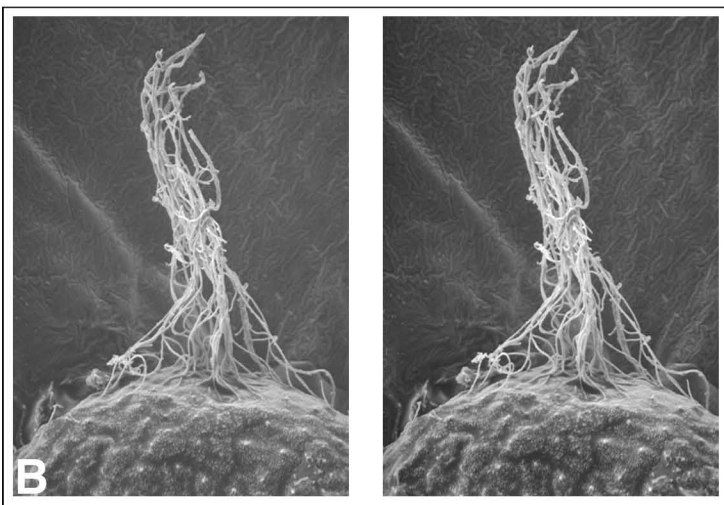
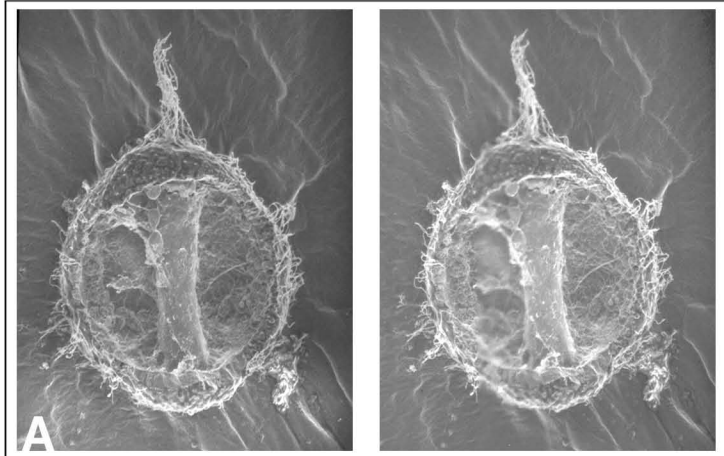


PLATE 47

TEM Views of Cilia and Cilia Collar Microvilli of Gastrulae and Larvae

- A-G. TEMs of longitudinal sections through the apical region of ectodermal cells. Panel (A) shows the three zones of the hyaline layer. OZ. Outer zone; IZ: inner zone; SL, support layer. The inner zone and support layer extend to the tips of the collar microvilli (CM). The outer zone extends along the shaft of the cilium. Below the support layer or apical lamina is an intervillous space (IV). Cortical vesicles (CV) are docked at the cell membrane. The cilium has three morphologically distinct components: a ciliary shaft (C), Translational region (TR), and Basal body. Beneath and surrounding the basal body complex is a well developed Golgi apparatus (G). In Panel (B) the striated rootlet (R) of the basal body is visible as are the basal plate (BP) of the cilium and Ruthenium Red (RR) proteoglycan aggregates along the outer surface of the ciliary shaft. In Panel (C), the RR granules are visible in the cross sections of two cilia. Panel (D) shows the cone shaped golgi complex associated with the basal body. The longitudinal sections in panels (E-G) show the collar microvilli and cupola like cavity surrounding the cilium containing partially preserved ECM.
- H-I. Panels (H and I) are cross sections of cilia surrounded by ten to twelve collar microvilli. Panel (H) is an oblique cross section. In panel (I), the two cross sections are at different levels along the cilium.

PLATE 47

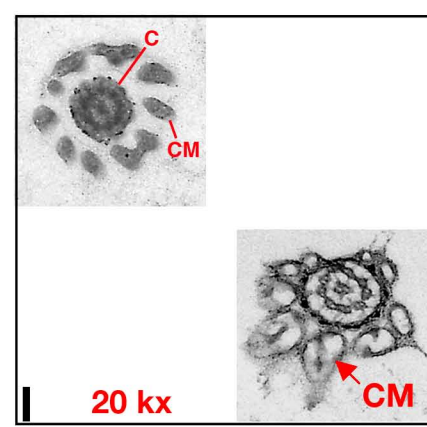
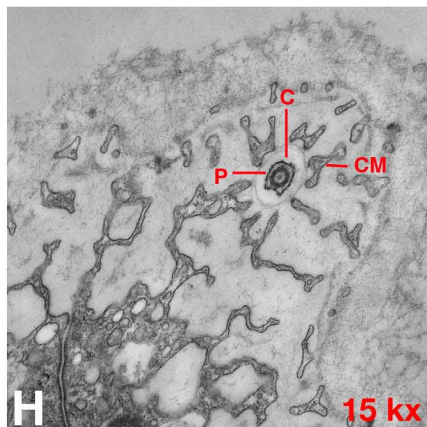
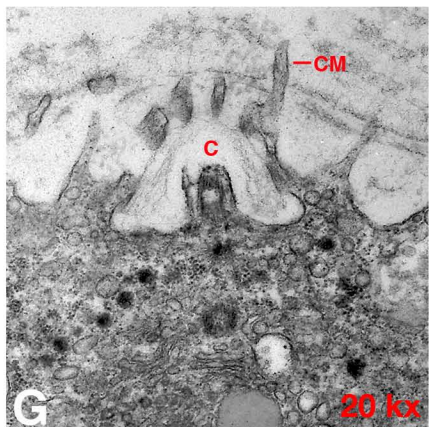
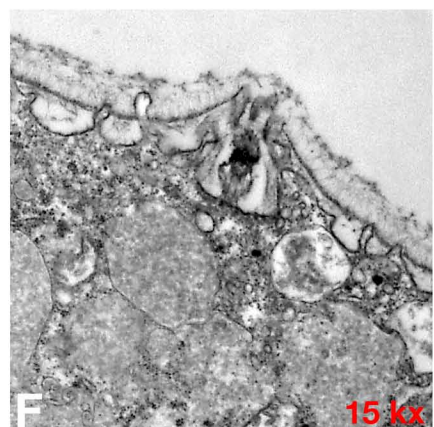
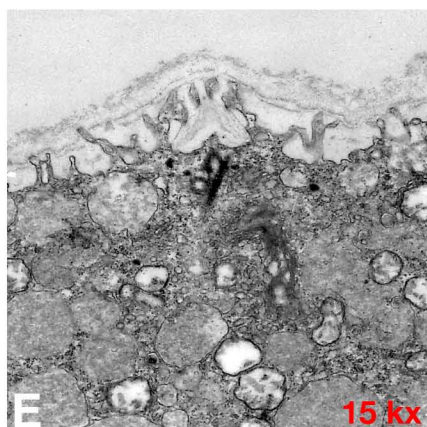
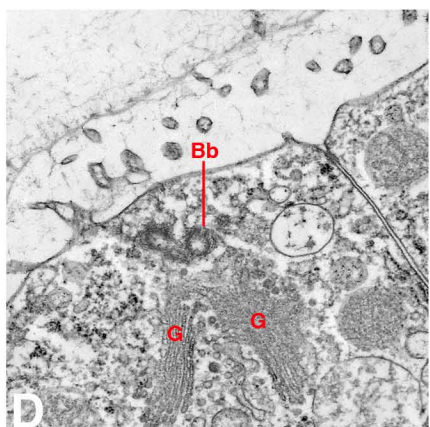
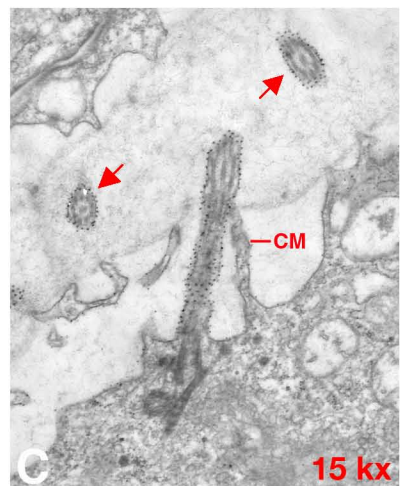
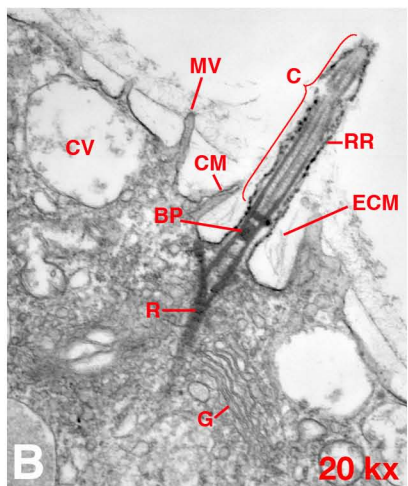
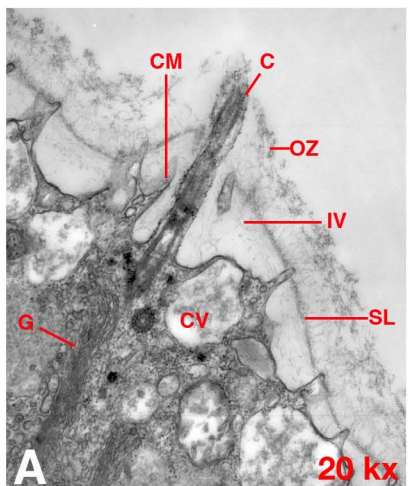
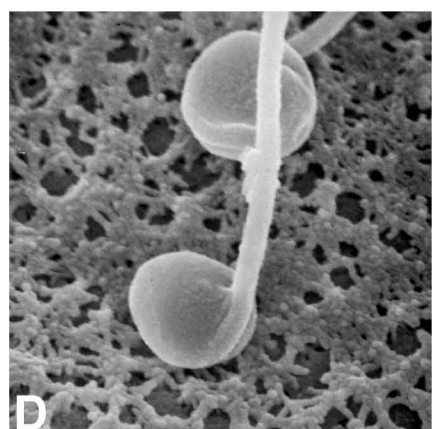
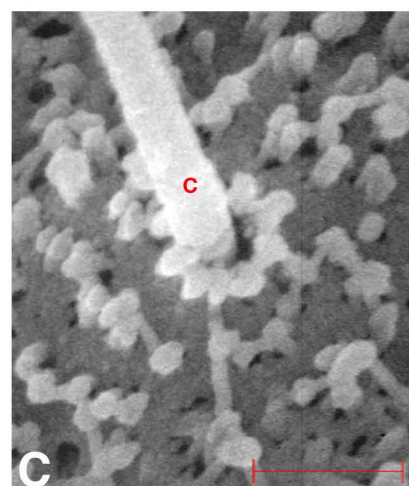
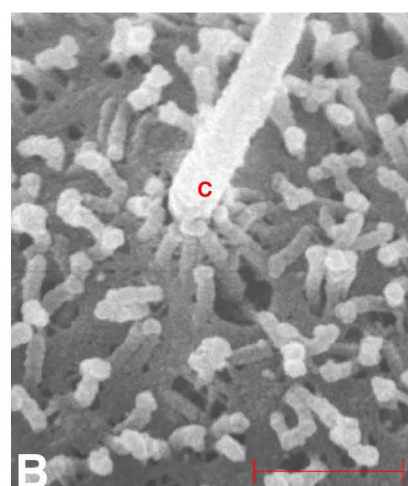
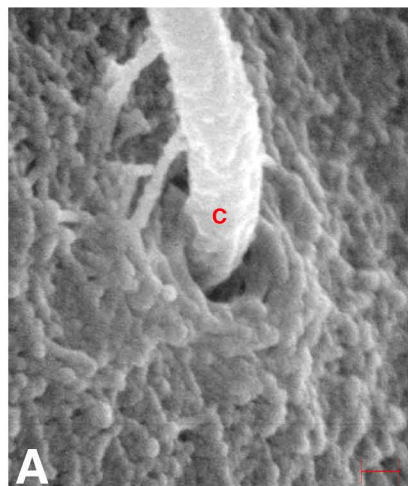


PLATE 48

- A- SEM views of individual cilia. In panel (A), the cilium protrudes through a “pore” in the intact hyaline layer. In panels (B and C) the hyaline layer was removed leaving the apical lamina, the exposed cell surface microvilli, and the collar microvilli surrounding the cilium. Bars: 0.1 μ m (A), 1.0 μ m (B and C).
- D- Abnormal lollipop cilia that are fixation artifacts in which the distal end of the ciliary membrane is inflated.
- G.

PLATE 48



33,600 X

Section 12:

Hyaline Layer of Gastrulae and Larvae

PLATE 49

Schematic Diagram of the Ultrastructure of the “Hyaline Layer” of Gastrulae and Larvae

The diagram is based on TEM and SEM images in the panels of plates 50 and 51

Abbreviations

- AL. Apical Lamina
- BL. Boundary Layer between the outer and inner zones of the hyaline layer
- C. Cilium
- ECM. Extracellular matrix between collar microvilli and cilium
- G. Golgi complex
- IV. Intervillous layer below apical lamina
- IZ. Inner zone of hyaline layer of which the main component is the calcium dependent protein, hyalin
- OJ. Occluding junction between epithelial cells
- OZ. Outer zone of hyaline layer with two distinct sub zones
- RR. Ruthenium red stained knobs on the surface of the ciliary shaft.

PLATE 49

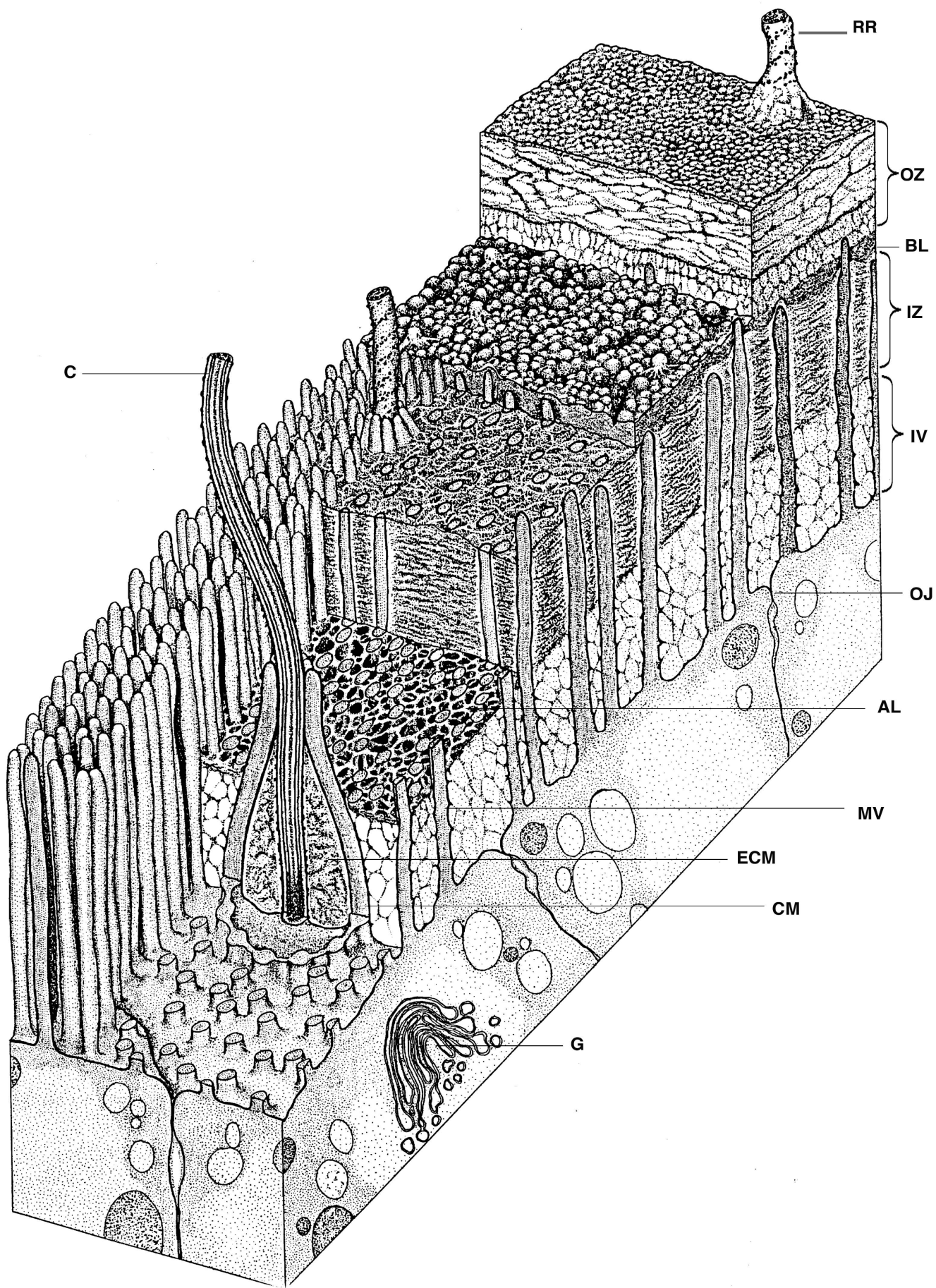


PLATE 50

TEMs of the “Hyaline Layer” and Distal Ends of Ectoderm Cells of Gastrulae Following Four Different Fixation Procedures

- A. Primary fixative, 4% gluteraldehyde in 0.2M cacodylate buffer; Post fixative, 1% Osmium tetroxide in 0.2 M cacodylate buffer.
- B. Cocktail fixative of 4% gluteraldehyde (GA) and 1% Osmium tetroxide (OS) with 1% Ruthenium Red (RR).
- C. Cocktail fixative (GA/OS) with 1% RR and 20mM Calcium chloride.
- D. Cocktail fixative (GA/OS) saturated with Alcain Blue.
- E. Freeze substitution fixation with Osmium tetroxide.

PLATE 50

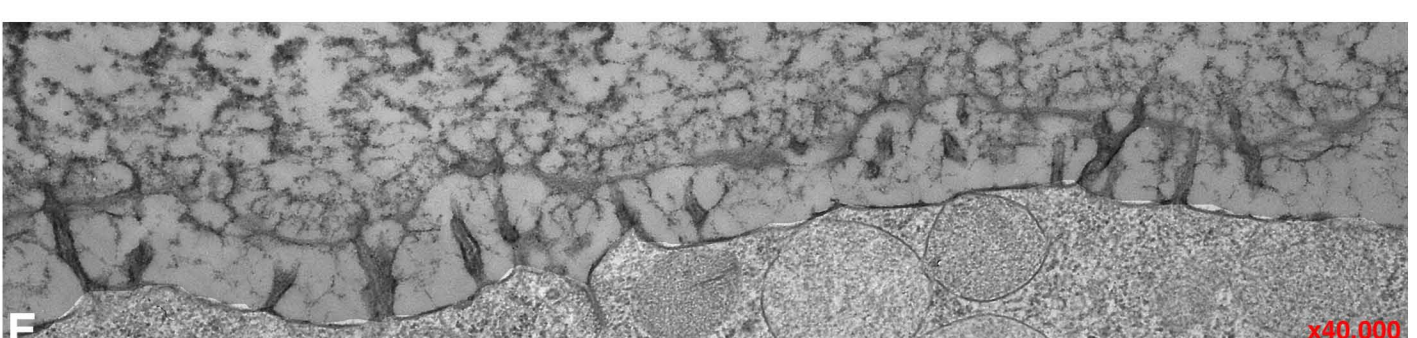
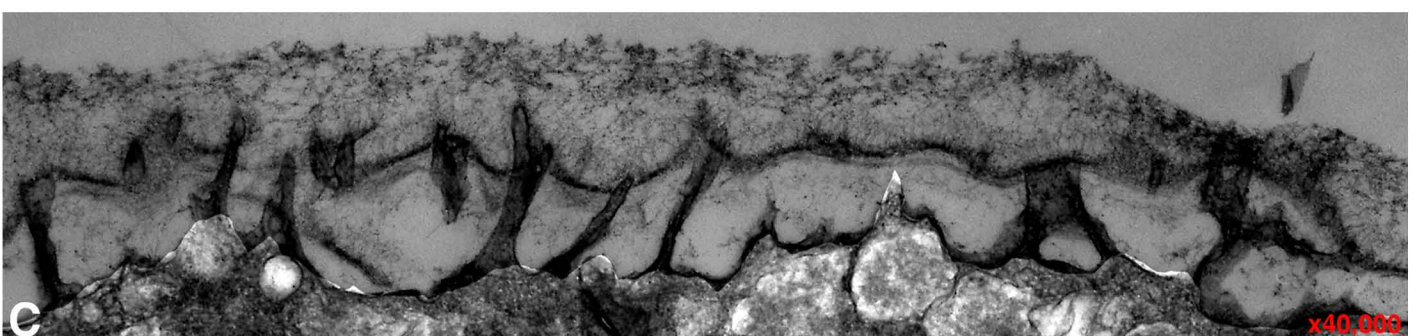
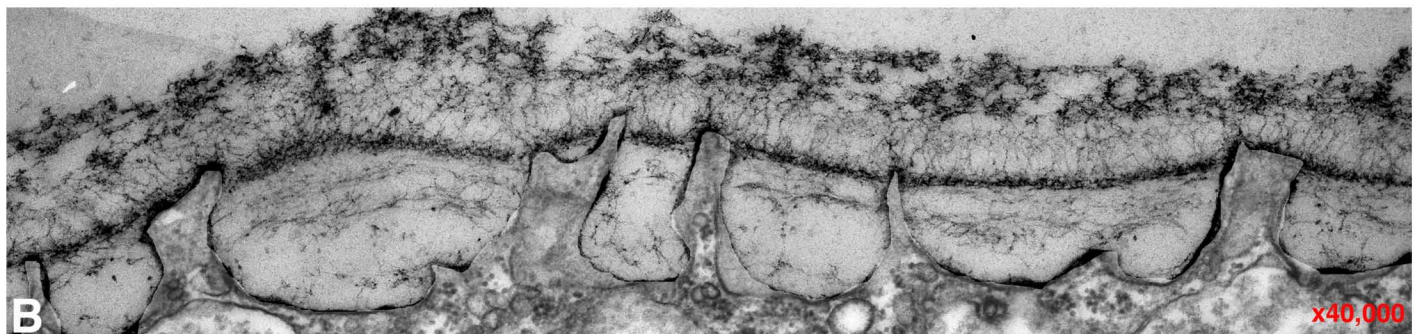
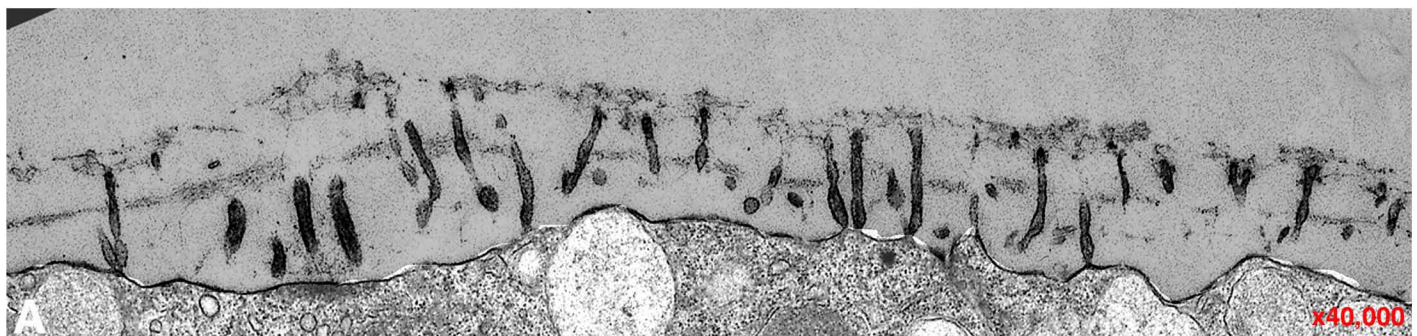
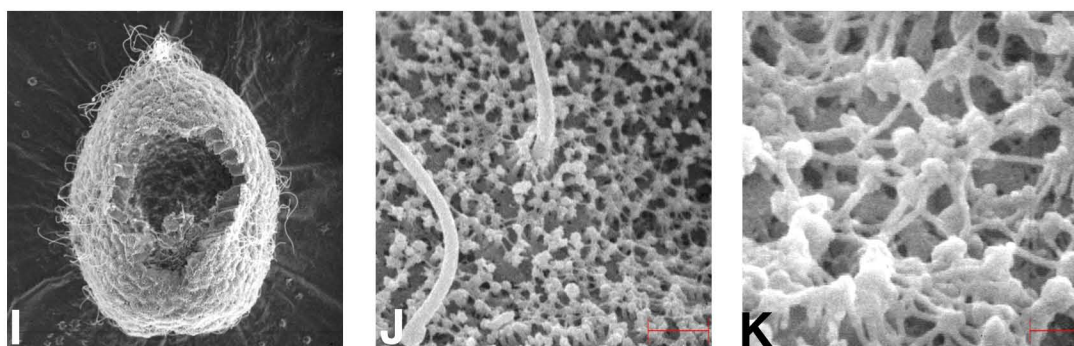
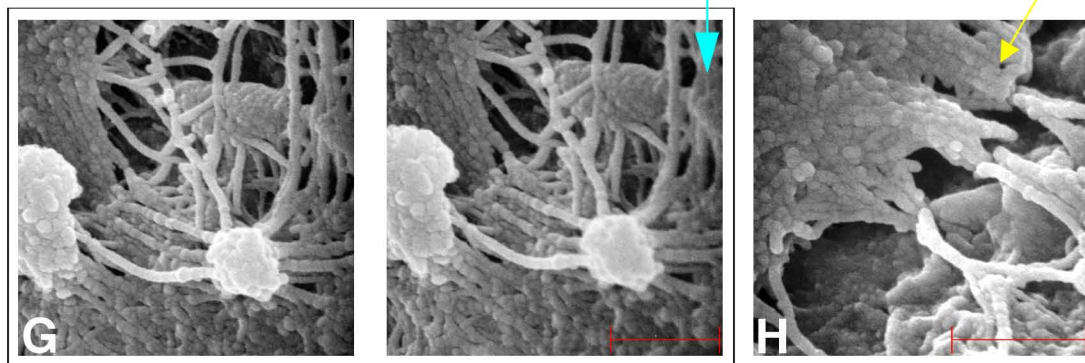
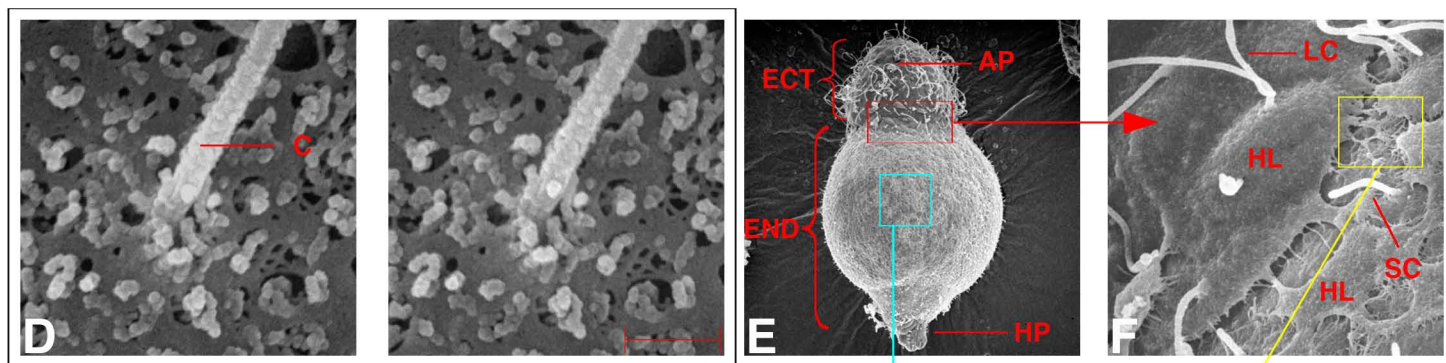
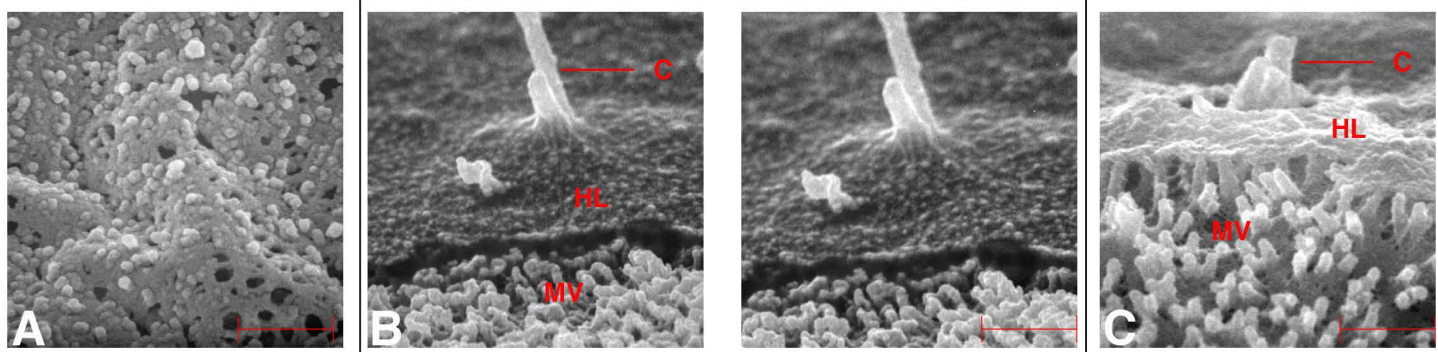


PLATE 51

SEMs of Surface Views of the “Hyaline Layer” and Apical Lamina of Gastrulae

- A. Outer surface of hyaline layer of a gastrula fixed in 2.5% GA in 0.4M cacodylate buffer. Bar, 1.0 μ m
- B. Stereo pair of outer surface of hyaline layer (HL), a cilium (C), and underlying microvilli (MV). Bar, 1.0 μ m.
- C. An oblique view of the hyaline layer and the underlying microvilli and basal lamina. Bar, 1.0 μ m.
- D. Stereopair on face view of the apical lamina, the microvilli and the collar microvilli surrounding the cilium. Bar, 1.0 μ m.
- E. Vegetalized, radialized exogastrula resulting from chronic treatment with 26mM LiCl. (E)
- H. Morphology of whole embryo; ectoderm (ECT) with long cilia and swollen endoderm (END) with short cilia not visible. (F) Transitional zone between the ectoderm and endoderm regions; short cilia (SC) of endoderm and long cilia (LC) of ectoderm. At a magnification of 5 kx, the surface of the hyaline layer (HL) of the ectoderm appears continuous while the HL of the endoderm appears retracted away from the short cilia and other regions of the surface of endoderm cells. (G) Stereo pair of the stretched HL over the endoderm cells shows at 30 kx the HL is composed of beaded strands, some of which converge upon aggregated centers. (H) At a magnification of 30kx the surface of the HL of outer ectoderm is a continuous granular sheet. Bar, 1.0 μ m.
- I-K. Treatment of gastrulae with calcium/magnesium free sea water (CMFSW) for 10 min. and fixed in 0.75% GA in CMFSW removes most of the hyaline layer but not the apical lamina. (I) Whole CMFSW treated gastrula. (J) Ectoderm surface shows collar microvilli around the base of a cilium. The outer surface of the apical lamina has fiber-like strands between microvilli whose tips are covered with hyaline layer material. (K) Remnants of the hyaline layer at a higher magnification. Bars: 1.0 μ m (j) ; 0.1 μ m (k).

PLATE 51



Section 13:

Extracellular Matrices

PLATE 52

LM and SEM Views of the Extracellular Matrices of the Cleavage Cavity and Blastocoel

- A, B. Light micrographs of resin embedded thick sections of FSF embryos. (A) 60-cell stage. (B) 216 cell stage. A: animal pole; V: vegetal pole, Cc, cleavage cavity; Pv: perivitelline space.
- C. Stereo pair SEM of a post 8th cleavage, embryo fixed at 5 hours post fertilization and dry fractured. Other views of the cleavage cavity ECM are shown in panel (M). Plate 10; panel (L), plate 11; and panel (P), plate 12.
- D. Stereopair SEM of mesenchyme blasutla.
- E. Stereopair SEM of a late mesenchyme blastula.
- F. Stereopair SEM of a late gastrula fractured along the A-V axis. Numerous ECM fibers extend radially from the archenteron basal lamina to the ectodermal wall basal lamina.
- G. Stereopair SEM of a dry fractured late gastrula in which the animal hemisphere ectoderm was removed. Arrow points to the 8 small micromeres descendants at the tip of the archenteron.
- H, I. SEMs of a prism larva fractured along the A-V axis. (H) Stereopair of the half of the embryo separated from the archenteron. (I) The other half of the embryo. A, archenteron. Ap. Apical plate. B. blastopore.
- J. Fractured prism larva in which the oral ectoderm was removed. A, archenteron; Ap, apical plate; B, bilaterally symmetrical blastopore; PMC aggregation center.

PLATE 52

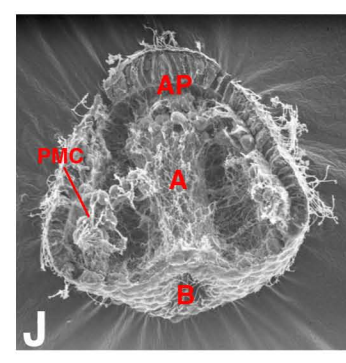
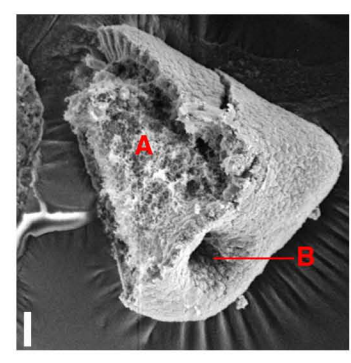
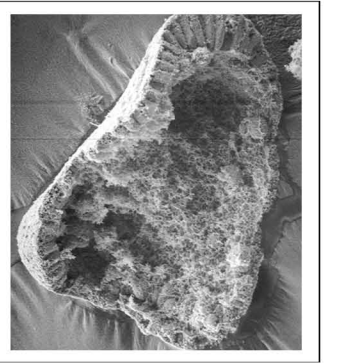
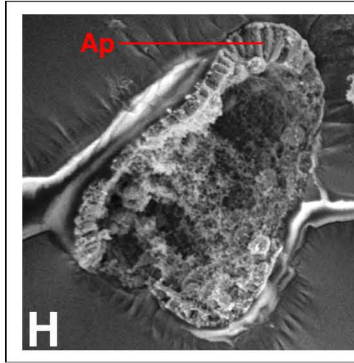
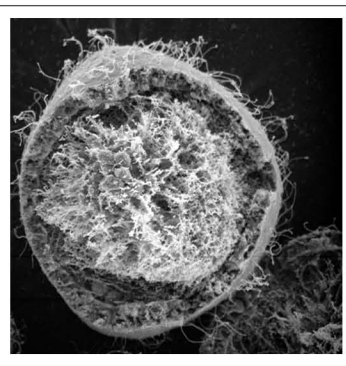
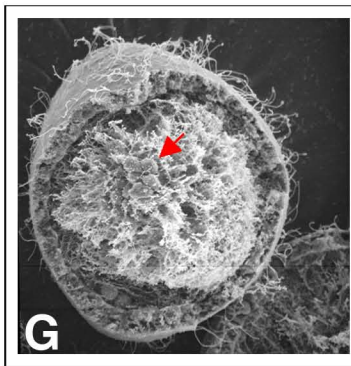
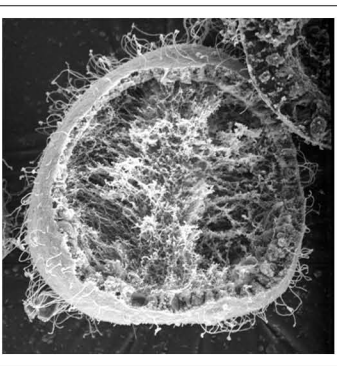
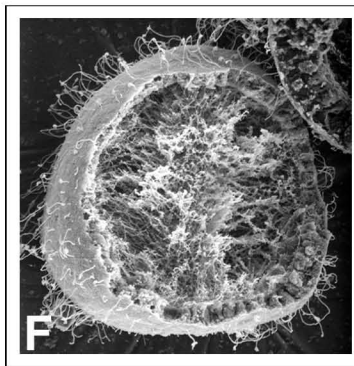
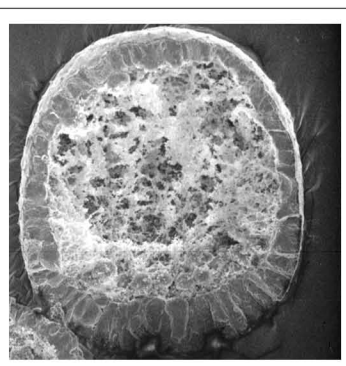
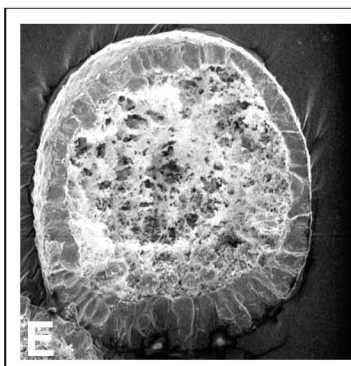
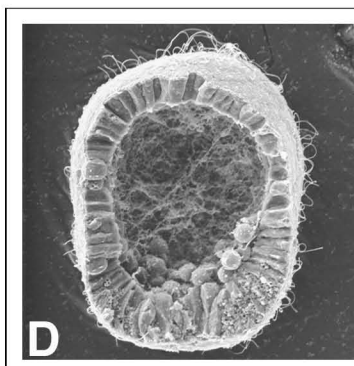
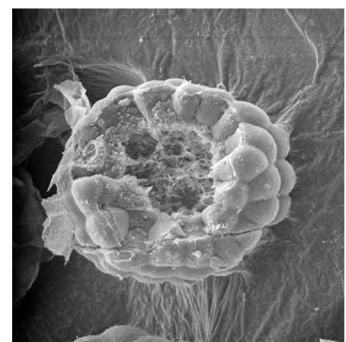
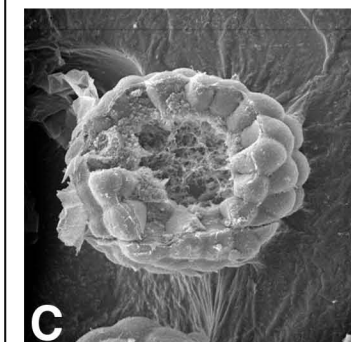
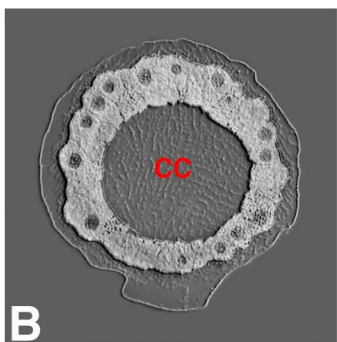
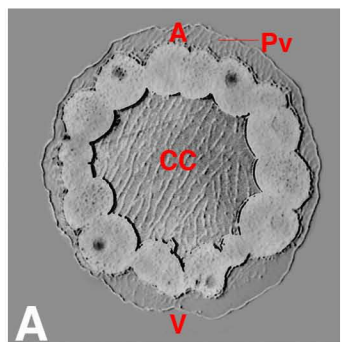


PLATE 53

ECM Vesicle (ECMV) Exudate, Coated Blastocoelic Fibers and Basal Lamina of Ectoderm

- A. SEM of extracellular matrix vesicle revealing aggregated contents. V. vessicle. Bar, 0.5 μm.
- B. Stereopair SEM of ECM vesicle contents that coat ECM fibers. Bar, 0.5μm
- C. SEM of ECM vesicles, their released contents and coated ECM fibers.
V, ECM vesicles. Bar, 0.5 μm
- D, E. Stereopair SEM of coated blastocoelic fibers. Bar, 0.5 μm.
- F.G. Stereopair SEM of the blastoceolic side of the epithelial basal lamina. (F) Bar: 1.0μm. (G) Bar, 1.0 μm.
- H. TEM of basal lamina (Bl) of ectodermal epithelium shows two distinct regions (1and 2) in the basal lamina distal to a surface coating of the cells. B:blastocoel; Is: intercellular space between two epithelial cells;
M, mitochondrion.

PLATE 53

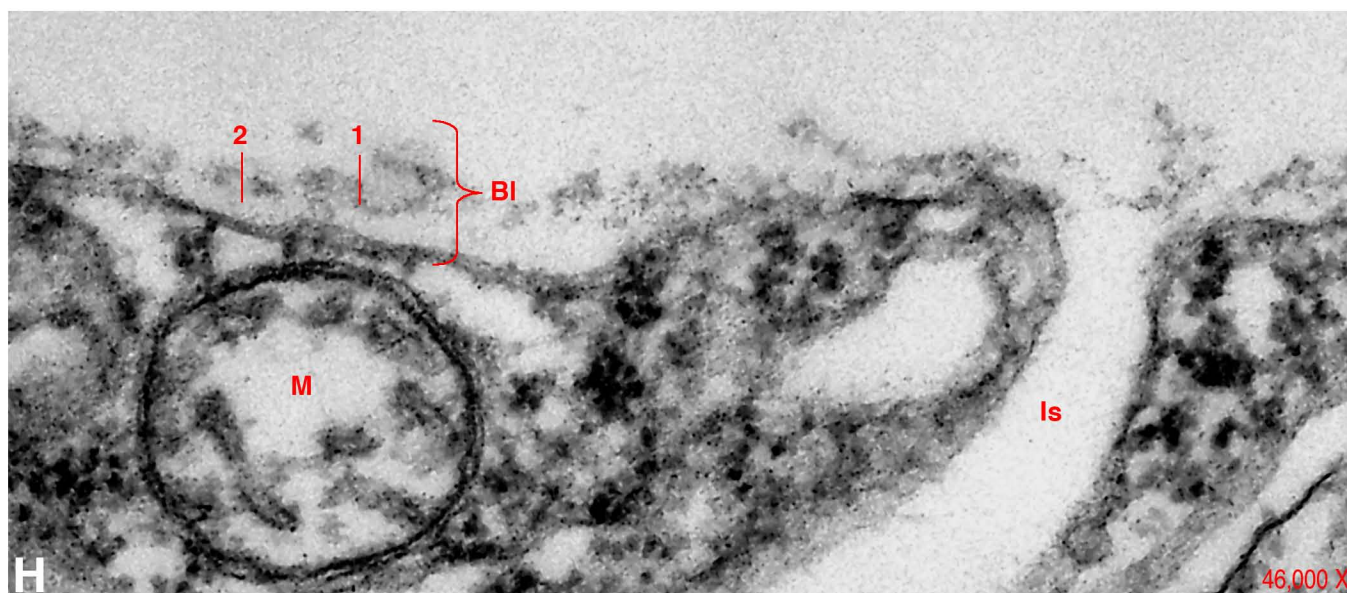
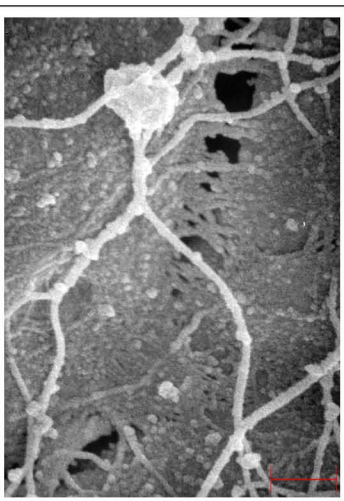
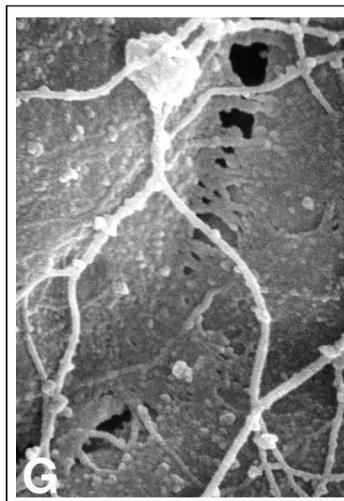
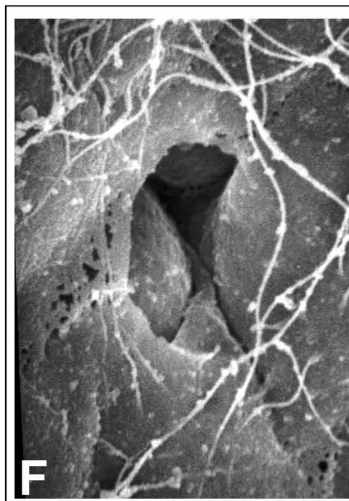
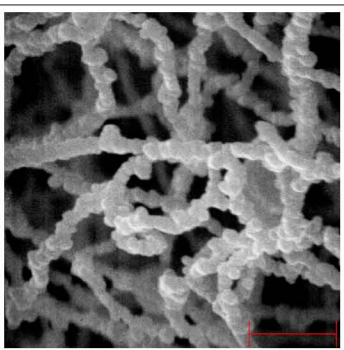
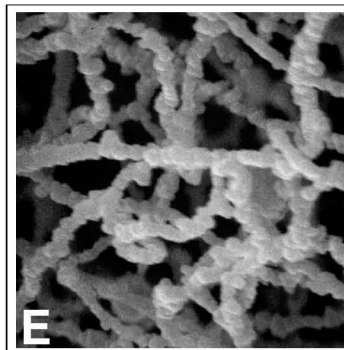
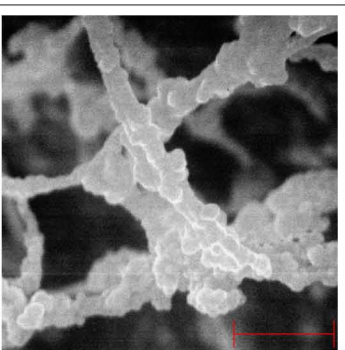
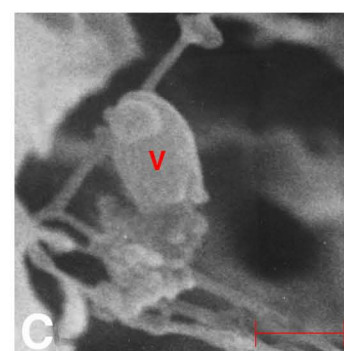
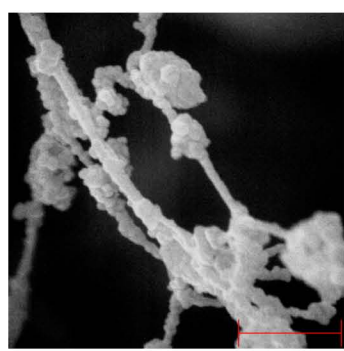
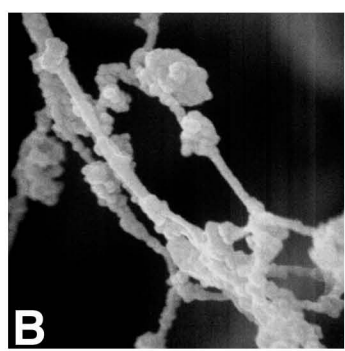
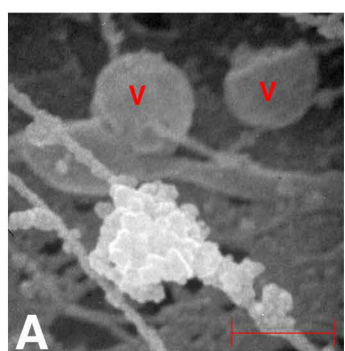


PLATE 54
Origins of Extracellular Matrix Vesicles (ECMV)

- A. SEM view of a dry fractured, hatched blastula. Vegetal hemisphere on left and animal hemisphere on right.
- B. Enlargement of boxed area in (A) shows numerous ECMVs of varying sizes at the vegetal pole in the area of the large and small micromere descendants surrounded by presumptive secondary mesenchyme cells.
Bar, 1.0 μ m.
- C, D. SEMs of vegetal pole region of a hatched blastula. (D) Enlargement of boxed area in (C) with numerous ECMVs over the flattened small micromere descendants area surrounded by presumptive primary mesenchyme and secondary mesenchyme cells with cytoplasmic extensions converging at the central area. Bar, 1.0 μ m.
- E, F. SEMs of a mesenchyme blastula fractured along the A-V axis. The enlarged boxed area in (F) shows numerous ECMVs over the blastoceleic ends of the secondary mesenchyme cells at this stage. The ingressed PMCs were in the other half of the fractured embryo.
Bar, 0.1 μ m.
- G, H. SEMs of the vegetal pole of a late mesenchyme blastula with elongated secondary mesenchyme cells (SMCs) surrounding the small micromere descendants (SMD). (H) Boxed area in (G) enlarged to show numerous ECMVs at the ends of the SMCs and apical protrusions that represent a type of holocrine secretion. Bar, 1.0 μ m.

PLATE 54

